UNIVERSITY OF UDINE
PhD COURSE IN BIOMEDICAL SCIENCES AND BIOTECHNOLOGY
XXVI CICLE

PhD THESIS

The ECM molecule EMILIN2: a dual role in the tumor microenvironment

PhD student
Alice Paulitti

TUTOR
Prof. Carlo Pucillo

SUPERVISOR
Dott. Maurizio Mongiat

ACADEMIC YEAR
2013/2014

TABLE OF CONTENTS

1 ABSTRACT

EMILIN2 is an extracellular matrix molecule belonging to the EDEN (EMI Domain ENdowed) protein family. The protein is characterized by the cysteine-rich EMI domain at the N-terminus, the hallmark of the family, α-helical domains at the C-terminus, a proline-rich motif adjacent to a collagenous stalk preceding the globular gC1q domain. Here we report that this molecule exerts a double function in the tumor microenvironment, simultaneously directly acting on cancer cells and, indirectly on the tumor vasculature.

First, based on sequence homology with the Cysteine Rich Domain (CRD) of the Frizzled receptors, we hypothesized that EMILIN2 could affect Wnt signaling activation and we demonstrated a direct interaction with the Wnt1 ligand. As a consequence, EMILIN2 negatively affects the viability, migration and tumourigenic potential of MDA-MB-231 breast cancer cells in a number of 2D and 3D in vitro assays. Moreover, *in vivo* experiments show that the ectopic expression of EMILIN2, as well as treatment with the recombinant protein, significantly reduce tumor growth in nude mice.

Second, based on our previously published evidences that treatment with EMILIN2 enhanced angiogenesis, we sought to corroborate these findings and shed light on the molecular mechanisms involved. EMILIN2 challenged ECs display an increased expression of IL-8 as assessed by a protein array, ELISA, Real Time and Western blot analysis. The induction of IL-8 production occurs through activation of EGFR following interaction with EMILIN2 and a consequent activation of the Jak2/STAT3 pathway. Similarly, EMILIN2 induces expression of IL-8 also by fibroblast, the major source of this molecule and EMILIN2 itself. Accordingly, manipulation of EMILIN2 expression by fibroblast lead to significant changes in EC behavior when challenged with the conditioned media derived from these cells in terms of both viability and random motility. Manipulation of EMILIN2 expression by fibroblast leads also to an altered EC spouting from spheroids in a 3D co-culture setting. In line with our findings the pro-angiogenic function of EMILIN2, which was tested in a number of *in vitro*, *ex vivo* and *in vivo* assays, was blocked by Cetuximab, an anti-EGFR monoclonal antibody. Taken together these results suggest that the expression of EMILIN2 in the microenvironment may significantly affect the growth and development of the tumors.

2 INTRODUCTION

2.1 The role played by tumor microenvironment in tumor progression

The tumor can be considered a complex organ where transformed cells characterized by high genomic instability and altered gene expression communicate with the surrounding microenvironment. The microenvironment is composed by a large variety of hematopoietic and mesenchimal cells including inflammatory, stem and progenitor cells, fibroblasts, myofibroblasts, endothelial and mural cells of the blood vessels that sustain tumor growth. The cellular moiety is surrounded by a complex network of extracellular matrix (ECM) molecules that sustain and communicate with the cells. Numerous studies have reported that the tumor microenvironment not only responds to and supports carcinogenesis but also can actively contribute to tumor initiation, progression and metastasis. It has been demonstrated that stromal cells can cause transformation of the adjacent cells through transient signaling that in some cases leads to the disruption of homeostatic regulation, including control of tissue architecture, adhesion, cell death and proliferation (Hu and Polyak, 2008).
Fibroblasts in particular are important members of the stromal microenvironment, as they maintain the adjacent epithelial homeostasis through the secretion of growth factors and direct mesenchymal-epithelial cell interactions. It is becoming increasingly clear that fibroblasts are also prominent modifiers of cancer progression. Knowledge of the role of resting and activated fibroblasts in cancer is still evolving. A subpopulation of fibrolasts, called cancer-associated fibroblats (CAFs), is an important promoter of tumor growth and development. CAFs directly stimulate tumor cell proliferation and angiogenesis through paracrine secretion of growth factors, hormones and cytochines in a context-dependent manner (Räsänen and Vaheri, 2010). Many of the CAF-secreted factors acting in isolation are sufficient to induce transformation of epithelial cells, indicative of a tumor-initiating capability of CAFs (Pietras and Ostman, 2010). Moreover CAFs can affect cancer progression by secreting and organizing altered ECM within the tumor stroma (Kalluri and Zeisberg, 2006).
Inflammtory cells can also deeply affect cancer cell behavior. Tumor associated macrophages (TAMs), which represent the majour inflammatory component of the stroma of many tumors, are strongly associated with tumor progression and metastasis. In contrast to the reactive macrophages which are characterized by a so-called M1 phenotype, TAMs are alternatively activated and aquire an M2 phenotype, thus promoting tumor growth, angiogenesis and metastasis (Mantovani et al., 2001). TAMs affect vascular density and ECM by secreting a vast array of pro-angiogenic factors and proteolytic enzymes including VEGF, FGF, PDGF, TNFα, MMPs, plasmin, urokinase-type plasminogen activator (uPA) and uPA receptor (uPAR) (Guruvayoorappan and Kuttan, 2008;Allavena et al., 2008). The key players in the setting of TAMs phenotype are several

microenvironmental chemoattractants including macrophage colony-stimulating factor (M-CSF), the CC chemokines CCL2, CCL3, CCL4, CCL5 and CCL8, and VEGF. In addition tumor-derived anti-inflammatory molecules such as IL-4, IL-10, TGF-β1 and prostaglandin E2 are essential for the function of TAMs and this suggests that exposure to IL-4 and IL-10 may induce monocytes in tumor to develop into polarized M2 macrophages (Mantovani et al., 2002). These immune cells often accumulate in necrotic areas and promote tumor development by secreting growth factors, chemokines and proteases (Lewis and Pollard, 2006a).

Various transgenic mice models and clinical data show that the presence of tumor-associated neutrophils often correlates with poor prognosis given their ability to stimulate tumor angiogenesis. The migration of neutrophils towards the tumors mainly mediated by CXC chemokines. CXCL8 (IL8), in particular, is overexpressed by various human tumor cell lines and stimulates neutrophil degranulation with the release of MMP9, a known matrix-degrading enzyme. MMP9 in turn cleaves the amino terminus of CXCL8 producing a tenfold more potent chemokine which creates a positive loop to recruit more neutrophils into the tumor and further stimulating angiogenesis. TNFα is also a key chemokine that stimulates neutrophil degranulation and the release of VEGF from the intracellular stores (Lewis and Pollard, 2006).

TGFβ, an immunosupressive cytokine frequently found in the tumor microenvironment and known to enhance tumor progression in later stages, is able to switch peripheral cytotoxic natural killers (NK cells) to a secretory dNK (decidual NK) phenotype. This latter type of NK cells is similar to decidual NK and is characterized by the capacity to promote angiogenesis, due to the production of several angiogenic factors including VEGF, PIGF and IL-8 (Noonan et al., 2008)

The ECM composition and the stroma's mechanical properties are also important determinants that can profoundly affect tumor cell behaviour. The ECM tensile strenght or stiffness can regulate cell growth, differentation and migration, as well as the recruitment of other types of tumor-associated cells. Moreover, the stiffness and the increased interstitial pressure of the tumor stroma influences drug diffusion through the tumor and also the intrinsic drug sensitivity of malignant cells (Augsten et al., 2010).

On the other end, tumor invasion and metastasis are accomplished through ECM breakdown mainly due to matrix metalloproteinases (MMPs) activation. The ECM disruption promotes abnormal inter- and intra-cellular signaling leading to dysregulation of cell proliferation, growth and cytoskeleton reorganization. In turn, the ECM degradation entails a release of growth factors and other ECM-derived molecules that in turn modulate the properties of the different tumor-resident cell types. An important event in tumor progression is the acquisition by cancer cells of the capability to dissociate from their original site and invade adjacent tissues and reach distant sites. Invasion involves the breaching of several barriers, including the basement membrane and the stromal matrix.

Other key elements of the tumor microenvironment are the single ECM components. The ECM is mainly composed by an intricate interlocking mesh of fibrillar and non-fibrillar collagens, elastic fibers, non collagenous glycoproteins such as proteoglycans (PGs) and glycosaminoglycans as hyaluronan (HA). Within these structural elements, the stroma is made also of matricellular proteins, a group of extracellular proteins that do not contribute directly to the formation of structural elements but serve to modulate cell-matrix interactions and cell functions (Steeg, 2006;Brooks et al., 2010). Tumors often display an altered ECM composition due to the factors produced by tumor and stroma cells. Most solid tumors exhibit a profoundly different ECM-protein profile compared to their normal counteparts. Many of these proteins, through the integrins or other cell surface molecules, affect tumor cells behaviour in terms of proliferation, apoptotic rate and migration.

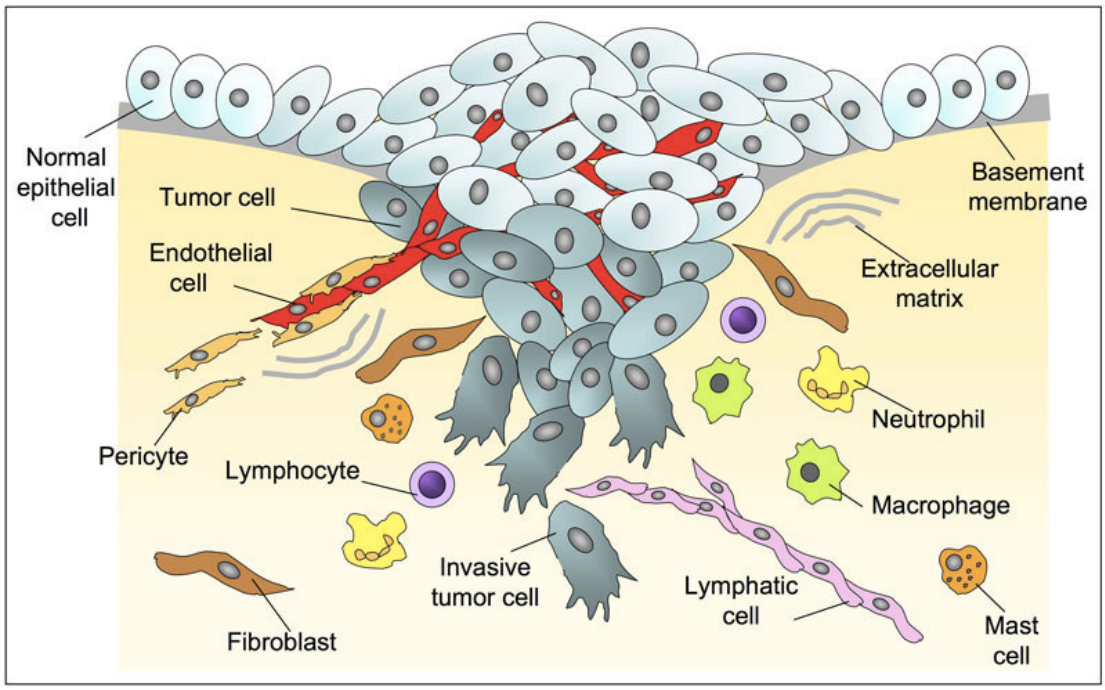

Fig.1: The tumor microenvironment. A large variability of cancer, stromal, hematopoietic and inflammatory cells contribute to the organization of the tumor microenvironment. Cells are supported and interact with a meshwork of different glycoproteins known as extracellular matrix (ECM) (Joyce and Pollard, 2009).

2.2 Wnt/β-Catenin signaling and tumor progression

WNTs are a family of 19 secreted glycoproteins (Papkoff et al., 1987) that have crucial roles in the regulation of diverse processes, including cell proliferation, survival, migration and polarity, specification of cell fate, and self renewal in stem cells. Perturbation of the levels of WNT ligands, or altered activities of the proteins that are necessary for WNT signal transuction, can result in defects in

embryonic development; additionally, abnormal WNT signaling in adults may contribute to disease aetiology (Anastas and Moon, 2013).

Aberrant overexpression of WNT1 induced by a proviral insertion at the Wnt1 locus, induces spontaneous mammary hyperplasia and tumours in mice (Nusse et al., 1984), and, similarly, *Wnt1* transgenic mice develop mammary tumors, suggesting a causative role for WNT1 in mammary tumorigenesis (Tsukamoto et al., 1988). Further studies demonstrated that WNT1 and other WNTs promoted the stabilization of free pools of β-catenin and the activation of β-catenin dependent transcription (Papkoff et al., 1996).

For example inherited inactivating mutations in adenomatous polyposis coli (*APC*), which is a negative regulator of β-catenin stability, are found in patients with familiar adenomatous polyposis, which can progress to colorectal carcinomas following concomitant activating mutations in *KRAS* and inactivating mutations in *TP53*. Both *APC* (90%) and *β-catenin* (10%) are also frequently mutated in colorectal cancers of non-familiar adenomatous polyposis patients (Segditsas and Tomlinson, 2006). Moreover overexpression of constitutively active β-catenin, or loss of APC function (both of which lead to hyperactivation of WNT-β-catenin signalling) can result in colorectal tumorigenesis in murine models (Morin et al., 1997).

It is now clear that WNTs modulate both β-catenin dependent (often referred to as “canonical”) WNT signaling, and β-catenin indipendent (often referred to as “non canonical”) WNT signaling pathways. In the canonical WNT signaling pathway, in the absence of WNT stimulation, a destruction complex which includes the APC, the glycogen synthase kinase 3β (GSK3β) the casein kinase Iα (CKIα) and AXIN, phosphorilates β-catenin, targeting it for ubiquitylation and proteasomal degradation. As a consequence, in the absence of WNTs, members of the TCF/LEF family of high-mobility-group transcription factors associate in a repressive complex with transducin-like enhancer protein (TLE) co-repressor proteins, which promote the recruitment of histone deacetylases (HDACs) to repress β-catenin target genes. The binding of WNT ligands, such as WNT3A and WNT1, to the frizzled (FZD) receptor and LRP5 or LRP6 co-receptors transduces a signal across the plasma membrane that results in the activation of the Dishevelled (DVL) protein. Activated DVL inhibits the destruction complex, resulting in the accumulation of β-catenin in the cytoplasm and its translocation into the nucleus where it can act as a co-activator for TCF/LEF-mediated transcription (Angers and Moon, 2009).

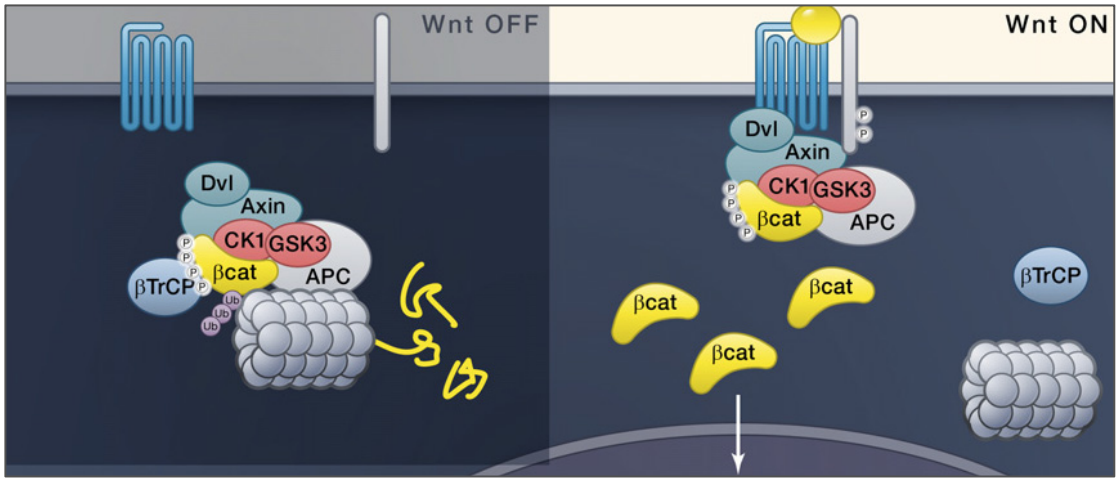

Fig. 2: The Wnt/β catenin signalling. In the absence of Wnt ligands, the destruction complex resides in the cytoplasm, where it binds and phosphorylates β-catenin, which is then ubiquitinated by β-TrCP. The proteasome recycles the complex by degrading β-catenin. Wnt induces the association of the intact complex with phosphorylated LRP. After binding to LRP, the destruction complex still captures and phosphorylates β-catenin, but ubiquitination by β-TrCP is blocked. Newly synthesized β-catenin accumulates (Clevers and Nusse, 2012).

On the contrary, some WNT ligands, such as WNT5A and WNT11, fail to stabilize β-catenin and regulate signalling pathways that are associated with cell polarity and migration. β-catenin indipendent WNT pathways are also initiated by the binding of these WNT ligands to frizzled (FZD) receptors in order to activate Dishevelled (DVL), which can then activate a variety of downstream effectors. Disruption of FZD receptors in fact, results in planar cell polarity defects (Habas et al., 2003). Moreover WNT5A and WNT11 can also induce a calcium flux, which results in the activation of various signalling pathways, such as protein kinase C (PKC), calcium/calmodulin-dependent protein kinase II (CAMKII) and JUN N-terminal kinase (JNK) (Kohn and Moon, 2005).
The precise mechanism by which a WNT stimulates β-catenin dependent versus β-catenin independent cellular responses are not fully elucidated, but probably involve the stimulation of distinct WNT receptors. Reported transmembrane WNT receptors include the ten members of the FZD family of G-protein-coupled receptors (GPCRs), as well as the receptor tyrosine kinase (RTKs) ROR1 and ROR2 and the RTK-like protein RYK (Angers and Moon, 2009; Kohn and Moon, 2005). All these findings suggest that WNT-β-catenin signalling, as well as β-catenin indipendent WNT signalling, can either promote or inhibit cancer progression in a context-dependent manner.

2.3 The role of angiogenesis in tumor progression

Blood vessels are a complex network of tubes that transport oxygenated blood and nutrients throughout the body.

The most essential component of blood vessels is the endothelial cell (EC). All vessels consist of a monolayer of EC, called the endothelium, arranged in a mosaic pattern around a central lumen through which blood can flow. Outside the endothelium there is an extracellular lining called the basement membrane (BM), separting the EC from the surrounding connective tissue. The connective tissue is composed of protein fibres, mainly laminin and collagen, and may contain peri-endothelial supporting cells. BM proteins has multiple binding sites for cell adhesion molecules and many motifs serve as ligands for cell surface receptors. When cell surface receptors bind to BM proteins, the consequent intracellular signaling pofoundly affects cell behavior. BM components guide cellular differentation and inhibit or promote cell proliferation and migration (LeBleu et al., 2007). Cell-cell contacts, mediated by cadherins, and cell-BM contacts, mediated by integrins, are essential and their loss can lead to local destabilization of the endothelium and EC apoptosis (Lobov et al., 2002). Pericytes are peri-endothelial cells present in the microvasculature. Capillaries infact, consist only of the endothelium, BM and pericytes. Larger vessels instead, have a thick wall of smooth muscle cells outside the BM lining. Both pericytes and smooth muscle cells play a particularly important role in maintaining blood vessels in the stable-state and are involved in the regulation of blood flow (Hirschi and D'Amore, 1996; Rucker et al., 2000). A layer of connective tissue, known as the stroma, separates the vessel from the functional tissue of an organ, the parenchyma. The stroma is principally composed of fibroblasts, which secrete a matrix of extracellular protein fibres, such as collagen and fibronectin (Raza et al., 2010).

Blood vessels' formation is tightly regulated and is one of the earliest events in organogenesis. It occurs through two processes: vasculogenesis and angiogenesis. Vasculogenesis is *de novo* formation of blood vessels from angioblasts. It occurs in the extraembryonic and intraembryonic tissues of the embryos. Vasculogenesis is a dynamic process that involves cell-cell and cell-ECM interactions directed spatially and temporally by growth factors and morphogens. This process includes the differentation of mesodermal stem cells into angioblasts which migrate under growth factors stimulation to form blood islands and give rise to ECs (Ema and Rossant, 2003).

In contrast angiogenesis is the formation of new vessels from the pre-existing vasculature. This complex process requires the interaction between different cell types, the ECM and several cytokines and growth factors. During angiogenesis, the capillary plexus is remodelled by sprouting, microvascular growth and finally by fusion into a mature and functional vascular bed. Angiogenesis also includes vessel penetration into avascular regions of the tissue and is crucially dependent on the correct interaction between pericytes, EC and stromal cells, such as fibroblasts, and their association with the ECM and vascular BM (Yancopoulos et al., 2000).

In adults angiogenesis takes place only in particular occasions including inflammation, wound healing, endometrial re-growth during the menstrual cycle, and ischemia to maintein the physiological homeostasis and tissue integrity (Carmeliet, 2003).
An effective angiogenesis requires multiple, sequential steps:

1) At first the expression of pro-angiogenic factors and mitogens for ECs, that guides ECs into avascular areas (Ferrara et al., 2003)

2) The second step is the activation of the membrane type 1 matrix metalloproteinase (MT1-MMP). It plays a majour role in ECM remodelling, by degrading several ECM components, including collagens, fibronectin, laminin and proteoglycans. Moreover the MT1-MMP induces the activation of the pro-MMP9 (Sato et al., 1996). As a result, ECs loose their contact with BM laminin and are exposed to interstitial collagen. This change triggers signalling cascades in ECs that lead to cytoskeleton reorganization and sprouting morphogenesis (Rhodes and Simons, 2007). As a consequence, these cells become motile and align into chords

3) Subsequently, once EC proliferation is arrested, pericytes and vascular smooth muscle cells are recruited to nascent vessels. This provides stabilization, remodelling and maturation signals (Folkman, 2006)

4) The contact between ECs and pericytes induces the expression of tissue inhibitor of metalloproteinase 2 (TIMP2) by ECs and TIMP3 by pericytes and the ECs' proteolytic phenotype is turned off (Saunders et al., 2006)

5) A further step is the tight sealing of the vessel lumen by adjacent ECs that are held toghether by tight junctions and adherent junctions (Bazzoni and Dejana, 2004). A BM is then produced by ECs in cooperation with surrounding cells to provide structural support and maintain EC quiescence (LeBleu et al., 2007)

6) The consequent step is the pruning of excess or unneeded vessels for optimal perfusion occuring during the maturation of new capillaries. This process is thought to be an adjustment to the oxygen surplus, while the surrounding ECM exerts mechanical strain that provides traction and orientation for angiogenic microvessels (Krishnan et al., 2008)

7) Finally, once tube formation is complete, the blood flow to the newly vascularized area induces an increase of the local oxygen levels, resulting in a decrease of the VEGF levels and the end of angiogenic process (Ferrara et al., 2003).

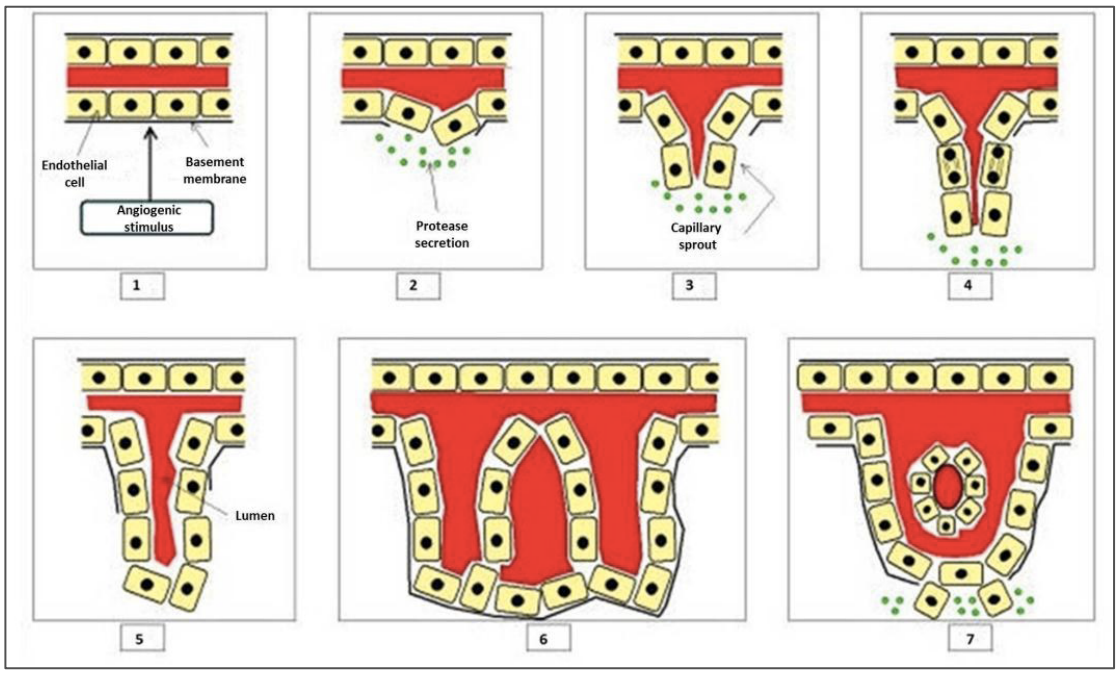

Fig. 3 Angiogenesis is a complex dynamic process. At least seven critical steps have so far been identified to occur during this tightly regulated process.

However angiogenesis not only occurs in physiological conditions but also in a broad range of human diseases. Aberrant angiogenesis is associated with an excess of growth-promoting signals and a lack of sufficient cues to spatially and temporally coordinate vessel growth, remodelling, maturation and stabilization. During pathological conditions, such as tumorigenesis, the angiogenic cascade is persistent and unresolved, fuelled in part by tumor-secreted factors and tumor hypoxia (Chung et al., 2010).

At the beginner tumors are avascular masses of host-derived cells that proliferate without controlling their growth (Papetti and Herman, 2002). An avascular tumor is reliant on passive diffusion for the supply of the required oxygen and nutrients and the removal of its waste products. This imposes a limiting size of approximately 2 mm to which it can grow (Folkman, 1971). Hypoxic tumor cells produce growth factors, but also some endogenous inhibitors of angiogenesis such as transforming growth factor-beta (TGF-β) (Bikfalvi, 1995). Macrophages, which congregate in the region of the abnormal growth, respond to the presence of the tumor by producing both pro and anti-angiogenic substances that diffuse through the tissue (Bingle et al., 2002). At the beginning, the inhibitors outweight the growth factors and the ECs remain quiescent. However, if the tumor produces enough growth factors and/or suppresses the expression of inhibitors, it may succeed in flipping the "angiogenic switch" and promote angiogenesis (Hanahan and Folkman, 1996). ECs from capillaries adjacent to the tumor become activated: they loose the tight

contacts with neighbouring cells (Papetti and Herman, 2002) and secrete proteases and proteolytic enzymes. These proteases first target the BM and allow the EC movement through the induced gaps into the ECM (Pepper, 2001). Following extravasation, the ECs continue to secrete proteolytic enzymes leading to ECM degradation. This creates a path along which the cells move and also allows the release of growth factors, that are normally sequestred by the matrix, thus augmenting the angiogenic signals (Hirschi and D'Amore, 1996). The ECs then form small sprouts which may initially take the form of solid strands of cells, but subsequently ECs form a central lumen, thereby creating the necessary structure for a new blood vessel (Pepper, 2001). However the vessels associated with solid tumors are characterized by a number of prominent abnormalities. These abnormalities have been hypothesized to have a significant impact on tumor growth, progression and response to various anticancer therapies. Among the structural and morphologic abnormalities there are the presence of excessively dilated blood vessels, vessels with areas containing absent or abnormal BM, vessels having extreme corkscrew-like tortuosities, a relative lack of supporting perivascular cellular elements such as pericytes, or abnormalities in the pericyte population and excessive vascular leakiness (Carmeliet, 2003). These aberrations can be quite variable within a solid tumor mass and such heterogeneity can also extend to the relative density of blood vessels, which can be quite high in certain areas and low in others (Cooney et al., 2006). Indeed blood flow and perfusion in tumors can be highly heterogeneous, with some areas being therefore deprived of oxygen and nutrients, leading to adjacent areas of elevated hypoxia. This may account for the slow growth of tumors in some reagions and a more rapid growth in others. In addition the marked leakiness/hyperpermeability of the tumor vasculature can lead to enhanced extravasation of high molecular weight plasma, proteins and fluid into the extracellular microenvironment within tumors. This can limit or retard the diffusion of certain drugs, especially monoclonal antibodies or vectors used for gene therapy, as well as immune effector cells from the blood through the interstitium of the tumors. Thus tumor blood vessels are necessary for progressive tumor growth and metastasis, but also limit the efficacy of anticancer drugs and treatments, including chemotherapy and radiation therapy.

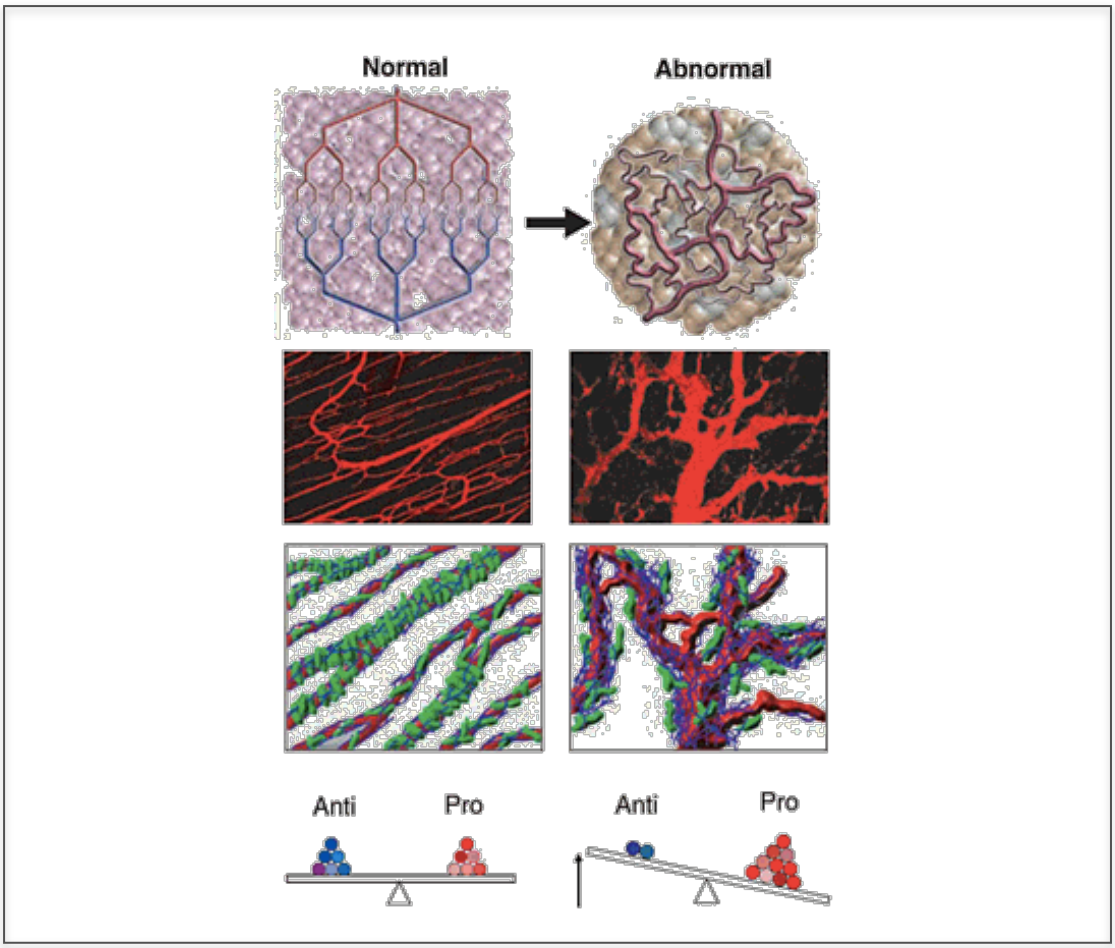

Fig. 4 Tumor angiogenesis. Unlike healthy blood vessels, tumor vessels consist of disorganized, leaky and primitive vascular networks, which display abnormal functions (Cooney et al., 2006)

2.4 Epidermal growth factor receptor in tumor angiogenesis

The epidermal growth factor receptor family comprises four structurally-related receptor tyrosine kinases: HER1 (EGFR, *erb*B1), HER2 (*neu*, *erb*B2), HER3 (*erb*B3) and HER4 (*erb*B4). All four HER receptors are composed of an extracellular reagion that consists of glycosylated domains; a transmembrane domain that contains a single hydrophobic anchor sequence, and an intracellular region that contains the catalytic tyrosine kinase domain, which generates and regulates intracellular signaling. EGFR was the first HER family member to be described and is one of the best characterized. EGFR is expressed by most normal cells, particularly those of epithelial origin, and in malignant tissues, but is not found in mature hematopoietic cells (Carpenter, 1987; Gullick, 1991). Known ligands for EGFR include epidermal growth factor (EGF), transforming growth factor (TGF)-α, amphiregulin, betacellulin, and epiregulin (Salomon et al., 1995). EGFR activation follows three basic steps: ligand binding, receptor dimerization (either EGFR homodimerization or heterodimerization with other HER family members), and activation of the receptor tyrosine kinase by way of

intramolecular phosphorylation. EGFR activation is followed by rapid endocytosis and degradation or recycling of the receptor and the ligand.
Activation of EGFR initiates or modifies intracellular signaling pathways that control normal cell growth and differentation (Yarden, 2001). Dysregulation or increased activity of EGFR-mediated signaling seems to confer a proliferative or malignant phenotype, possibly by alterating signaling pathways that are involved in cell cycle progression, proliferation, apoptosis, angiogenesis and metastasis. Many different solid tumors express EGFR, including breast, head and neck, colon, ovarian, nonsmall cell lung, pancreatic, bladder and glioblastoma tumors (Salomon et al., 1995).
One of the most interesting roles of EGFR lies in tumor angiogenesis. Angiogenic factors can be produced by tumor cells themselves and by other cell types, such as endothelial cells, fibroblasts, smooth muscle cells/pericytes, and infiltrating immune cells. These factors initiate the angiogenic process by activating ECs and inducing the angiogenic switch. Vascular endothelial growth factor (VEGF) has been identified as the major tumor angiogenesis factor that is involved in endothelial cell activation (Ferrara and Alitalo, 1999). Many other growth factors, such as interleukin 8 (IL-8), EGF and basic fibroblasts growth factor (bFGF) are proangiogenic. Conversely endogenous proteins such as thrombospondin, angiostatin, endostatin and tumstatin, endorepellin and MULTIMERIN2 inhibit angiogenesis (Fox et al., 1996; Bouma-ter Steege et al., 2001; Maeshima et al., 2002; Mongiat et al. 2003; Lorenzon et al., 2007; Lorenzon et al., 2012). Indeed the EGFR activates several signaling cascades in response to epidermal growth factor stimulation. One of these signaling events involves tyrosine phosphorylation of signal transducer and activator of transcription 3 (STAT3) (Xia et al., 2002) that subsequently induces the production of the pro angiogenic chemochine IL-8 (Gharavi et al., 2007).
An increased body of evidence suggests that the EGFR pathway is involved intimately in tumor angiogenesis in many tumor types. In addition to EGFR expression on tumor cells, ECs within tumors express EGFR (Kim et al., 2003). The EGFR ligands, EGF and TGF-α, exert renown proangiogenic functions (Fox et al., 1996). Expression of EGFR and TGF-α correlates with tumor microvessel density in invasive breast cancer (de Jong et al., 1998).
It is likely that the EGFR pathway modulates angiogenesis by way of upregulation of VEGF or other key mediators in the angiogenic process (Goldman et al., 1993; O-Charoenrat et al., 2002). EGFR levels strongly correlate with the expression of MMPs and VEGF in many cases of head and neck squamous cell carcinoma (O-Charoenrat et al., 2002). These data suggest that EGFR may play a role in the progression of head and neck squamous cell carcinoma by way of up-regulation of MMPs or VEGF. The most convincing evidence of the involvement of EGFR in angiogenesis, is provided by the antiangiogenic effects of agents that block EGFR in preclinical models. For example Cetuximab is a human:murine chimeric anti-EGFR IgG_1 that has demonstrated antitumor activity in EGFR-

expressing tumor cells in vitro and in vivo (Prewett et al., 1998). Treatment of a variety of EGFR-exprissing tumor cells with cetuximab resulted in down-regulation of one or more angiogenic mediators, including VEGF, IL-8 and bFGF, *in vitro* and *in vivo* (Bruns et al., 2000).

2.5 The EMILIN protein family

EMILINs are a family of ECM glycoproteins whose distinguishing feature is the presence of a cystein-rich EMI domain at the N-terminus. In addition most of the members of this family also display a gC1q-like domain at the C-terminus (Doliana et al., 2000; Mongiat et al., 2000). These proteins can be divided into three groups:

- The first group is characterized by the presence of the EMI domain at the N-terminus, a coiled-coil region and a gC1q domain at the C-terminus, and includes MULTIMERIN1 (Hayward et al., 1991), MULTIMERIN2 (Christian et al., 2001), EMILIN1 (Doliana et al., 2000), and EMILIN2 (Doliana et al., 2001).
- The second group includes only one gene named EMILIN3. The protein displays a structure similar to that of the first group, except for the lack of the gC1q domain (Leimeister et al., 2002). EMILIN3 exhibits a different expression pattern compared to other EMILIN/MULTIMERIN proteins and is able to function as an extracellular regulator of TGF-β activity (Schiavinato et al., 2012).
- The third cluster includes two genes, Emu1 and Emu2, which share only the presence of EMI domain at N-terminus with the previous group but display a completely different structure compared to the other members, given that most of their sequence is collagenous, (Leimeister et al., 2002).

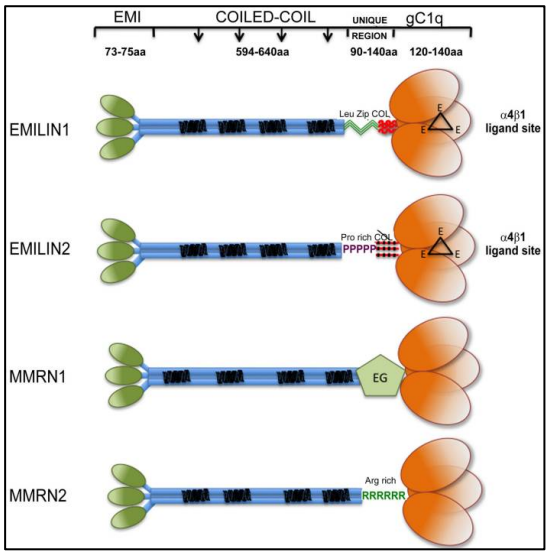

Fig. 5 Graphical view of EMILIN/Multimerin family members. (EMI) EMI domain; Coiled-coil region; (C1q) gC1q-like domain; (PR) prolin-rich domain; (RR) arginine-rich domain; (EG) region with partial similarity with EGF domain (Colombatti A. et al., 2011).

2.5.1 MULTIMERIN1

MULTIMERIN1 (MMRN1) is a soluble S-S linked homopolymer stored in platelets, megakaryocytes, and ECs and deposited in the Extracellular Matrix (ECM) (Hayward, 1997; Adam et al., 2005). It plays an important homeostatic control in platelets aggregation, it binds to collagen and it is able to enhance von Willebrand factor-dependent platelet adhesion to collagen, thus supporting thrombus formation. MMRN1 infact supports the adhesion of platelets, neutrophils and ECs via integrin $\alpha_v\beta_3$ and $\alpha_{IIb}\beta_3$ (Adam et al., 2005). Moreover MMRN1 has a high affinity for factor V (Jeimy et al., 2008) and this facilitates the co-storage in platelet α-granules. When MMRN1 is released from platelets during platelet activation, it regulates thrombin formation limiting thrombus formation. Unfortunately all these multiple functions have not been assigned to any of the domains of MMRN1 apart from cell adhesion that depends on an RGD sequence at the N-terminus (Adam F. et al., 2005).

2.5.2 MULTIMERIN2

MULTIMERIN2 (MMRN2) also known as EndoGlyx-1, was identified during a screeneng for new antigenic markers of the vascular endothelium, using a monoclonal antibody raised against the human umbilical vein EC (Sanz-Moncasi et al., 1994). MMRN2 is characterized by a short cluster of charged aminoacids, located between the coiled-coil region and the C1q-like domain. In an extensive immunohistochemical survey of normal human fetal and adult tissues as well as in human cancer tissues, MMRN2 was found to be expressed only at the blood vessel endothelium level. This includes capillaries, veins, arterioles and molecular arteries, but no immunoreactivity was seen in the sinusoidal ECs of the spleen and liver. In neoplastic tissues MMRN2 is depositated along tumor capillaries and in the “hot spots” of neoangiogenesis (Sanz-Moncasi et al., 1994). Moreover it was recently published by our group a paper in which we demonstrated that MMRN2 is a crucial player in the regulation of EC function, neo-angiogenesis and hence tumor growth. In particular we demonstrated that VEGF may be sequestered by MMRN2 and be less available for the engagement to the receptors (Lorenzon et al., 2012).

2.5.3 EMILIN1

EMILIN1 is the archetype molecule of the family and it was originally identified during the isolation of elastic-specific glycoproteins. EMILIN1 is a 115 KDa glycoprotein specifically localized at the interface between the amorphous

elastin surface and the microfibrils, hence the acronym (Elastin Microfibril Interface Located proteIN) (Bressan et al., 1993). EMILIN1 is highly expressed at the level of large blood vessel wall and in the connective tissue of a wide array of organs (Colombatti et al., 1985). During mouse development EMILIN1 mRNA is expressed along the blood vessels and perineural mesenchyme (Braghetta et al., 2002). Moreover intense labeling is identified in the mesenchymal component of many organs including lung and liver and in different mesenchymal condensations such as limb bud and branchial arches. During late gestation times EMILIN1 is widely distributed in the interstitial connective tissue and in smooth muscle cell rich tissues. After birth, the EMILIN1 mRNA expression levels decline with the age increase. EMILIN1 has different functions:

- As an ECM component, it has adhesive and migratory properties for different cell types. It is a ligand for the $\alpha_4\beta_1$ integrin and the interaction occurs through the gC1q domain (Spessotto et al., 2003).
- It binds the immature form of the pro-TGF-β via the EMI domain, thus preventing TGF-β maturation by furin-convertases. As a consequence EMILIN1-deficient animals display an hypertensive phenotype likely due to a decrease diameter of the arteries which is significantly narrower in EMILIN1-null mice compared to the wild type mice (Raman and Cobb, 2006).
- EMILIN1 is also highly expressed along the lymphatic vessels and it was demonstrated to be an important costituent regulating the structure and function of lymphatic vessels, as well as limphangiogenesis (Danussi et al., 2008). In fact EMILIN1 deficency results in hyperplasia and enlargement of the superficial and visceral lymphatic vessels which often display an irregular pattern. Moreover EMILIN1 deficency leads to a significant reduction of anchoring filaments, and this correlates with the functional defects observed, such as mild lymphedema, an enhanced lymph leakage and a highly significant decrease of lymph drainage. EMILIN1-deficient mice also develop larger lymphangiomas if compared to wild type mice (Danussi et al., 2012).

In conclusion EMILIN1 deficency causes skin and lymphatic vessel hyperplasia and structural anomalies in lymphatic vasculature. An EMILIN1-negative microenvironment promotes tumor cell proliferation as well as dissemination to lymph nodes (Danussi et al., 2012).

2.5.4 EMILIN2

EMILIN2 was cloned following a two-yeast hybrid screening using the globular C1q domain of EMILIN1 as a bait. The analysis of the primary structure revealed that this protein shares a similar domain organization pattern with EMILIN1 except for a proline-rich (41%) segment of 56 residues between the potential coiled-coil region and the collagenous stalk which is distinctive of EMILIN2. The

mRNA expression of EMILIN2 is more restricted compared to that of EMILIN1 both in first steps of development and in the adult. Highest levels of the protein are present in fetal heart and adult lung of mice, whereas differently from EMILIN1, adult aorta, small intestine and appendix show very low expression (Doliana et al., 2001). In embryos EMILIN2 expression is more restricted compared to that of EMILIN1; early expression includes somites, neural tube and mesenchyme of branchial arches, limb buds, invertebral disks and perineural tissue. Weak staining is also found in mesenchymal cells of most organs, including lung, liver, intestine and bladder at the beginning of organogenesis. The strongest EMILIN2 expression is detected in the heart, starting at E8.5 and reaching highest levels at E11.5. Labelling is restricted to the myocardium, while the endocardium is negative. In this organ EMILIN2 mRNA expression is stable up to E11.5 and then fades, becoming undetectable at E14.5. Unlike other members of the family, staining for EMILIN2 is found in the central nervous system where labelling is still present at E16.5. In adult tissues EMILIN2 mRNA expression is mostly evident in spleen and uterus while it is weak in kidney and gut (Braghetta et al., 2002; Leimeister et al., 2002). Moreover EMILIN2 was shown to be one of the majour basilar membrane components in the coclea (Amma et al., 2003). A study aimed at investigating immune-specific genes from a compendium of microarray expression data among different myeloid cells revealed high EMILIN2 mRNA levels in monocytes, macrophages and dendritic cells (Abbas et al., 2006).

At the functional level EMILIN2 was found to significatly impair tumor growth inducing tumor cell apoptotic death. EMILIN2 was demonstrated to adopt a totally different mechanism from other ECM proteins that promote cell death; in fact it bears the unique property to directly interact with and activate death receptors, in particulat DR4. The activation of the extrinsic apoptotic pathway leads to a dramatic decrease of tumor cell viability and to anti-tumorigenic properties as demonstrated by *in vivo* and *in vitro* studies (Mongiat et al., 2007). Followinging intratumoral treatemnts with E2 to induce tumor cell death an unexpected function of EMILIN2 was found. It infact stimulated blood vessel development (Mongiat et al., 2010). This pro-angiogenic property was also confirmed by Bronisz and his group. In particular blocking EMILIN2 expression in fibroblasts using a specific blocking antibody or siRNA, reduces EC proliferation (Bronisz et al., 2012).

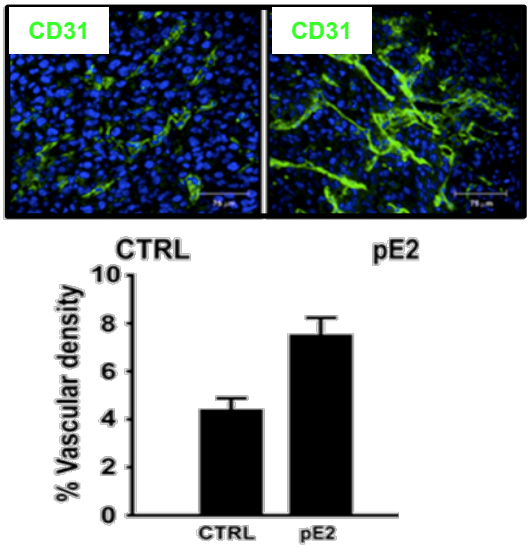

Fig. 6 EMILIN2 in vivo pro-angiogenic effect. EMILIN2 treated tumors displayed an increased angiogenesis. CD31 staining is reported in green (Mongiat et al., 2010).

EMILIN2 represents a negative regulator of tumor development: the gene is frequently methylated in breast, lung and colorectal tumors and this suppression correlates with poor clinical outcome and increased limph node metastasis in breast cancer patients (Hill et al., 2010). Moreover we have recently found that EMILIN2 exerts a tumor suppressive effect also by attenuating the Wnt signaling pathway in brest cancer cells. The function of EMILIN2 as a tumor supressive protein impairing Wnt signalling activation and the discovery of the molecular mechanisms responsible for the EMILIN2 pro-angiogenic properties were the subject of my PhD program and will be further explicated in this thesis.

3 AIMS

EMILIN2 is an extracellular matrix protein that exerts contradictory effects within the tumor microenvironment: it induces apoptosis in a number of tumor cells, but it also enhances tumor neo-angiogenesis.
The down-regulation of EMILIN2 expression by gene methylation in breast cancer suggested that EMILIN2 could affect the progression of this type of tumor, even if breast cancer cells were not sensible to the pro-apoptotic effect of the protein.

The first aim of this work was to identify the mechanism by which EMILIN2 attenuates breast tumor cell viability.
Based on sequence homology with the Cysteine Rich Domain (CRD) of the Frizzled receptors, we hypothesized that EMILIN2 could affect Wnt signaling activation and we focused our attention on the molecular mechanism by which the protein inhibited the Wnt signaling. EMILIN2 markedly reduced β-catenin activation in MDA-MB-231 cells, thus we sought to verify if EMILIN2 attenuated the Wnt1-induced cell proliferation. Finally we verified whether EMILIN2 could also impair Wnt1-driven breast tumor cell growth *in vivo*.

The second aim of my project was to dissect the molecular mechanisms by which EMILIN2 regulates the angiogenic processes, that are known to profoundly affect tumor growth and development. Since EMILIN2 is expressed by fibroblasts, as recently demonstrated in literature, we decided to challenge the endothelial cells (ECs) with conditioned media from Normal Human Dermal Fibroblasts (NHDF) over-expressing EMILIN2 and to assess the ECs' behavioral changes. The angiogenic potential of EMILIN2 was verified both *in vitro*, *ex vivo* and *in vivo* and the molecular mechanisms assessed in these contexts. Finally we show preliminary data of the role of EMILIN2 in tumor angiogenesis .

4 RESULTS

4.1 EMILIN2 affects breast cancer cell behaviour

Data from the literature indicate that the EMILIN2 gene is methylated in breast cancer and as a consequence the expression of this molecule is down-regulated in this type and other type of tumors (Hill et al. 2010). This finding suggests that EMILIN2 could affect breast cancer development.
To address this question we first over-expressed EMILIN2 in MDA-MB-231, which do not secrete this molecule, and we observed a reduced cell viability in different high-expressing clones (**Fig. 1A** and **B**). In addition MDA-MB-231 cells over-expressing EMILIN2 migrated significantly less (**Fig. 1C**) and displayed fewer filopodia protrusions (**Fig. 1D**).

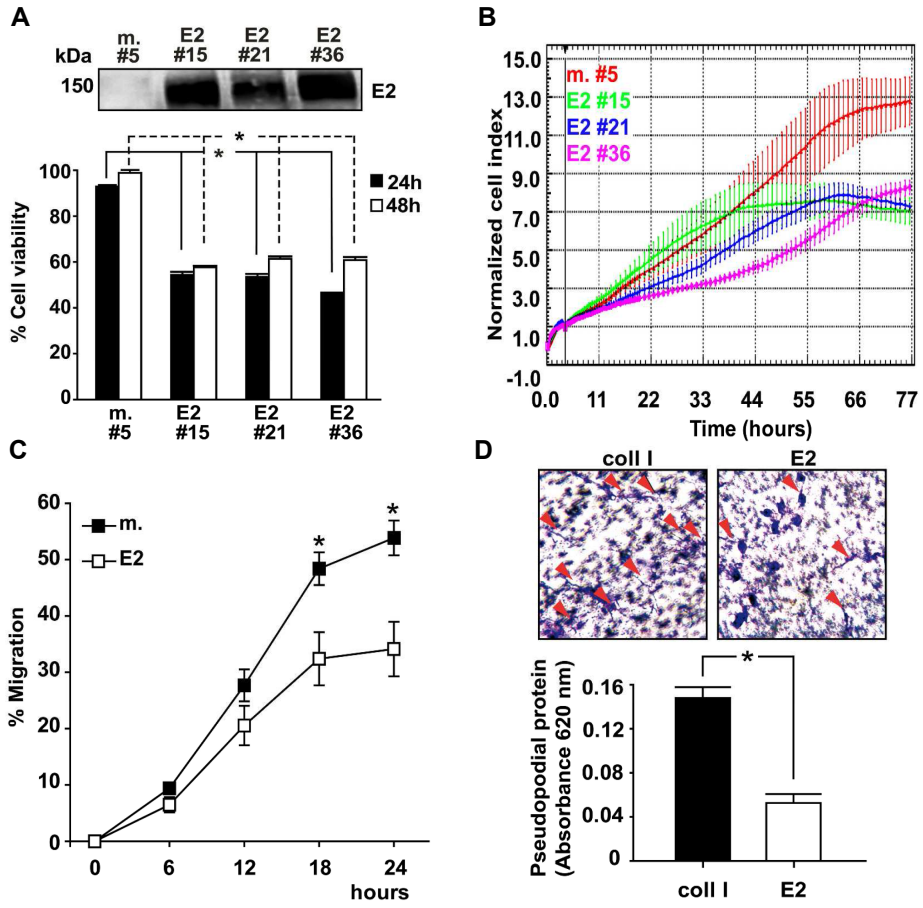

Fig. 1 EMILIN2 reduces MDA-MB-231 cell viability and motility. (a) Top panel: Western blotting analysis of the conditioned media from MDA-MB-231 cells stably transfected with the pcDNA-EMILIN2 construct (clones #15, 21, and 36). Mock-transfected clone 5 (m. #5) was used as a control; bottom: graph reporting the % of cell viability of the different clones at 24 and 48 hours after seeding as assessed by MTT assay. (b) Time course analysis of cell proliferation as assessed through the xCELLigence instrument. c) Graph reporting the migration of EMILIN2 and mock transfected MDA-MB-231 cells as assessed by transwell migration assay. (d) relative quantification (bottom panel) and representative images (top panel) of the pseudopodial emissions (indicated by arrows) by MDA-MB-231 cells treated with type I collagen (coll I) or EMILIN2 (E2).

4.2 EMILIN2 affects the Wnt signalling pathway through the interaction with Wnt ligands

During the search for new EMILIN2 molecular partners that could account for inhibition of breast cancer cell proliferation, we noticed that the cysteine-rich EMI domain shared 42% homology with the CRD domains of the Frizzeld receptors. The highest homology involved a group of amino acid residues indispensabile for the interaction with Wnt ligands (**Fig. 2**). These observations led to the hypothesis that EMILIN2 could be an extracellular regulator of the Wnt signaling pathway.

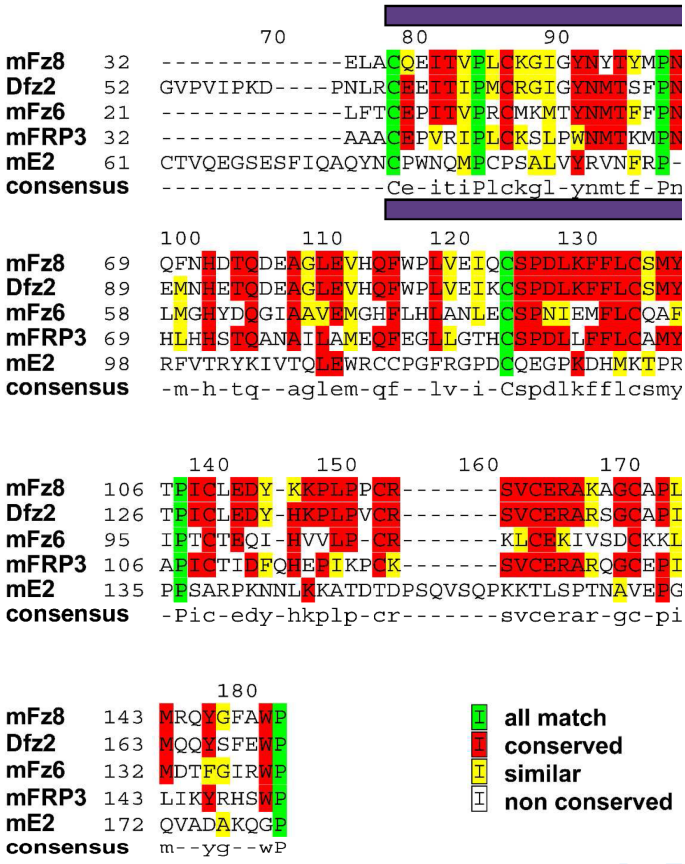

Fig. 2 The cystein-rich EMI domain of EMILIN2 shares homology with the Frizzled Receptors and with the secreted Frizzled Related Proteins. Sequence alignment of mouse Frizzled 8 (mFz8), Frizzled 6 (mFz6), Frizzled Related Protein 3 (mFRP3), EMILIN2 (mE2) and Drosophila Frizzled 2 (DFz2). The region responsible for the interaction with Wnt ligands is highlighted by violet lines.

Considering this homology we hypothesized that EMILIN2 and Wnt ligands could represent new molecular partners and that the interaction required the EMI domain. Indeed we performed a solid-phase binding assay and the results

indicated that EMILIN2 and Wnt1 interacted (**Fig. 3A**). The binding was confirmed by both His-(EMILIN2) and Flag-(WNT1) pull down experiments (**Fig. 3B**). Moreover, as expected, the EMI domain of EMILIN2 was necessary for the interaction, since there was no binding when the Δ5 EMILIN2 deletion mutant (Δ5E2) lacking this domain was used (**Fig. 3C**and **D**).

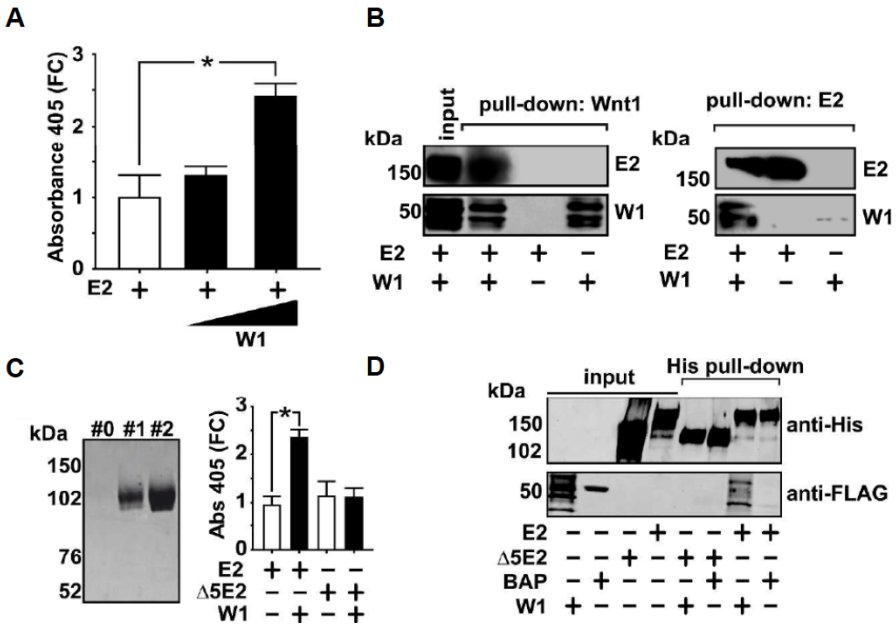

Fig. 3 EMILIN2 binds to Wnt1. (A) Graph representing the results from a solid-phase binding assay following coating of ELISA plates with EMILIN2 (E2) and incubation with 30 or 100 ng of purified FLAG-tagged Wnt1. (B) Western blotting analysis of the Histidine and FLAG pull-down experiment following incubation of His-tagged EMILIN2 (E2) with cell lysates from MDA-MB-231 cells transfected with a FLAG-tagged Wnt1 construct (Wnt1 +) or empty vector (Wnt1 -). (C) Left: image representing the SDS-PAGE analysis following Comassie staining of different fractions of the His-tagged recombinant Δ5E2 deletion mutant purification. Right: graph representing the results from a solid-phase binding assay following coating of ELISA plates with EMILIN2 (E2) or the Δ5E2 deletion mutant and incubation with 100ng of purified FLAG-tagged Wnt1. The binding is expressed as absorbance fold change (FC) at 405 nm. (D) Western blotting analysis of the Histidine and FLAG pull down experiment following incubation of the His-tagged EMILIN2 deletion mutant (Δ5E2) with cell lysates from MDA-MB-231 cells transfected with a FLAG-tagged Wnt1 construct (W1). His-tagged EMILIN2 and FLAG-tagged BAP were used as a positive and negative controls, respectively.

We then wandered whether this interaction affected Wnt signaling. To address this question we challenged Fz8-transfected E293 cells with recombinant EMILIN2. Type I collagen and DKK1 were used as negative and positive control, respectively. First we co-transfected E293 cells with a murin pcDNA-Wnt1 construct (W1) and increasing amounts of a murin pcDNA-EMILIN2 (E2) construct and the TOPflah reporter revealed a decreased activity of β-catenin

when EMILIN2 was ectopically expressed (**Fig. 4A**). Next, we co-transfected E293 cells with the murin pcDNA-Wnt1 construct (W1) and/or the pcDNA Frizzled 8 construct (Fz8) and we treated the cells with collagen I, EMILIN2 or with the Δ5E2 deletion mutant. Also in this case EMILIN2 but not the Δ5E2 deletion mutant , decreased the activity of β-catenin (**Fig. 4B**).

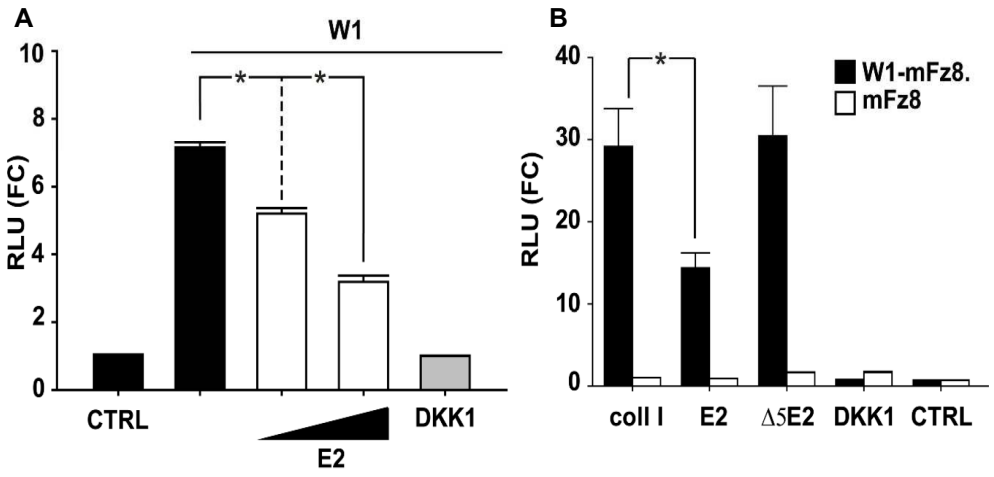

Fig. 4 EMILIN2 affects Wnt signalling. (A) Graph representing the analysis of β-catenin activity as assessed by TOPflash analysis. E293 cells were co-transfected with murin pcDNA-Wnt1 (W1), 50ng or 100ng of murin pcDNA-EMILIN2(E2), pCS2-DKK1 (DKK1) as a control and the reporters..,,. (B) Representative graph of the analysis of β-catenin activity. E293 cells were co-transfected with murine pcDNA-Wnt1 and/or pcDNA-Frizzled-8 (Fz8) and pCS2-DKK1 (DKK1) as a control. Cells were then treated with equimolar amounts of type I collagen (coll I), EMILIN2 (E2) or the Δ5 EMILIN2 deletion mutant (Δ5E2).

4.3 The effect of EMILIN2 on MDA-MB-231 cells in terms of proliferation and motility is Wnt dependent

We next verified if the inhibition of Wnt signalling occured also in breast cancer cells. To assess if EMILIN2 was able to attenuate the Wnt-driven LRP6 and β-catenin activation, we generated Wnt1 over-expressing MDA-MB-231 stable clones. As expected EMILIN2 was able to impair the activation of β-catenin and LRP6, as well as the cell viability, as shown in **Fig. 5A** and **B,** respectively.

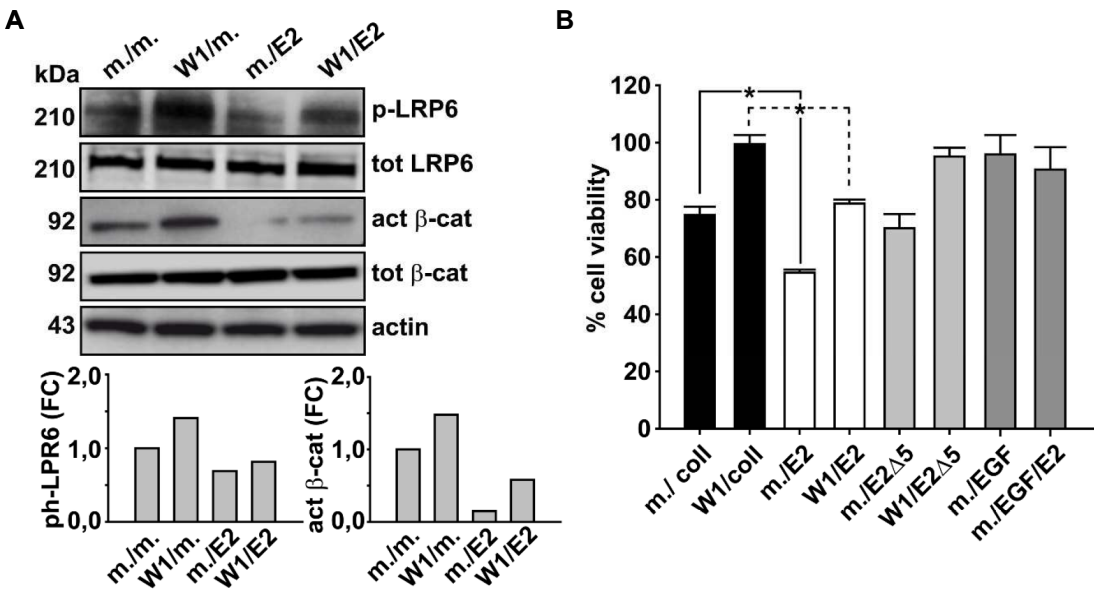

Fig. 5 EMILIN2 inhibits the viability of MDA-MB-231 cells affecting the Wnt signaling. (A) On top: Western blotting analysis of β-catenin (actβ-cat) and LRP6 (p-LRP6) activation in MDA-MB-231 cells transfected with empty (m.), Wnt1 (W1) or EMILIN2 (E2)pcDNA vectors. Bottom: quantification of the bands fold change (FC). (B) Graph representing the results of the MTT assay of MDA-MB-231 cells co-transfected with empty (m.), or Wnt1 (W1) vectors and treated with collagen type I (coll I), EMILIN2 or the EMILIN2 deletion mutant (Δ5E2).

We next verified whether EMILIN2 could affect the Wnt-driven motility of breast cancer cells. To this end we performed a Matrigel^{MT} evasion assay using MDA-MB-231 cells transfected with empty (m.) or Wnt1 pCMV (W1) constructs and we treated them with equimolar amounts of type I collagen (coll I) or EMILIN2 (E2). We observed that EMILIN2 significantly and specifically reduced the Wnt1-induced evasion of the cells from the Matrigel. Instead, MDA-MB-231 cells challenged with EGF were not affected by EMILIN2 treatment (**Fig. 6**).

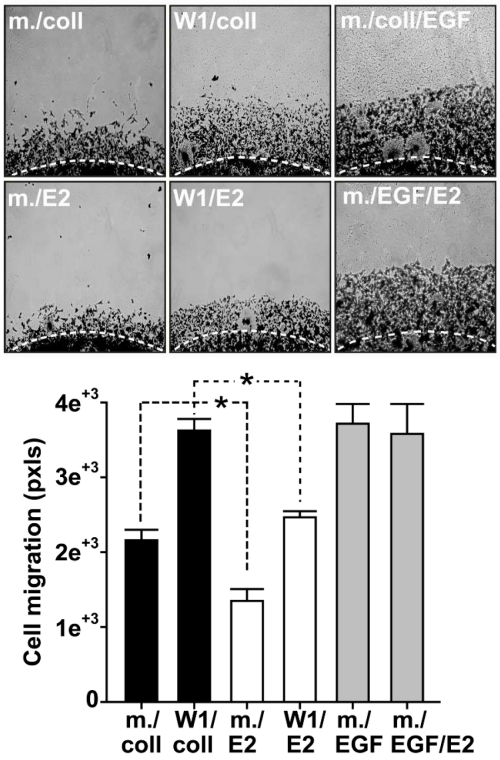

Fig.6 EMILIN2 reduces the Wnt-driven breast cancer cell migration. Top: representative images of the Matrigel evasion assay performed using MDA-MB-231 cells transfected with the empty (m.) or Wnt1 pCMV (W1) constructs. The cells were then treated with equimolar amounts of type I collagen (coll I) or EMILIN2 (E2). Cells treated with EGF were used as a control.

4.4 EMILIN2 inhibits the Tumorigenic potential of MDA-MB-231 in vivo impairing the Wnt signaling

The findings that EMILIN2 inhibited breast cancer cell proliferation and motility, prompted us to study the potential anti-tumorigenic effect of EMILIN2 *in vivo*. We first analyzed the capacity of MDA-MB-231 cells to form colonies when embedded in agarose gel. As expected, EMILIN2 transfected MDA-MB-231 cells developed significantly fewer and smaller colonies compared to the control (**Fig. 7A**). Moreover we also analyzed the colony number and size from soft agar colony assay using Wnt1 over-expressing cells treated with conditioned media containing or not EMILIN2. As shown in **Fig.7B**, we observed that the effect induced by EMILIN2 in mock cells was striking also with Wnt1 over-expressing cells.

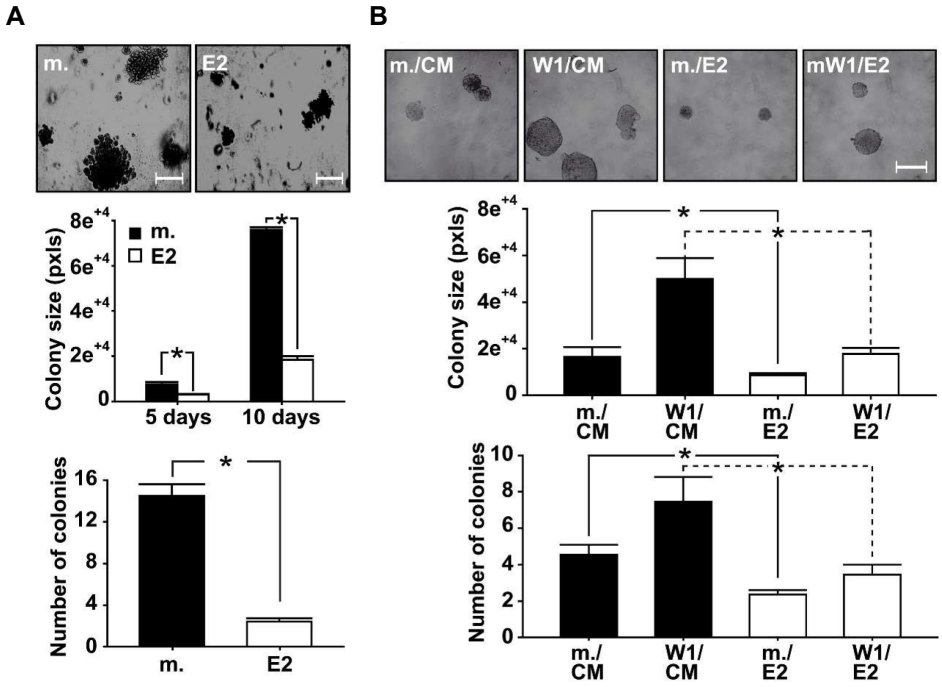

Fig. 7 EMILIN2 reduces clonogenicity. (A) Representative images (top) and quantification of the colony size (middle) and colony number (bottom) of soft agar assays using MDA-MB-231 cells transfected with the empty (m.) or EMILIN2 (E2) pcDNA vectors. (B) Representative images (top) and quantification of the colony size (middle) and colony number (bottom) from soft agar assays using MDA-MB-231 cells transfected with the empty (m.) or Wnt1 (W1) pCMV vectors and treated with conditioned media containing or not EMILIN2 (E2 and CM respectively).

We next verified the anti-tumorigenic potential of EMILIN2 *in vivo*. To this end we injected orthotopically transduced EMILIN2 MDA-MB-231 cells in nude mice and, as expected, we observed that the over-expression of EMILIN2 led to the formation of smaller tumors compared with the control (**Fig. 8A**). The smaller size of the EMILIN2 over-expressing tumors was not due to an activation of apoptosis as shown in **Fig. 8B**.

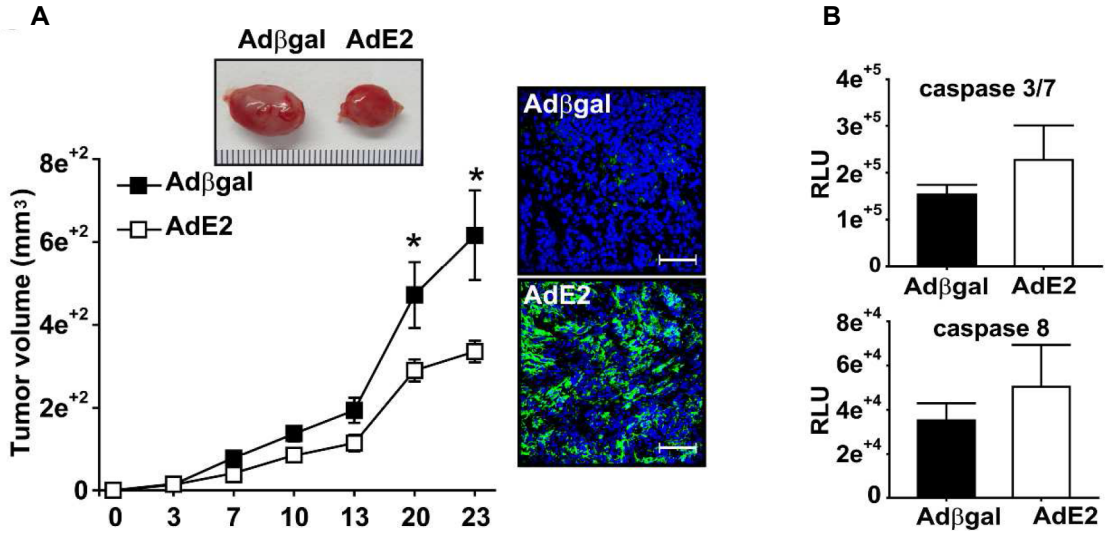

Fig. 8 EMILIN2 reduces tumor growth in vivo. (A)Representative images (top) and graph representing the tumor curves (bottom) following orthotopic injection of MDA-MB-231 cells transduced with the β-galactosidase (Adβgal) or EMILIN2 (AdE2) adenoviral constructs in nude mice. Right panel, immonofluorescence analysis of the intra-tumoral deposition of EMILIN2 by the transduced tumor cells. (B) Graph representing the analysis of the active caspase 3/7 and caspase 8 in tumors from Adβgal and AdE2 transduced cells as assessed with the Caspase-Glo assays.

To assess whether the smaller size of the EMILIN2 over-expressing tumors was due to an inhibition of the Wnt signaling induced by this molecule, we analyzed the levels of the active β-catenin in the tumor samples. In accordance with our in vitro results and as shown in **Fig. 9A** and **B**, the tumors from EMILIN2 over-expressing cells displayed a significant decrease of active β-catenin.

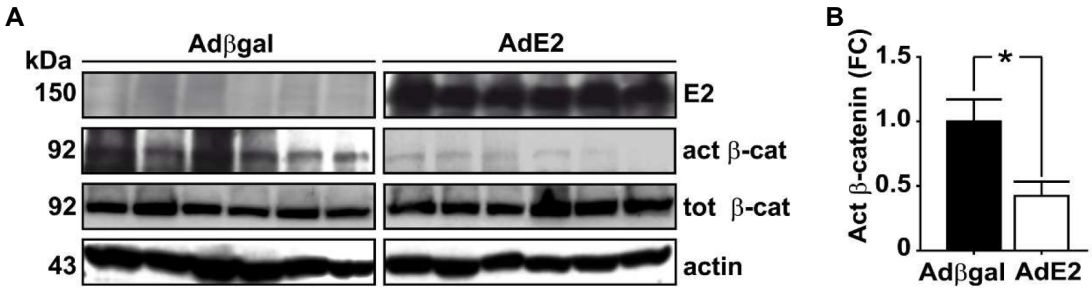

Fig. 9 The EMILIN2 over-expressing tumors display decreased levels of active β-catinin (A) Western blotting analysis of EMILIN2 expression and β-catenin activation performed on six tumor samples from Adβgal and AdE2 transduced MDA-MB-231 cells. Actin was used as a normaliser. (B) Graph representing the quantification of the fold change (FC) of the active β-catenin bands reported in A.

To investigate if EMILIN2 could also impair Wnt1 driven breast tumor cell growth in vivo, we injected cells over-expressing Wnt1 and transduced with the β-galactosidase or EMILIN2 adenoviral vectors in nude mice. Also in this case EMILIN2 decreased the Wnt1-induced tumor growth (**Fig. 10A**) and this impairment was induced by a reduction of the cell proliferation rate, as demonstrated by the decreased Ki67 staining (**Fig. 10B**).

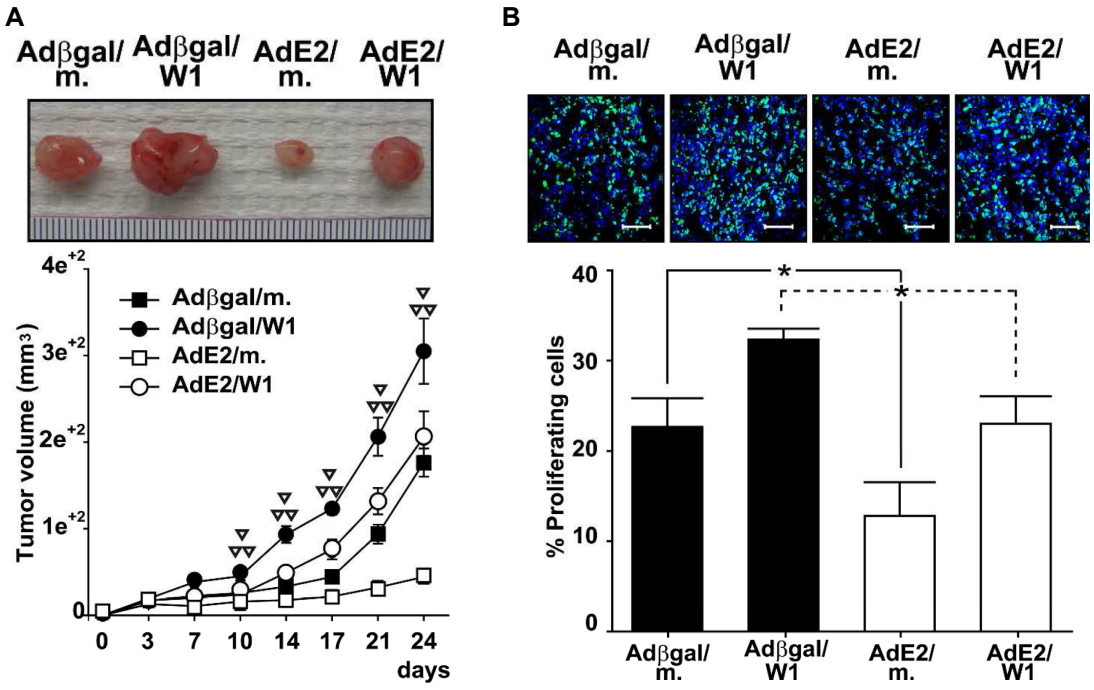

Fig. 10 EMILIN2 inhibites breast tumor growth impairing Wnt signaling. (A) Top panel: representative images of the tumors obtained following orthotopic injection in nude mice of MDA-MB-231 cells transfected with empty (m.) or Wnt1 (W1) pCMV vectors and/or transduced with EMILIN2 (AdE2) or β-galactosidase (Adβgal) adenoviral constructs. Bottom: graph representing the tumor growth curves. (B) Top panel: representative images of the Ki67 immunofluorescence analysis performed on tumor sections from the experiment in A.

Moreover, to simulate a therapeutic approach, we injected MDA-MB-231 cells over-expressing or not Wnt1 and we challenged the grown tumors with EMILIN2 every other day. As shown in **Fig. 11A**, this treatment strongly reduced tumor growth even when boosted by Wnt1 over-expression. To test whether EMILIN2 expression was appreciable in human normal breast tissues and could account for a significant control of Wnt signaling activation we analyzed the expression of EMILIN2 in normal and tumoral human tissues. The results are reported in Fig. **11B** and indicate that at least in these samples, EMILIN2 expression is detectable in normal breast tissues and is down-regulated in tumor tissues as previously reported. In accordance to our study, an in silico meta-analysis of gene expression profiles performed on a cohort of breast cancers showed an inverse

correlation between EMILIN2 and Wnt target genes (**Fig. 11C**). Taken together, these results demonstrated that high EMILIN2 expression negatively affected the proliferation and dissemination of breast cancer cells by directly attenuating the Wnt signaling pathway.

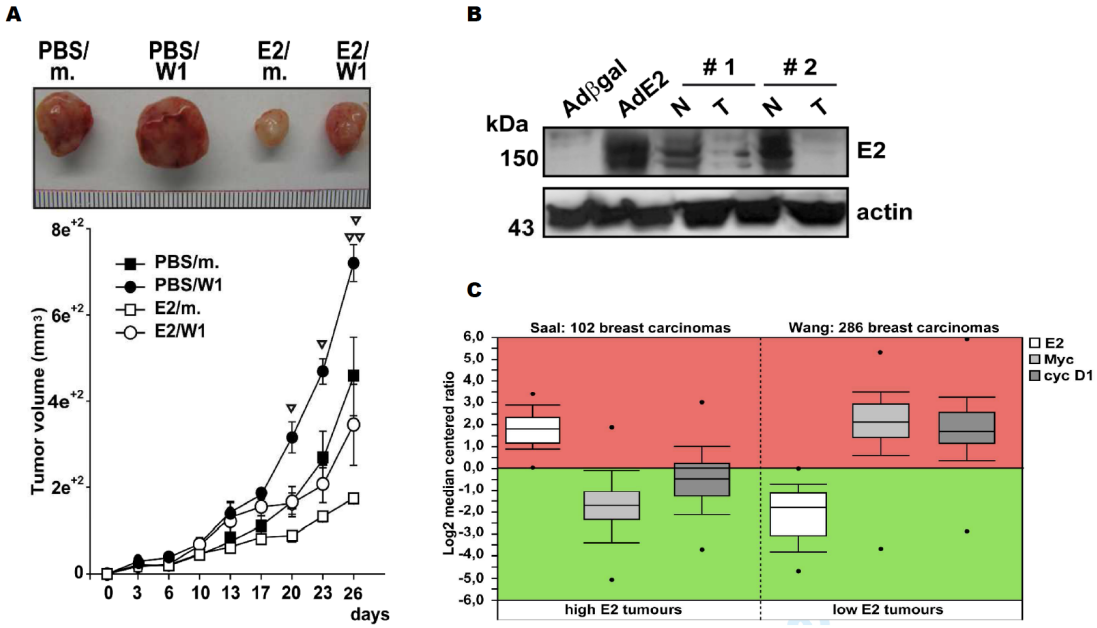

Fig. 11 EMILIN2 inhibits Wnt1 induced tumor growth. (A) Top panel: representative images of the tumors obtained following orthotopic injection of MDA-MB-231 cells transfected with empty (m.) or Wnt1 (W1) pCMV vectors and treatment with PBS or recombinant EMILIN2 (E2). Bottom: graph representing tumor growth curves. (B) Western blot analysis of EMILIN2 expression in normal (N) and tumoural (T) human breast tissues (sample #1 and #2) compared to the expression of EMILIN2 by in vivo grown MDA-MB-231cells transduced with the control (Adβgal) or the EMILIN2 (AdE2) adenoviral vectors. Actin was used as a normalizer. (C). Expression profile of the Wnt target genes Myc and Cyclin D1 (cyc D1) in high- and low-EMILIN2 expressing tumors, as reported in the Saal et al. (Saal et al. 2007) and Wang et al. (Wang et al. 2005) dataset, respectively, available in the Oncomine database. Axin2 was not included in these two datasets. The dataset were selected based on the following criteria: high number of cases, consistency of the expression pattern of Wnt target genes and consistency in the analysis with different reporters.

4.5 The over-expression of EMILIN2 induces IL8 production in ECs and fibroblasts

In a recent study carried out in our laboratory we have identified the pro-apoptotic region of EMILIN2 (Mongiat et al. 2010). The analysis of the tumor sections from the *in vivo* studies revealed an unexpected additional function of

EMILIN2: on one hand it induced apoptosis of the HT1080 sarcoma cell line injected in nude mice, on the other hand it also triggered angiogenesis .
The pro-angiogenic effect of EMILIN2 was confirmed by Ostrowski and his group, who demonstrated that EMILIN2 was expressed by fibroblasts and that blocking EMILIN2 expression reduced the ability of fibroblasts to stimulate EC proliferation (Bronisz et al. 2012a).
On these grounds, we decided to study the molecular mechanism by which EMILIN2 was able to stimulate angiogenesis and to this end we first performed a protein array analysis in order to determine if EMILIN2 could affect the expression of pro- or anti-angiogenic molecules. Among the 27 molecules analyzed in the array, we observed that the protein whose expression was altered the most by the over-expression of EMILIN2 in HUVEC cells was interleukin 8 (IL8) (**Fig. 12A**). This finding was also confirmed by Real-Time PCR, ELISA, and Western blot analysis (**Fig. 12C**, **D** and **E**).

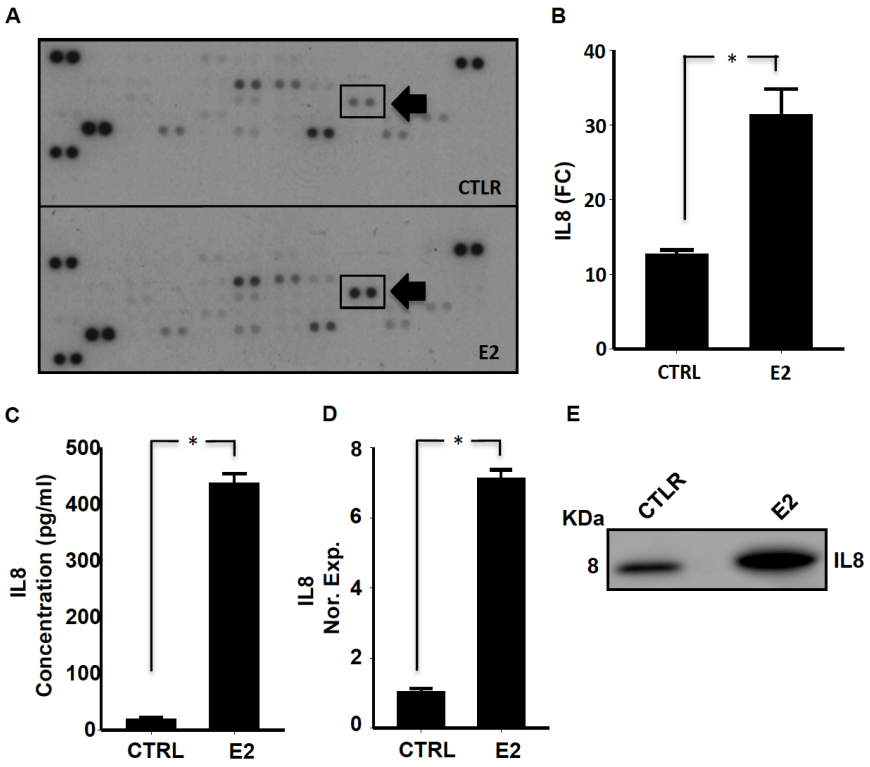

Fig.12 EMILIN2 induces IL8 production by the ECs. (A) Image of the angiogenesis protein array following incubation of the membrane with lysates from HUVECs transduced with EMILIN2 (AdE2) or β-galactosidase (Adβgal) adenoviral constructs (E2 and CTRL respectively). The spots corresponding to IL8 are boxed and highlighted by an arrow. (B) Quantitative analysis of the spots corresponding to IL8 as assessed with the Imaging Tool software. (C) Graph representing the concentrations of IL8 in the supernatants of HUVECs transduced with the EMILIN2 (AdE2) or β-galactosidase (Adβgal) adenoviral constructs as assessed with a commercially available ELISA test. (D) Graph representing the Real-Time PCR analysis of the relative IL8 expression by HUVEC cells transduced with the EMILIN2 (AdE2) or β-galactosidase (Adβgal) adenoviral constructs. (E) Western blotting analysis of IL8 expression in the supernatants of HUVEC cells transduced with the EMILIN2 (AdE2) or β-galactosidase (Adβgal) adenoviral constructs.

Fibroblast are a main source of both EMILIN2 (Bronisz et al. 2012) and IL8 (Fukui et al. 2013), hence we over-expressed EMILIN2 in NHDF cells to verify if the molecule could effectively trigger IL8 production and this was indeed the case (**Fig. 13**).

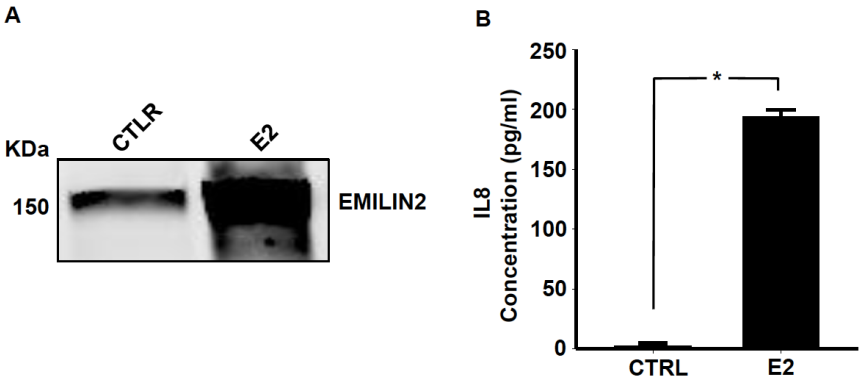

Fig. 13 EMILIN2 induces IL8 production in fibroblasts. (A) Western blotting analysis of supernatants of NHDF cells transduced with the EMILIN2 (AdE2) or β-galactosidase (Adβgal) adenoviral constructs. (B) Graph representing the concentrations of IL8 in the supernatants of NHDF cells transduced with the EMILIN2 (AdE2) or β-galactosidase (Adβgal) adenoviral constructs as assessed with a commercially available ELISA kit.

4.6 Conditioned Media from EMILIN2 challenged fibroblast affect ECs behavior

The finding that EMILIN2 boosted IL8 production by fibroblasts suggested that this could have been the mechanism by which EMILIN2 positively affects angiogenesis, given also the importance of fibroblasts in this process. We thus decided to corroborate this hypothesis by inducing EMILIN2 over-expression in fibroblasts and then tested the effects of the conditioned media on ECs behavior. As shown in **Fig. 14**, conditioned media from EMILIN2 challenged fibroblasts increased the EC proliferation rate (**Fig. 14A**) and also affected the motility of these cells, both in terms of distance (**Fig. 14B**) and speed (**Fig. 14C**).

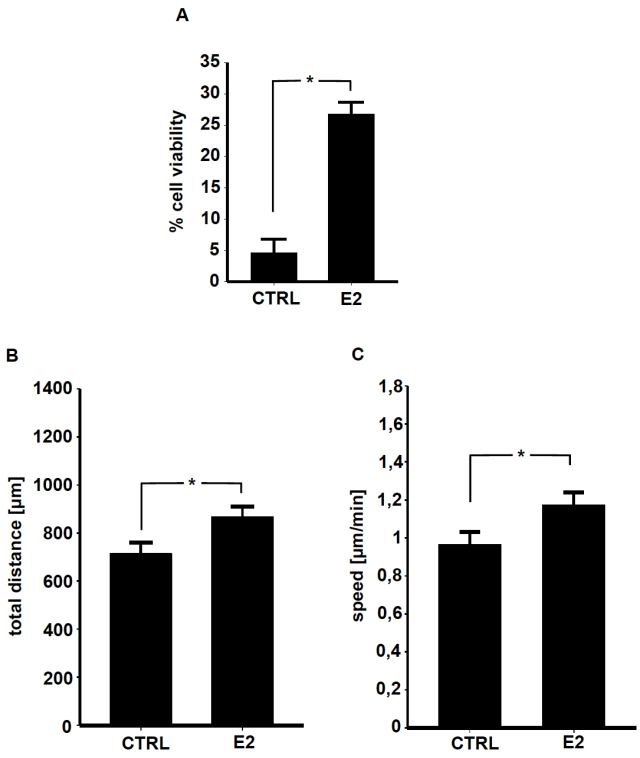

Fig. 14 Conditioned media from EMILIN2-challeged Fibroblasts affect ECs behavior. (A) Graph representing the viability of HUVEC cells treated with supernatants from NHDF cells transduced with the EMILIN2 (AdE2) or the β-galactosidase (Adβgal) adenoviral constructs as assessed by MTT assays. (B) Graph representing the analysis of the distance covered by HUVEC cells treated with supernatants from NHDF cells transduced with the EMILIN2 (AdE2) or β-galactosidase (Adβgal) adenoviral constructs. (C) Graph representing the analysis of the speed of HUVEC cells treated with supernatants from NHDF cells transduced with the EMILIN2 (AdE2) or the β-galactosidase (Adβgal) adenoviral constructs.

4.7 EMILIN2 binds the EGF receptor (EGFR) activating the Jak2/STAT3 pathway

Given that EMILIN2 is an extracellular molecule, we assumed that it could trigger the activation of a cell surface receptor that could prompt the production of IL8. To address this hypothesis we over-expressed EMILIN2 in ECs and performed an RTK protein array analysis. The results of this analysis indicated that receptors that exert a pivotal role in angiogenesis such as VEGFR1 and VEGFR2 were not affected by EMILIN2, and the sole RTK activated by the molecule was the EGF receptor (EGFR) (**Fig. 15**).

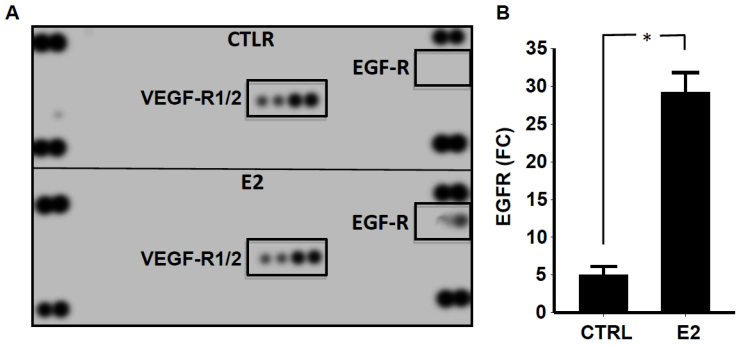

Fig. 15 EMILIN2 activates the EGFR at the EC surface.(A) Image of the RTK array analysis following incubation of the membrane with lysates from HUVEC cells transduced with the EMILIN2 (AdE2) or the β-galactosidase (Adβgal) adenoviral constructs (E2 and CTRL respectively). (B) Quantitative analysis of the spots corresponding to phosphorylated EGFR as assessed with the ImageTool software.

In support of these findings, an *in silico* analysis performed by Veljkovic and his group following the EIIP/ISM Bioinformatics Concept (Veljkovic et al. 2007) indicated that EGFR and EMILIN2 are potential molecular interactors (**Fig. 16A**). To further verify this putative interaction we performed a solid phase assay: EMILIN2 was coated on the wells of an ELISA plate and incubated with a recombinant fragment of the only extracellular portion of EGFR (EGFR-Fc). The results reported in **Fig. 16B** confirmed that EMILIN2 binds to EGFR and demonstrate that the interaction involves the extracellular region of the receptor. Finally, the interaction was also validated through a Histidine pull-down experiment (**Fig. 16C**).

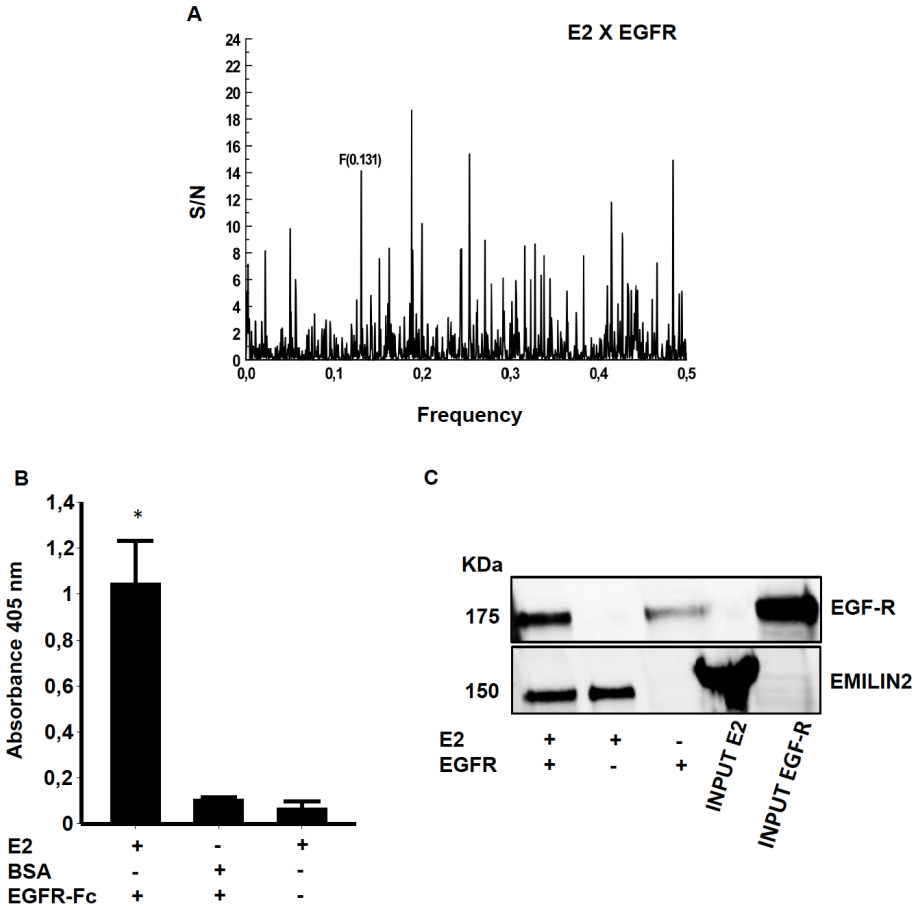

Fig. 16 EMILIN2 binds the EGFR. (A) Graph representing the *in silico* analysis according to the EIIP/ISM Bioinformatics Concept. (B) Graph representing the absorbance detected following an ELISA test performed following immobilization of EMILIN2 (E2) (0,5µg/well) or BSA to which soluble EGFR-Fc was added (100ng/well). Values represent the mean ± s.e. of three independent experiments. (C) Western blotting analysis of the Histidine pull-down experiment following incubation of His-tagged EMILIN2 (E2) with A431cell lysates as a source of EGFR (EGFR).

The activation of EGFR induces the activation of the Jak2/STAT3 pathway (Xia et al. 2002), and this pathway is the major regulator of IL8 transcription (Gharavi et al. 2007). Hence we over-expressed EMILIN2 in HUVEC cells and, as expected, we observed an increased phosphorylation of jak2 and STAT3 (**Fig. 17A**). Interestingly, when we treated the cells with both EMILIN2 and EGF, the activation of STAT3 was significantly increased compared with cells treated with only EMILIN2 (**Fig. 17B**).

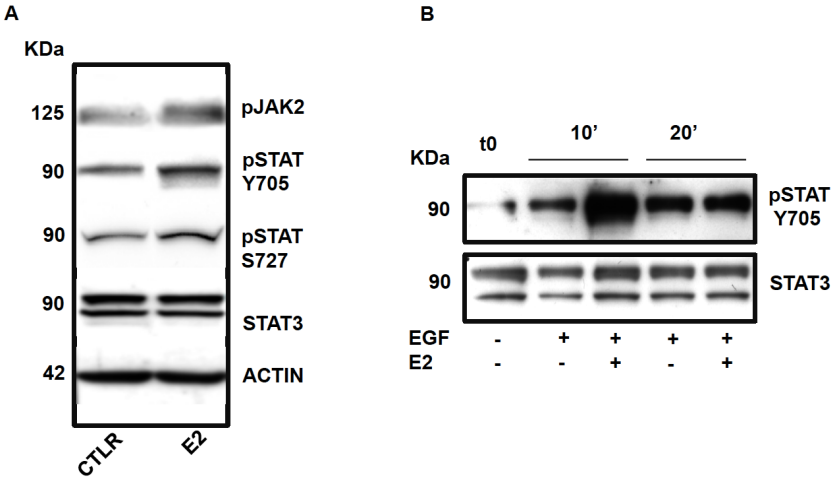

Fig. 17 EMILIN2 affects jak2/STAT3 pathway. (A) Western blotting analysis of Jak2 and STAT3 in HUVEC cell lysates following treatment with EMILIN2 (E2) or PBS as a control (CTRL). (B) Western blotting analysis of STAT3 phsphorylation HUVEC cell lysates following treatment with EMILIN2 (E2), EGF (EGF) or both for 10 or 20 min.

Since HUVEC cells express low levels of EGFR, to study the activation of the receptor in response to EMILIN2 treatment we used A431 cells, that are known to express high levels of EGFR on their cell surface. A431 cells were challenged with EMILIN2, EGF or both of them and as expected EMILIN2 induced a significant activation of EGFR and STAT3 compared with non treated cells. Moreover the cells treated with both EMILIN2 and EGF induced a further increased phosphorylation of EGFR and STAT3 and these effects were particularly evident after 10 and 20 minutes of treatment (**Fig. 18**).

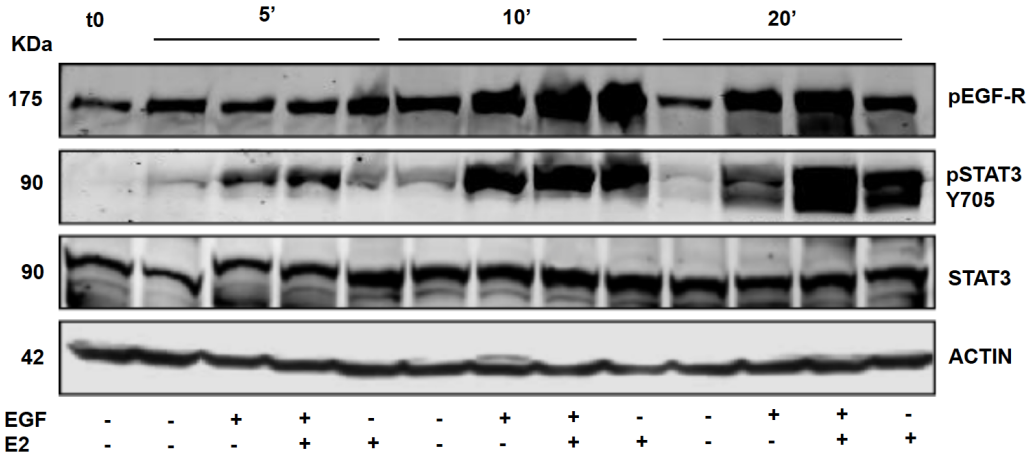

Fig. 18 EMILIN2 activates EGFR and subsequently the jak2/STAT3 pathway. Western blotting analysis of EGFR and STAT3 phosphorylation in A431 cell lysates following treatment with EMILIN2 (E2), EGF or both.

4.8 Inactivation of EGFR blocks the EMILIN2 pro-angiogenic effects

Cetuximab is a human:murine chimeric anti-EGFR IgG_1 that blocks EGFR function and does not cross-react with other members of the family. We thus thought to employ Cetuximab to further demonstrate that to exert its pro-angiogenic functions EMILIN2 requires a functional EGFR. In accordance to our hypothesis and in support of our findings, as shown in **Fig. 19**, Cetuximab inhibited the EMILIN2-driven IL-8 production in HUVEC cells.

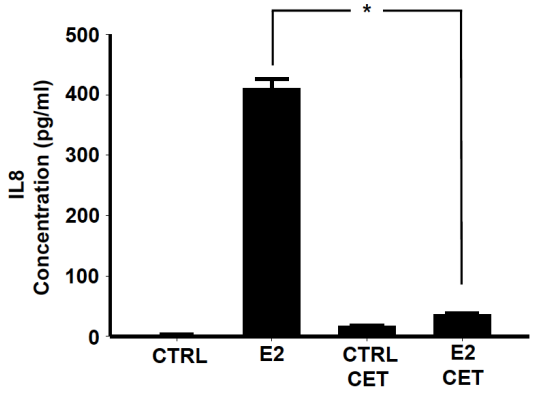

Fig. 19 Cetuximab blocks the EMILIN2-driven IL-8 production in HUVEC cells. Graph representing the concentrations of IL-8 in supernatants from HUVEC cells transduced with the EMILIN2 (AdE2) or the β-galactosidase (Adβgal) adenoviral constructs, and challenged with Cetuximab, as assessed with a specific ELISA kit.

We next verified whether the blockage of the EMILIN2-driven IL-8 production by Cetuximab could also reflect on an impaired EC behavior. As shown in **Fig. 20A**, the increase of EC viability prompted by EMILIN2 was rescued in presence of the antibody. Similarly, the use of Cetuximab blocked the increased EC random motility induced by EMILIN2, both in terms of distance and speed (**Fig. 20C**, **20D**), further demonstrating that the effects of EMILIN2 on EC behavior are EGFR-dependent. To demonstrate that the pro-proliferative effects of EMILIN2 on ECs are dependent on the increased IL-8 production induced by EMILIN2, we performed a proliferation assay using an antibody that blocks the receptor for IL-8 (αCXCR1). As shown in **Fig. 20B**, the αCXCR1 impaired the effect of EMILIN2, thus confirming our hypothesis.

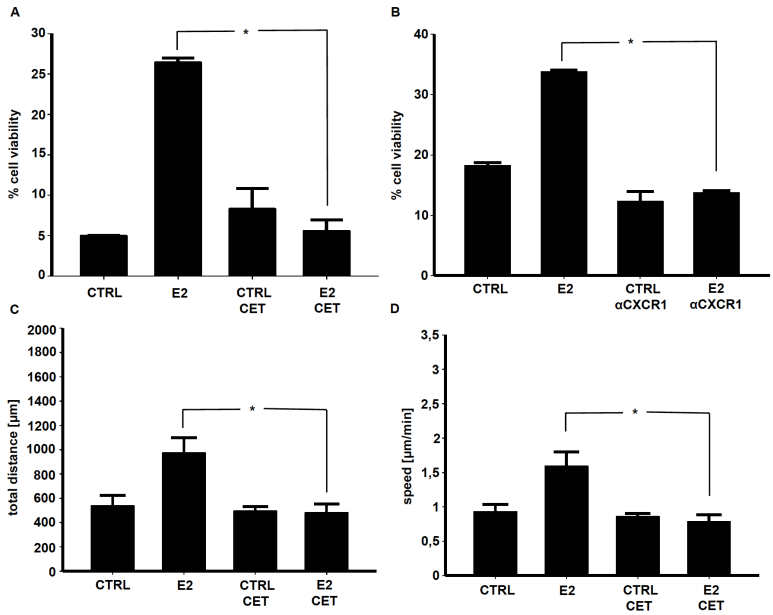

Fig. 20 The EMILIN2 effects on EC behavior depend on EGFR activation and IL-8 production. (A)Graph representing the viability of HUVEC cells following treatment with recombinant EMILIN2 (5µg/ml) and/or Cetuximab (60µg/ml) as assessed by MTT assay. (B) Graph representing the viability of HUVEC cells treated with recombinant EMILIN2 (5µg/ml) and/or αCXCR1 (1µg/ml) as assessed by MTT assay. (C) Graph representing the analysis of the distance covered by HUVEC cells treated with supernatants from NHDF cells transduced with the EMILIN2 (AdE2) or the β-galactosidase (Adβgal) adenoviral constructs, in the presence or not of Cetuximab (60µg/ml). (D) Graph representing the analysis of the speed of HUVEC cells treated with supernatants from NHDF cells transduced with the EMILIN2 (AdE2) or the β-galactosidase (Adβgal) adenoviral constructs, in the presence or not of Cetuximab (60µg/ml).

4.9 EMILIN2 induces EC sprouting in a 3D context

We next tested the pro-angiogenic role of EMILIN2 in a more sophisticated setting verifying the efficiency in developing new sprouts in a 3D context. To set up the 3D in vitro angiogenesis assay, HUVEC cells were coated onto cytodex microcarriers and embedded into a fribrin gel. The gel was then overlayed with NHDF cells transduced with the EMILIN2 or the β-galactosidase adenoviral constructs. Spheroids were challenged with EGF or AG1478, a chemical inhibitor of the EGFR and incubated for 7 days. Following the incubation the structures were fixed and stained with anti-CD31 antibody. As shown in **Fig. 21**, while EMILIN2 and EGF treated spheroids developed numerous and long vessels' sprouts, control and AG1478 treated spheroids failed to efficiently form sprouts. These results indicate that the over-expression of EMILIN2 significantly increase angiogenesis in a 3D context and confirm that this effect is dependent of EGFR activation.

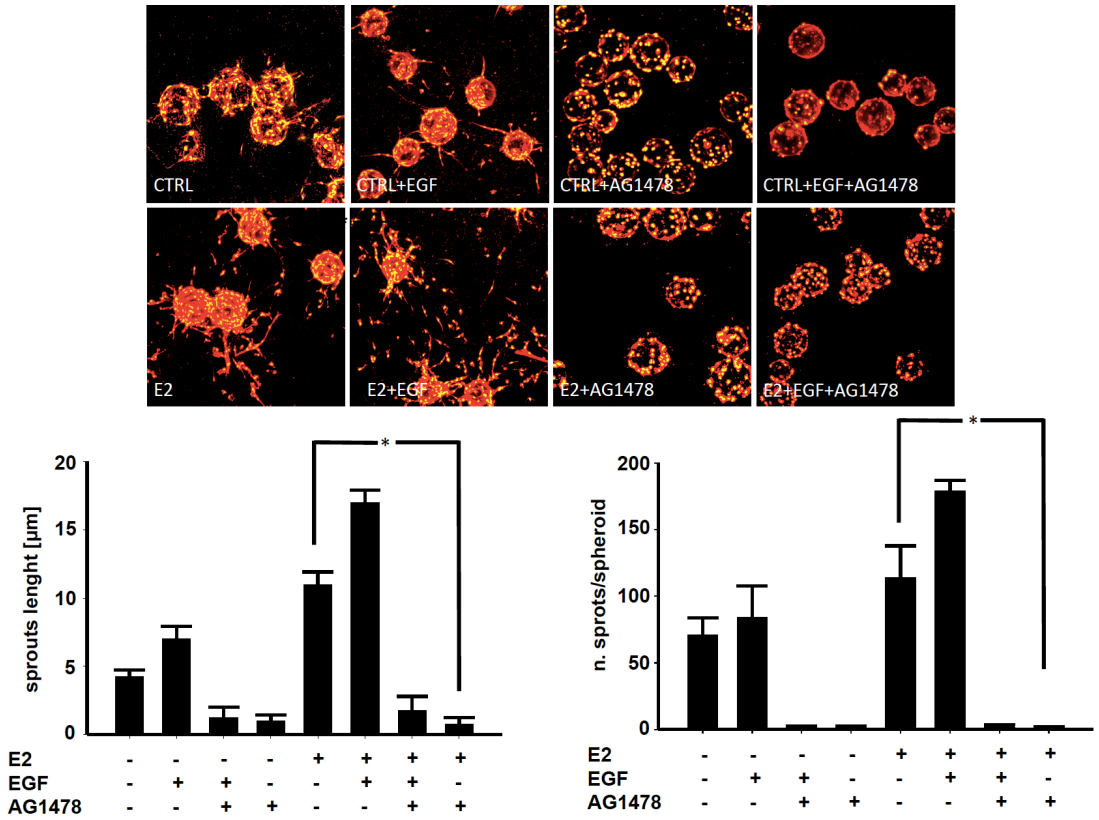

Fig. 21 EGFR blockage strikingly impares the EMILIN2-induced vessels' sprouts in a 3D setting. Top panels: representative images obtained following a 3D in vitro angiogenesis assay using HUVEC cells coated onto cytodex microcarriers and embedded into a fribrin gel. On top of the gel NHDF cells over-expressing or not EMILIN2 were seeded. Spheroids were treated with EGF and/or the chemical inhibitor of EGFR AG1478. Spheroids were stained with α-CD31 (vessels) and SYTOX (nuclei). Bottom: graphs representing the evaluation of the length and the number of the sprouts as assessed by the Volocity 3D software. Values represent the mean ± s.d. of three independent experiments.

4.10 EMILIN2 induces angiogenesis in an *ex vivo* model

To investigate if EMILIN2 could also impair angiogenesis in a more complex systems we set up an *ex vivo* rat aortic ring assay. In particular aortic rings from Fischer 344 male rats were isolated and cultivated on rat type I collagen containing or not EMILIN2. We used both murine and human recombinant EMILIN2, and as shown in the preliminary results reported in **Fig. 22**, the aortas treated with EMILIN2 displayed a stricking increase of the microvascular formations. Our future plan is to repeat the experiment in the presence of Cetuximab to block EGFR and/or of αCXCR1 to block the receptor for IL-8, to confirm also in this setting that the EMILIN2 pro-angiogenic effects depend on the activation of EGFR and the consequent production of IL-8..
Next the pro-angiogenic function of EMILIN2 was also demonstrated *in vivo*. Our

preliminary data exploiting the zebrafish model in collaboration with the University of Padua, indicate that the morpholino targeting EMILIN2 induces a striking reduction of the intersomitic vessels (data not shown). We are thus planning to corroborate these results and strengthen the molecular mechanism involved exploiting this *in vivo* model.

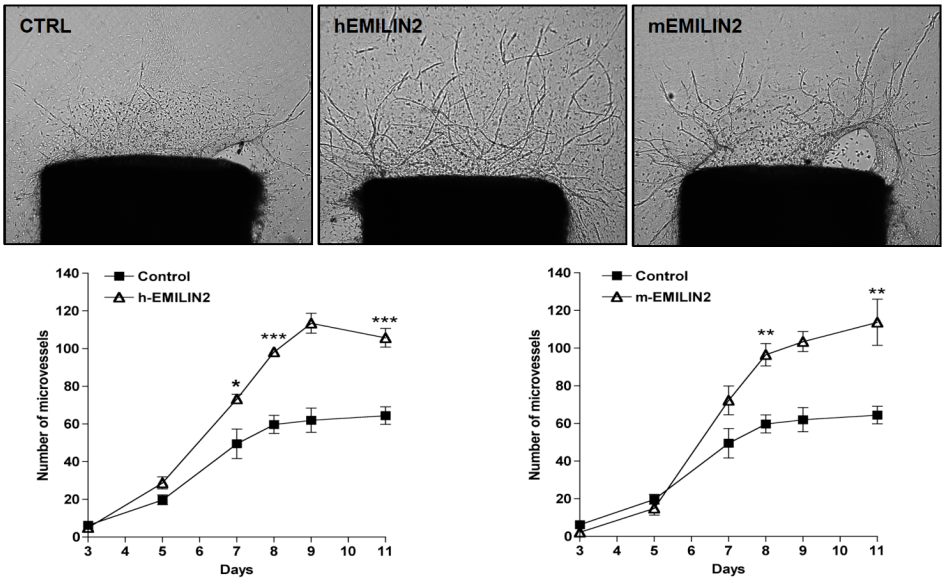

Fig. 22 EMILIN2 induces a striking increase of newly formed microvessels in aortic ring assays. Top: representative images of rat aortic rings treated with 5μg/ml of recombinant murine EMILIN2 (mEMILIN2), human EMILIN2 (hEMILIN2) or PBS as a control (CTRL). Bottom: graphs representing the number of microvessels formed following the treatment.

4.11 The tumor vessels from EMILIN2 KO mice are exceedingly dismorphic

Given that, despite its demonstrated role in angiogenesis, the knockout of EMILIN2 in mice does not lead to obvious dysfunctions of the vascular system, we hypothesized that more evident alterations could occur in pathological conditions, where the angiogenic processes are less tightly regulated. To address this hypothesis we subcutaneously injected syngenic B16-F10 melanoma cells in C57BL/6 WT or EMILIN2 knockout mice. Tumors were let growth till they reached the size of ~300 mm^3, excised and the vessels analyzed by TEM microscopy. As shown in the preliminary results reported in **Fig. 23**, tumor-associated vessels from EMILIN2 KO mice displayed a poorly homogeneous and highly dismorphic endothelium.

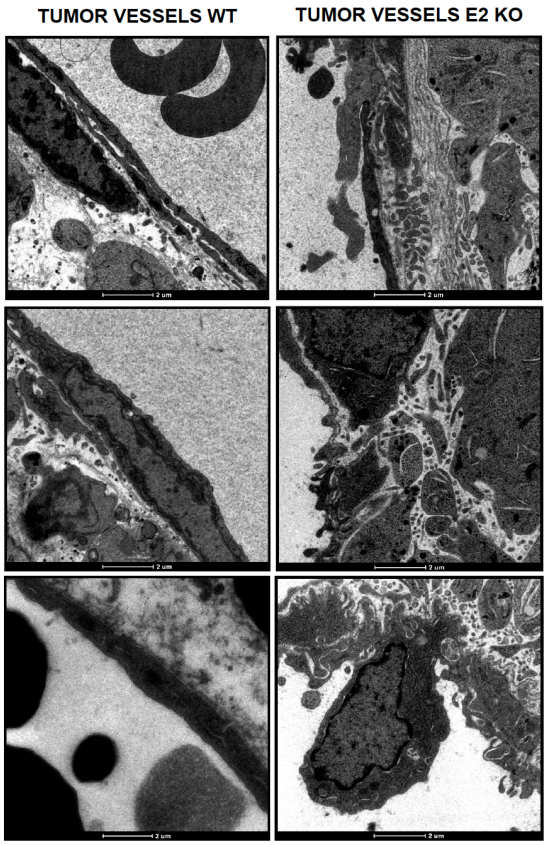

Fig. 23 Tumor vessels from EMILIN2 knockout mice display a strikingly altered endothelium. Representative images of the TEM microscopy performed on the tumor vessels from WT (left panels) and EMILIN2 knockout (right panels) mice.

The results reported in this thesis describe a dual role of EMILIN2: on one hand it reduces tumor growth by affecting directly breast cancer cells and inhibiting Wnt signaling. On the other hand it stimulates angiogenesis by binding EGFR and regulating IL8 production.

5 DISCUSSION

Our published data suggest that the ECM molecule EMILIN2 may play two different and apparently contradictory roles in the tumor microenvironment. In fact, in our previous studies we demonstrated that on one hand EMILIN2 inhibits tumor growth by activating apoptosis and, on the other hand, it induces new vessels formation.
The subject of investigation of my PhD program and the results reported in the present thesis are in line with these results and grant further evidences of the role of EMILIN2 in the regulation of tumor growth. I mainly focused on two different aspects:
- First, the effect of EMILIN2 in the regulation of breast cancer cell growth. The results presented here highlight a further mechanism by which EMILIN2 exerts a tumor suppressive function affecting the activation of the Wnt signaling pathway;
-The second aspect of my investigations dealt with the identification of the molecular mechanisms responsible for the EMILIN2-driven regulation of EC function and pro-angiogenic effects.
These two aspects will be discussed separately.

5.1 Role of EMILIN2 in the regulation of Wnt signaling.

In this study, recently accepted for publication by the Journal of Pathology (Marastoni et al., in press) we identified EMILIN2 as a novel molecular partner of Wnt1 and we demonstrated that this interaction led to a significant inhibition of the Wnt signaling in breast cancer cells. EMILIN2 in fact, decreased the activation of β-catenin and the phosphorylation of LPR6, thus altering the expression of β-catenin target genes. Moreover EMILIN2 reduced the Wnt-driven breast cancer cell migration as demonstrated by the Matrigel evasion assays.
The first clue indicating that EMILIN2 could have been involved in the regulation of Wnt signaling came with the observation that the EMILIN2 EMI domain shared sequence homology with the CRD domain of the Frizzled receptors. And in particular the highest homology involved a stretch of amino acid residues that are critical for Wnt binding (Dann et al. 2001).
The pleiotropic functions of EMILIN2, pro-apoptotic for a number of tumor cell lines (Mongiat et al. 2007), pro-angiogenic (Mongiat et al., 2010) and Wnt signaling regulatory function described in this thesis (Marastoni et al., in press), may likely be due to its multimodular structure.
As to why MDA-MB-231 cells are only sensitive to the regulation of Wnt signaling by EMILIN2 but are not affected by its pro-apoptotic effects is still not clear. It is possible that EMILIN2 treatment may alter the expression of the death receptors at the cell surface, as also observed with the treatment with TRAIL (Yoshida et al. 2009). The region responsible for the interaction between EMILIN2 and Wnt ligands is the EMI domain, since the use of a deletion mutant lacking this domain

abolished the effect. *In silico* analyses also showed a potential and highly specific interaction with Wnt2 (unpublished observation), suggesting that EMILIN2 could also interact with other Wnt ligands. It cannot be excluded that the EMI domain may represent a potential reservoir of Wnt molecules that could compete with Wnt receptor(s) depending on the relative affinities.
In line with our results, EMILIN2 is frequently methylated in tumors and this suggests that decreased levels of EMILIN2 expression deprives the tumor microenvironment of the inhibitory effect on Wnt signaling, granting an advantage to cancer cells. As a consequence tumor microenvironments with lower concentrations of EMILIN2 display higher expression of c-Myc, cyclin D1 and Axin2 and thus are more permissive to cancer progression. In our model, in an EMILIN2-rich microenvironment, EMILIN2 sequesters Wnt ligands inhibiting the interaction with their receptors. This leads to a decreased expression of c-Myc, cyclin D1 and Axin2 and to a better prognosis for breast cancer patients. On the contrary, in an EMILIN2-deprived microenvironment, Wnt ligands are free to engage their receptors thus efficiently activate the Wnt signaling cascade leading to a worse prognosis for breast cancer patients (**Fig. 1**).

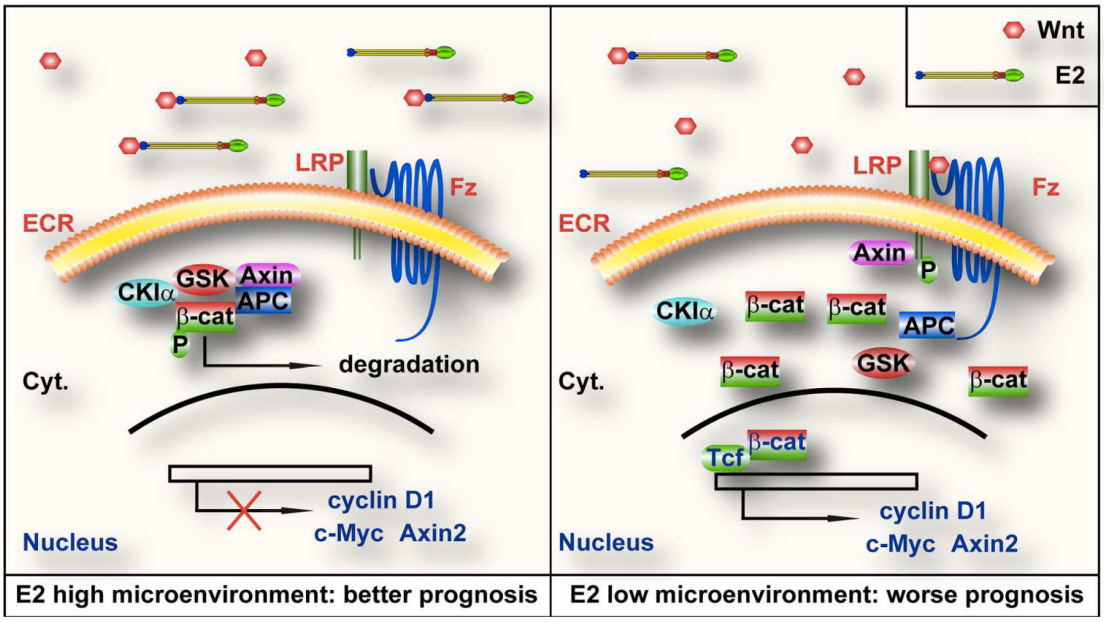

Fig. 1 A low EMILIN2 expression in human breast tumors correlates with an increased expression of β- catenin target genes. Schematic representation of the effects of low or high concentrations of EMILIN2 (E2) in the tumor microenvironment on the regulation of the Wnt signaling pathway. The extracellular region (ECR), cytoplasm (cyt.) and nuclear compartments of breast cancer cells are indicated and color-coded; the components of the β-catenin (β-cat) destruction complex casein kinase α (CKIα), Axin, GSK3β (GSK) and APC, as well as the LPR6 (LRP) and Frizzled (Fz) receptors are indicated. Protein phosphorylation is indicated by a P.

5.2 Role of EMILIN2 in angiogenesis

The second aspect of my investigation dealt with the identification of the molecular mechanisms responsible for the EMILIN2 pro-angiogenic effects. The increased angiogenesis observed in tumors treated with EMILIN2 (Mongiat et al., 2010), prompted us to further analyze this function of the molecule and to verify by which mechanisms EMILIN2 could affect ECs behavior and therefore play a key role in the regulation of angiogenesis.

We first manipulated the expression pattern of HUVEC cells to induce EMILIN2 expression through adenoviral transduction. The over-expression of EMILIN2 by these cells led to a significant increase of cell proliferation and motility and changes in the expression of cytokines and other molecules involved in angiogenesis in particular IL-8.

Since ECs do not normally express EMILIN2 but fibroblasts are an important source of both IL-8 and EMILIN2 (Fukui et al. 2013), in other set of experiments we manipulated NHDF cells to over-express EMILIN2 and we used supernatants from these cells to challenge HUVEC cells. The over-expression of EMILIN2 by NHDF cells significantly increased the EC proliferation rate and motility.

To further shed light on the molecular mechanisms governing the EMILIN2 pro-angiogenic effects we chose to carry out a broad analysis of the RTKs supposedly activated on the surface of ECs challenged with EMILIN2. The results of this analysis indicated that EMILIN2 induced a prominent activation of the EGFR.

Despite the fact that the expression of EGFR by ECs is controversial (Jouan-Hureaux et al. 2012, Doherty et al. 1999) we have generated preliminary results indicating that HUVEC cells express this receptor, despite at low levels. However our data indicate that the levels of EGFR are sufficient to induce IL-8 production in these cells and a consequent increased proliferation and migration. In fact, these effects are lost when using EGFR-blocking agents.

In addition, we have further dissected the molecular mechanisms that linked EMILIN2 to EGFR and IL-8 production. In particular we found that EMILIN2 following the binding to the EGFR receptor, activates the jak2/STAT3 pathway, which is one of the most important regulators of the IL-8 production (Gharavi et al., 2007).

The use of both EMILIN2 and EGF in a series of experiments lead to an activation of EGFR that was higher compared to the use of EMILIN2 and EGF alone, indicating that the two molecules may produce additive effects. It is yet not known whether EMILIN2 acts alone in the activation of EGFR even though is likely that it may enhance the activity of EGF present in the medium. Preliminary *in silico* analyses not yet experimentally corroborated, demonstrate that EMILIN2 and EGF are very likely potential interactors. In this scenario the binding of EGF to EMILIN2 may enhance the affinity of EGF for EGFR and EGFR activation may arise following the formation of a trimolecular complex. It cannot

be excluded though, that EGFR activation may also occur following the binding of EMILIN2 to other EGFR ligands such as EGF.
The EMILIN2 pro-angiogenic effects and the mechanisms involved were tested in a number of *in vitro*, *ex vivo* and *in vivo* tests including 2D cultures, spheroid based angiogenesis tests, aortic ring assays and the zebrafish model.
As to whether the increase of angiogenesis prompted by EMILIN2 leads to the formation of functional vessels or, on the contrary to unproductive angiogenesis as described for components of the Notch signaling pathway remains yet to be determined. In this second scenario EMILIN2 may have a "double-edge sword" role: on one hand attacking directly cancer cells by inducing apoptosis and impairing Wnt signaling activation, on the other hand reducing the rate of functional vessels within the tumors thus leading to their starvation.
In this context, the analysis of the syngenic B16-F10 tumors grown in WT and EMILIN2 knockout mice by TEM microscopy, revealed that the endothelium of the vessels from the knockout mice was more discontinuous and less uniform compared to the endothelium from the tumor vessels from WT mice suggesting that in pathological conditions EMILIN2 may leads to the formation of less organized and functional vessels.
Taken together the results presented in this thesis indicate that EMILIN2 displays a dual role in the tumor microenvironment. EMILIN2 targets directly breast cancer cells impairing their growth and motility by negatively modulating Wnt signaling activation. Simultaneously EMILIN2 activates angiogenesis. Indeed EMILIN2 is produced by fibroblast and it induces the activation of EGFR following the binding to the receptor. This leads to the activation of the Jak2/STAT3 pathway and IL-8 production. Moreover following EMILIN2 stimulation also fibroblasts secrete IL-8 thus inducing both a paracrine and autocrine loop of activation of ECs. (**Fig. 2**).

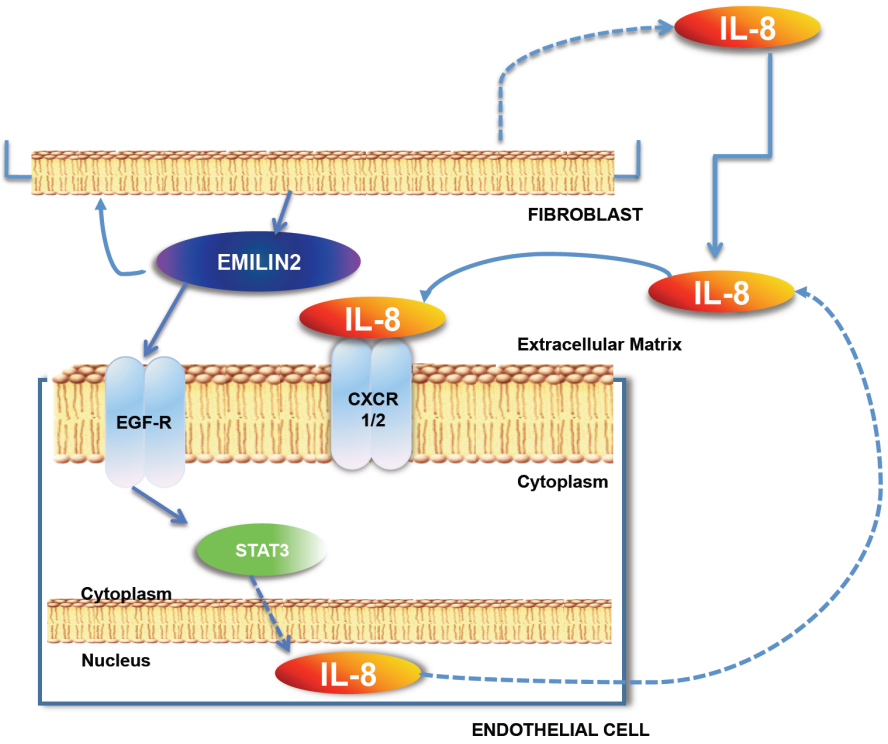

Fig.2 EMILIN2 activates IL-8 production in ECs and fibroblasts. Schematic representation of the effects of EMILIN2 produced by fibroblasts on ECs. EMILIN2 binds to the EGFR thus inducing IL-8 production. As a consequence IL-8 activates ECs affecting both thier proliferation rate and their motility. Moreover, by a yet unknown mechanism, EMILIN2 induces IL-8 expression also in fibroblasts thus acting both in a paracrine and autocrine fashion. Protein phosphorylation is indicated by a P.

6 MATERIALS AND METODS

6.1 Cell lines

The MDA-MB-231 and A431 cell lines were obtained from ATCC and cultured in Dulbecco's modified Eagle medium (DMEM) containing 10% fetal bovine serum (FBS) (GIBCO BRL). HUVEC (Human Umbilical Vein Endothelial Cells) were isolated from the human umbilical cord vein. Cells were cultured in M199 medium (GIBCO) supplemented with 20% FBS, 1% Penicillin-Streptomycin, 50 mg/ml heparin (SIGMA) and bovine brain extract (0,5%). Cells were grown in flasks pre coated with 1% porcine skin gelatin. 293-EBNA (Epstein-Barr Nuclear Antigen) cells were a gift from Rupert Timpl and cultured in DMEM, 10% FBS. The NHDF cell line was obtained from LONZA and cultured in Dulbecco's modified Eagle medium (DMEM) containing 10% fetal bovine serum (FBS) (GIBCO BRL). All cells were maintained al 37°C in a humidified 5% CO2 atmosphere.

6.2 Isolation of HUVEC cells

HUVEC were obtained from human umbilical cord veins according to Jaffe method (Jaffe et al., 1973). A sterile technique was utilized during all the required manipulations. Briefly, both ends of the cord were cut off and the vein was perfused with a Phosphate Buffer Saline (PBS) solution containing 50 mg/ml gentamycin and 250 ng/ml fungizone to wash out the blood. Then one end of the cord was tightly clamped and a 0,25% Collagenase A (Roche) solution pre warmed at 37°C was injected in the vein to facilitate EC detachment. After 20 minutes of incubation at room temperature, the collagenase solution was flushed out from the cord and the vein was washed with M199 medium. The collected cells were then centrifuged for 10 min at 500g, resuspended in M199 complete medium and seeded onto gelatin-coated flasks.

6.3 Antibodies and other reagents

The anti-EMILIN2 monoclonal antibody was obtained upon immunization of a rabbit with 150mg of a recombinant EMILIN2 fragment corresponding to the N-terminal gC1q domain preceded by the proline-rich domain. The antibody was affinity purified from the rabbit serum by means of the CNBr-activated Sepharose 4B resin (Amersham, GE-Healthcare, Milan, Italy)..The anti-β-actin and anti-FLAG antibodies, the FLAG peptide, the anti-FLAG M2 affinity gel, the FLAG-tagged BAP, the human type I collagen and the low-melting agarose were from Sigma-Aldrich (Milan, Italy). The Maxwell 16 Mouse Tail DNA Purification kit and Maxwell 16 instrument, the Dual Luciferase assay kit and the pRL-CMV-

Renilla vector were from Promega (Milan, Italy). The pseudopodia kit and the anti-active β catenin antibodies were from Millipore (Milan, Italy). The total β-catenin was from Abcam (Cambridge, UK). The anti-total and anti-phosphoLRP6 antibodies were from Cell Signaling Technology (Danvers, MA, USA). The anti histidine antibody was from Abgent (San Diego, CA). The Ni-NTA agarose was from QIAGEN (Milan, Italy); the secondary AlexaFluor-conjugated antibodies and TO-PRO-3 were from Invitrogen (Milan, Italy). The Matrigel™ was from BD Biosciences (Milan, Italy). The secondary HRP-conjugated antibodies were from Amersham (GE Healthcare, Milan, Italy) and Trueblot was from eBiosciences (San Diego, CA, USA). The EGF was from Peprotech (Rocky Hill, NJ, USA). The Wnt1 pCMV6-Neo vector was from Origene (Rockville, MD, USA). The mouse Wnt1, the Fz8-pcDNA and the Xenopus-Dickkopf (DKK) pCS2 construct, the TOPflash TCF reporter and Renilla plasmids, were a gift from Prof. S. Piccolo (University of Padua, Italy). The phosphor-EGFR and the EGFR antibodies were from Sigma-Aldrich (Milan, Italy). The STAT3 and the phosphor-STAT3 (Y705 and S727) were from Santa Cruz Biotechology Inc. (California, USA). Cetuximab was a gift from department of farmacology of the National Cancer Institute, CRO Aviano (Italy).

6.4 Cell transfection, expression and purification of recombinant proteins and Adenoviral constructs

Cell Transfection, Recombinant Protein Production and Adenoviral Transduction RNA for PCR analysis was extracted from manipulated/treated MDA-MD-231 cells or tumour samples with the Trizol reagent (Invitrogen, Milan, Italy); reverse transcription was performed using AMV-RT and exanucleotides (Promega, Milan, Italy).
MDA-MB-231 were transfected with the various vectors using FuGene6 reagent (Promega,Milan, Italy). Wnt1 stable clones were obtained through selection with 600 μg/ml of G418. E293 cells were transfected with the relative pCEP-Pu constructs using the FuGene6 reagent and were then selected with 250 μg/ml of G418 and 0.5 μg/ml of puromycin. Confluent cells were incubated in serum-free medium for 48 hours, and the media were collected. The proteins were purified by means of the Ni-NTA or anti-FLAG beads. The EMILIN2 Δ5 deletion mutant was amplified by PCR with the following oligonucleotides:
5'-CTAGCTAGCGACGGTTCTTGACCTCCAGTCT-3' and
5'-CGGGATCCTTAATGGTGATGGTGATGATGGAGGTGGGAAAGGAA-3' using the EMILIN2 full-length construct as a template. For EMILIN2 over-expression, tetracycline-inducible recombinant adenoviruses were constructed according to the manufacturer's instructions using the Adeno-X Tet-On Expression System 2 (Clontech Laboratories, Milan Italy). HUVEC were co-transduced with a

regulatory virus Adeno-X Tet-On and the EMILIN2 recombinant virus at a specific multiplicity of infection ratio (400 : 160). Doxycycline was employed at a final concentration of 0.5 mg/ml.

6.5 Real Time PCR

RNA for Real-Time PCR analysis was extracted from manipulated HUVEC cells with the Trizol reagent (Invitrogen, Milan, Italy); reverse transcription was performed using AMV-RT and exanucleotides (Promega, Milan, Italy). Real-Time PCRs was then performed using RealMasterMix SYBR ROX (5Prime, Hamburg, Germany) and the following oligonucleotides to assess IL-8 expression:
Forward: 5'-CATTGACCAAGGAAATCGGC-3',
Reverse: 5'-CACAGAGATAGTTACAGCCATACC-3'
The comparative Ct method ($2^{-\Delta\Delta Ct}$) was applied for the analysis.

6.6 ELISA and Solid Phase binding assays

EMILIN2/mock conditioned media were coated onto ELISA plates, blocked with 2% BSA and incubated anti-EMILIN2 antibody followed by a HRP-conjugated secondary antibody incubation; the substrate (0.5 mg/ml of ABTS/0.1 M sodium citrate solution containing 0.01% H2O2) was then added and the absorbance measured at 405 nm. For the EMILIN2-Wnt1 interaction studies, 0.1 μg/well of His-tagged EMILIN2 and the 5 deletion mutant were coated onto ELISA plates and incubated with ~ 30 or ~100ng of FLAG-tagged Wnt1 and the binding detected with an anti-FLAG antibody.
For EMILIN2-EGFR interaction studies, EMILIN2 (0,5μg) was immobilized onto ELISA plates, blocked with 2% BSA and incubated with 100ng soluble EGFR-Fc from Abcam (Cambridge, UK).
For IL-8 detection we used the Human IL-8 ELISA kit from Immunological Sciences (Roma, Italy). EMILIN2/mock conditioned media were coated onto ELISA plates provided by the Kit and the analysis performed according to the manufacturer instructions.

6.7 Western blot analysis

Cells were lysed in cold HNTG buffer (0,1% TrytonX100, 20mM HEPES pH 7.5, 10% glycerol, 150 mMNaCl) containing a protease inhibitors cocktail (Roche) and 1 mM sodium orthovanadate. After incubation on ice for 20 min, the lysates

were centrifuged at max speed for 20 min at 4°C and the supernatants recovered.
For the phosphorylation studies, cells were then lysed in a cold specific buffer (1mM $CaCl_2$, 1mM $MgCl_2$, 15mM Tris-HCl pH 7.2, 150mM NaCl, 1% TrytonX100, 0,1% SDS, 0,1% Na Deoxycholate) containing 25 mM NaF, 1 mM DTT, 1 mM Na_3VO_4 and the protease inhibitors cocktail (Roche). Proteins resolved in 4% to 20% Criterion Precast Gels (Bio-Rad, Milan, Italy) were transferred onto Hybond-ECL nitrocellulose membranes, blocked with 5% dry milk in TBS-T buffer, probed with the appropriate antibodies, and developed using enhanced chemiluminescence (Amersham Biosciences, Milan, Italy). Membranes were then expesed to X-ray films. Alternatively, the Odyssey Infrared Imaging System was used (Li-COR Biosciences, Lincoln, NE, USA). Human tissues were provided by the CRO-Biobank.

6.8 Histidine and Flag pull-down experiments

For EMILIN2-Wnt1 interaction analysis E293 or MDA-MB-231 cells transfected with the FLAG-tagged Wnt1 pcDNA construct were lysed in HNTG buffer (20 mM HEPES [pH=7.5], 150 mMNaCl, 0.1% Triton X-100, 10% glycerol). 60μg of cell lysates were incubated with 7μg of His-tagged EMILIN2 or the His-tagged Δ5 deletion mutant. The FLAG-BAP protein was used as control. Proteins were captured with the anti-FLAG-conjugated or Ni-NTA beads and analyzed by Western Blotting.
For EMILIN2-EGFR interaction analysis, 7μg of soluble EGFR-Fc were incubated with 7 μg of His-tagged EMILIN2. Proteins were captured with Ni-NTA beads and analyzed by Western Blotting.

6.9 Angiogenesis array

To verify which cytokines could be altered by EMILIN2 we have employed the Human Angiogenesis Antibody array from R&D Systems consisting of 55 different antibodies recognizing molecules important in angiogenesis spotted in duplicate on nitrocellulose membranes.. For this analysis HUVEC cells were transduced with the EMILIN2 or the control adenoviral vectors. The incubation was conducted for 1h. Following incubation, the cells were lysed and the lysates diluted to a final volume of 1,5 ml with the provided buffer. Cell lysates were deposited over the array and incubated overnight at 4°C. Streptavidin-HRP and chemiluminescent detection reagents were added and the membrane analyzed as a Western Blot.

6.10 RTKs array

Analysis of Tyrosine Kinase Receptors (RTKs) activation following treatment of ECs with EMILIN2 was evaluated using the Human Phospho-Receptor Tyrosine Kinase kit (R&D Systems) consisting of 42 different antibodies recognizing phosphorylated human RTKs spotted in duplicate on nitrocellulose membranes. For this analysis HUVEC cells were incubated with conditioned media from HUVEC cells transduced with the EMILIN2 or the control adenoviral vectors (collected 72 h post transduction). The incubation was conducted for 30'. Following incubation, the cells were lysed and the lysates diluted to a final volume of 1,5 ml with the provided buffer. Cell lysates were deposited over the array's membrane and incubated overnight at 4°C. A pan HRP-conjugated anti-phospho-tyrosine antibody was then used to detect phosphorylated tyrosines by chemiluminescence. The spots were revealed by exposure to X-ray films.

6.11 MTT assay

Cell proliferation was evaluated using MTT assay. Cells were transduced (or not) with the adenoviruses, as previously described, or treated with the indicated molecules or conditione media and 72 hours later cell viability was analyzed. The MTT (3-(4,5-Dimethylthiazol-2-yl)-2,5-diphenyltetrazolium bromide, a tetrazole) reagent was added to the cells at a final concentration of 0,3 mg/ml and incubated for 4 hours at 37°C in serum free medium. MTT is processed into to purple formazan crystals by the mitochondria of living cells. The medium was then discarded and the crystals solubilized with dimethyl sulfoxide (DMSO). The reduced form of the colorimetric substrate was then quantified at the spectrophotometer at 560 nm.

6.12 Luciferase assay

HEK-293-T cells were transfected with the FuGene6. The day after, cells were treated w/wo 12.5nM of type I collagen, EMILIN2, or the Δ5 deletion mutant. Cells transfected with the pCS2-DKK-1 construct served as a negative control. Using the Dual Luciferase assay kit, luciferase activity was normalized to Renilla following measurement with a luminometer (PerkinElmer, Waltham, MA, USA). As an alternative, MDA-MB-231 and HEK-293-T cells were co-transfected with empty or Wnt1 pCMV vectors, empty or EMILIN2 pcDNA vectors and TopFlash and Renilla constructs.

6.13 Random motility

$5x10^3$ HUVEC cells were seeded on 48 well plates in M199 medium containing 5% FBS. Cells were then treated with the supernatants from NHDF over-expressing or not EMILIN2, or with recombinant EMILIN2 (5μg/ml) and/or Cetuximab (60μg/ml). The movement of cells was monitored over time with the microscope LEICA AF6000 Imaging System (LEICA, Wetzlar, Germany). Cell distance and speed were calculated with the dedicated software.

6.14 Transwell migration assay and quantification of pseudopodia

8μm FluoroBlok™inserts (BD, Milan, Italy) were coated with 20μg/ml type I collagen and blocked with 1% BSA. Following overnight starvation, mock and EMILIN2 transfected MDA-MB-231 cells were fluorescently tagged with 5μg/ml DiI lipophilic dye (Invitrogen, Milan, Italy) and plated in the upper chamber. Migration was monitored by independent fluorescence detection from the top and bottom sides of the membrane with a GENios Plus microplate fluorometer (TECAN Italia, Milan, Italy). For pseudopodia analysis, starved MDA-MB-231 cells were seeded on type I collagen or EMILIN2 coated membranes. Complete medium was used as a chemoattractant and the analysis was performed after 90 minutes using the appropriate kit.

6.15 Soft agar colony and Matrigel evasion assay

$5x10^3$ MDA-MB-231 cells/well were included in 0.4% low-melting-point agarose, placed on top of a 0.6% agarose layer, challenged with EMILIN2, and pictures were taken after 10 days. The colony number and area of clones formed by more than 10 cells were measured using Image Tool software.
For the Matrigel evasion assay 3x105/ml mock and/or Wn1-transfected cells were included in MatrigelTMdrops containing 12,5nM of recombinant EMILIN2 or type I collagen or 50ng/ml of EGF. Pictures were taken after six days following crystal violet staining.

6.16 3D in vitro angiogenesis assay

For the 3D *in vitro* experiments we have set up a previously described angiogenesis assay (Nakatsu M. N. *et.al* , 2007). Briefly, 4 x 10^2 HUVEC cells per cytodex microcarrier were employed. HUVEC cells were incubated with the beads for 4 hours at 37°C, shaking every 20 minutes. After the incubation time,

the coated beads were transferred into a flask containing complete medium and were incubated overnight at 37°C. The next day the coated beads were embedded into a fibrin gel with or without EMILIN2 (5μg/ml). Normal or EMILIN2 over-expressing NHDF cells were layered on top of the gel. The NHDF cells provide the required soluble factors that promote EC sprouting from the surface of the beads. Vessels sprouts were allowed to form for 7 days. Spheroids were fixed with 4% (w/v) paraformaldehyde for 15 minutes at room temperature and stained with the anti-CD31 antibody (vessels) and with SYTOX (nuclei). Pictures were captured at the Confocal microscope .

6.17 Aortic ring assay

The rat aortic ring assays were performed as previously described (Baker et al. 2012). Breefly, aortic rings were isolated from Fisher 344 male rats and cultivated for 8 days on rat type I collagen. The rings were treated with 5 μg/ml of murine or human EMILIN2 and fixed in 4% (w/v) paraformaldehyde. Pictures were taken with the contrast phase microscope (Nikon Eclipse TS100), At least 20 rings per grup were analyzed and the vessel number evaluated by counting.

6.18 In vivo tumor growth studies and sample analysis

$1.5x10^6$ MDA-MB-231 cells transduced with the β-galactosidase or EMILIN2 adenoviralconstructs and re-suspended in 3 mg/ml of Matrigel were injected in the mammary fat pad of six nude mice per group. Ten nude mice were injected with MDA-MB-231 cells transfected with Wnt1 or mock pCMV constructs and/or transduced as above. Once the tumors had reached the size of about 30 mm^3, adenoviral expression was induced with 1 mg/ml of doxycycline and 2.5% sucrose added to the drinking water. Twenty nude mice were injected with $1.5x10^6$ MDA-MB-231 cells over-expressing or not Wnt1 and treated with 10 μg of purified EMILIN2 or PBS (five each) every other day. Another ten mice were orthotopically injected with 5x105 MDA-MB-231 cells transfected with the EMILIN2 or empty pcDNA vectors and sacrificed after 35 days. Tumor sizes were measured with a caliperand the volume calculated with the following formula: $(\pi \times \text{length} \times \text{width}^2)/6$.

$5x10^5$ B16-F10 cells were injected subcutaneously in 2 EMILIN2-/- and wild type C57BL/6 mice. Once, after about 7 days, tumors reached the size of about 50 mm^3 the mice were sacrified, the tumors were removed and fixed in a solution containing PFA 4%, Glutheraldeide2,5% and Cacodilate buffer 0,1M. Tumors were then sent to Dott. Federico Caicci, dept of Biology, University of Padova (Italy) for the TEM analysis.

All the in vivo studies were approved by the Institutional Ethics Committee.

6.19 Software and data analysis

Graphs and statistical analyses were performed using SigmaPlot (Systat Software Inc. SanJose, CA, USA) or Graphpad Prism 5 (Graphpad Software Inc. La Jolla, CA, USA); sequence analysis was performed with Workbench tools (http://workbench.sdsc.edu; San Diego, CA, USA); gene expression data were queried using the Oncomine database (https://www.oncomine.org); densitometric analyses were performed with Quantity one (Bio-Rrad, Milan, Italy); image measurements were taken with the Image Tool Software (http://en.biosoft. net/draw/ImageTool.html; San Antonio, TX, USA). Pictures were obtained using a digitalcamera or a Leica AF6000 Imaging System (Leica Microsystems, Milan, Italy).

7 REFERENCES

Adam, Frédérick, Shilun Zheng, Nilesh Joshi, David S Kelton, Amin Sandhu, Youko Suehiro, Samira B Jeimy, et al. "Analyses of Cellular Multimerin 1 Receptors: In Vitro Evidence of Binding Mediated by alphaIIbbeta3 and alphavbeta3." *Thrombosis and Haemostasis* 94, no. 5 (November 2005): 1004–1011. doi:10.1160/TH05-02-0140.

Allavena, Paola, Cecilia Garlanda, Maria Grazia Borrello, Antonio Sica, and Alberto Mantovani. "Pathways Connecting Inflammation and Cancer." *Current Opinion in Genetics & Development* 18, no. 1 (February 2008): 3–10. doi:10.1016/j.gde.2008.01.003.

Amma, Lori L, Richard Goodyear, Jonathan S Faris, Iwan Jones, Lily Ng, Guy Richardson, and Douglas Forrest. "An Emilin Family Extracellular Matrix Protein Identified in the Cochlear Basilar Membrane." *Molecular and Cellular Neurosciences* 23, no. 3 (July 2003): 460–472.

Anastas, Jamie N., and Randall T. Moon. "WNT Signalling Pathways as Therapeutic Targets in Cancer." *Nature Reviews Cancer* 13, no. 1 (Gennaio 2013): 11–26. doi:10.1038/nrc3419.

Andl, Claudia D., Takaaki Mizushima, Kenji Oyama, Mark Bowser, Hiroshi Nakagawa, and Anil K. Rustgi. "EGFR-Induced Cell Migration Is Mediated Predominantly by the JAK-STAT Pathway in Primary Esophageal Keratinocytes." *American Journal of Physiology - Gastrointestinal and Liver Physiology* 287, no. 6 (December 1, 2004): G1227–G1237. doi:10.1152/ajpgi.00253.2004.

Angers, Stephane, and Randall T Moon. "Proximal Events in Wnt Signal Transduction." *Nature Reviews. Molecular Cell Biology* 10, no. 7 (July 2009): 468–477. doi:10.1038/nrm2717.

Archbold, H C, Y X Yang, L Chen, and K M Cadigan. "How Do They Do Wnt They Do?: Regulation of Transcription by the Wnt/β-Catenin Pathway." *Acta Physiologica (Oxford, England)* 204, no. 1 (January 2012): 74–109. doi:10.1111/j.1748-1716.2011.02293.x.

Armengol, C, S Cairo, M Fabre, and M A Buendia. "Wnt Signaling and Hepatocarcinogenesis: The Hepatoblastoma Model." *The International Journal of Biochemistry & Cell Biology* 43, no. 2 (February 2011): 265–270. doi:10.1016/j.biocel.2009.07.012.

Augsten, Martin, Christina Hägglöf, Cristina Peña, and Arne Ostman. "A Digest on the Role of the Tumor Microenvironment in Gastrointestinal Cancers." *Cancer Microenvironment: Official Journal of the International Cancer Microenvironment Society* 3, no. 1 (2010): 167–176. doi:10.1007/s12307-010-0040-9.

Azzolin, Luca, Francesca Zanconato, Silvia Bresolin, Mattia Forcato, Giuseppe Basso, Silvio Bicciato, Michelangelo Cordenonsi, and Stefano Piccolo. "Role of TAZ as Mediator of Wnt Signaling." *Cell* 151, no. 7 (December 21, 2012): 1443–1456. doi:10.1016/j.cell.2012.11.027.

Baker, Marianne, Stephen D Robinson, Tanguy Lechertier, Paul R Barber, Bernardo Tavora, Gabriela D'Amico, Dylan T Jones, Boris Vojnovic, and Kairbaan Hodivala-

Dilke. “Use of the Mouse Aortic Ring Assay to Study Angiogenesis.” *Nature Protocols* 7, no. 1 (January 2012): 89–104. doi:10.1038/nprot.2011.435.

Bazzoni, Gianfranco, and Elisabetta Dejana. “Endothelial Cell-to-Cell Junctions: Molecular Organization and Role in Vascular Homeostasis.” *Physiological Reviews* 84, no. 3 (July 2004): 869–901. doi:10.1152/physrev.00035.2003.

Bhanot, P, M Brink, C H Samos, J C Hsieh, Y Wang, J P Macke, D Andrew, J Nathans, and R Nusse. “A New Member of the Frizzled Family from Drosophila Functions as a Wingless Receptor.” *Nature* 382, no. 6588 (July 18, 1996): 225–230. doi:10.1038/382225a0.

Bikfalvi, A. “Significance of Angiogenesis in Tumour Progression and Metastasis.” *European Journal of Cancer (Oxford, England: 1990)* 31A, no. 7–8 (August 1995): 1101–1104.

Bingle, L, N J Brown, and Claire E Lewis. “The Role of Tumour-Associated Macrophages in Tumour Progression: Implications for New Anticancer Therapies.” *The Journal of Pathology* 196, no. 3 (March 2002): 254–265. doi:10.1002/path.1027.

Bouma-ter Steege, J C, K H Mayo, and A W Griffioen. “Angiostatic Proteins and Peptides.” *Critical Reviews in Eukaryotic Gene Expression* 11, no. 4 (2001): 319–334.

Braghetta, Paola, Alessandra Ferrari, Paola de Gemmis, Miriam Zanetti, Dino Volpin, Paolo Bonaldo, and Giorgio M Bressan. “Expression of the EMILIN-1 Gene during Mouse Development.” *Matrix Biology: Journal of the International Society for Matrix Biology* 21, no. 7 (November 2002): 603–609.

Bressan, G M, D Daga-Gordini, A Colombatti, I Castellani, V Marigo, and D Volpin. “Emilin, a Component of Elastic Fibers Preferentially Located at the Elastin-Microfibrils Interface.” *The Journal of Cell Biology* 121, no. 1 (April 1993): 201–212.

Bronisz, A, J Godlewski, J A Wallace, A S Merchant, M O Nowicki, H Mathsyaraja, R Srinivasan, et al. “Reprogramming of the Tumour Microenvironment by Stromal PTEN-Regulated miR-320.” *Nature Cell Biology* 14, no. 2 (February 2012): 159–167. doi:10.1038/ncb2396.

Brooks, Susan A, Hannah J Lomax-Browne, Tracey M Carter, Chloe E Kinch, and Debbie M S Hall. “Molecular Interactions in Cancer Cell Metastasis.” *Acta Histochemica* 112, no. 1 (2010): 3–25. doi:10.1016/j.acthis.2008.11.022.

Bruns, C J, C C Solorzano, M T Harbison, S Ozawa, R Tsan, D Fan, J Abbruzzese, et al. “Blockade of the Epidermal Growth Factor Receptor Signaling by a Novel Tyrosine Kinase Inhibitor Leads to Apoptosis of Endothelial Cells and Therapy of Human Pancreatic Carcinoma.” *Cancer Research* 60, no. 11 (June 1, 2000): 2926–2935.

Carmeliet, Peter. “Angiogenesis in Health and Disease.” *Nature Medicine* 9, no. 6 (June 2003): 653–660. doi:10.1038/nm0603-653.

Carpenter, G. “Receptors for Epidermal Growth Factor and Other Polypeptide Mitogens.” *Annual Review of Biochemistry* 56 (1987): 881–914. doi:10.1146/annurev.bi.56.070187.004313.

Christian, S, H Ahorn, M Novatchkova, P Garin-Chesa, J E Park, G Weber, F Eisenhaber, W J Rettig, and M C Lenter. “Molecular Cloning and Characterization of EndoGlyx-1, an EMILIN-like Multisubunit Glycoprotein of Vascular Endothelium.” *The Journal of Biological Chemistry* 276, no. 51 (December 21, 2001): 48588–48595. doi:10.1074/jbc.M106152200.

Chung, Alicia S, John Lee, and Napoleone Ferrara. “Targeting the Tumour Vasculature: Insights from Physiological Angiogenesis.” *Nature Reviews. Cancer* 10, no. 7 (July 2010): 505–514. doi:10.1038/nrc2868.

Clevers, Hans, and Roel Nusse. “Wnt/β-Catenin Signaling and Disease.” *Cell* 149, no. 6 (June 8, 2012): 1192–1205. doi:10.1016/j.cell.2012.05.012.

Colombatti, A, G M Bressan, I Castellani, and D Volpin. “Glycoprotein 115, a Glycoprotein Isolated from Chick Blood Vessels, Is Widely Distributed in Connective Tissue.” *The Journal of Cell Biology* 100, no. 1 (January 1985): 18–26.

Cooney, Matthew M, Willem van Heeckeren, Shyam Bhakta, Jose Ortiz, and Scot C Remick. “Drug Insight: Vascular Disrupting Agents and Angiogenesis--Novel Approaches for Drug Delivery.” *Nature Clinical Practice. Oncology* 3, no. 12 (December 2006): 682–692. doi:10.1038/ncponc0663.

Cox, G, and K J O’Byrne. “Matrix Metalloproteinases and Cancer.” *Anticancer Research* 21, no. 6B (December 2001): 4207–4219.

Dann, Charles E., Jen-Chih Hsieh, Amir Rattner, Divya Sharma, Jeremy Nathans, and Daniel J. Leahy. “Insights into Wnt Binding and Signalling from the Structures of Two Frizzled Cysteine-Rich Domains.” *Nature* 412, no. 6842 (Luglio 2001): 86–90. doi:10.1038/35083601.

Danussi, Carla, Alessandra Petrucco, Bruna Wassermann, Teresa Maria Elisa Modica, Eliana Pivetta, Lisa Del Bel Belluz, Alfonso Colombatti, and Paola Spessotto. “An EMILIN1-Negative Microenvironment Promotes Tumor Cell Proliferation and Lymph Node Invasion.” *Cancer Prevention Research (Philadelphia, Pa.)* 5, no. 9 (September 2012): 1131–1143. doi:10.1158/1940-6207.CAPR-12-0076-T.

Danussi, Carla, Paola Spessotto, Alessandra Petrucco, Bruna Wassermann, Patrizia Sabatelli, Monica Montesi, Roberto Doliana, Giorgio M Bressan, and Alfonso Colombatti. “Emilin1 Deficiency Causes Structural and Functional Defects of Lymphatic Vasculature.” *Molecular and Cellular Biology* 28, no. 12 (June 2008): 4026–4039. doi:10.1128/MCB.02062-07.

De Jong, J S, P J van Diest, P van der Valk, and J P Baak. “Expression of Growth Factors, Growth-Inhibiting Factors, and Their Receptors in Invasive Breast Cancer. II: Correlations with Proliferation and Angiogenesis.” *The Journal of Pathology* 184, no. 1 (January 1998): 53–57. doi:10.1002/(SICI)1096-9896(199801)184:1<53::AID-PATH6>3.0.CO;2-7.

De Luca, Antonella, Adele Carotenuto, Annamaria Rachiglio, Marianna Gallo, Monica R Maiello, Donatella Aldinucci, Antonio Pinto, and Nicola Normanno. “The Role

of the EGFR Signaling in Tumor Microenvironment." *Journal of Cellular Physiology* 214, no. 3 (March 2008): 559–567. doi:10.1002/jcp.21260.

Doherty, J K, C Bond, A Jardim, J P Adelman, and G M Clinton. "The HER-2/neu Receptor Tyrosine Kinase Gene Encodes a Secreted Autoinhibitor." *Proceedings of the National Academy of Sciences of the United States of America* 96, no. 19 (September 14, 1999): 10869–10874.

Doliana, R, S Bot, P Bonaldo, and A Colombatti. "EMI, a Novel Cysteine-Rich Domain of EMILINs and Other Extracellular Proteins, Interacts with the gC1q Domains and Participates in Multimerization." *FEBS Letters* 484, no. 2 (November 3, 2000): 164–168.

Doliana, R, S Bot, G Mungiguerra, A Canton, S P Cilli, and A Colombatti. "Isolation and Characterization of EMILIN-2, a New Component of the Growing EMILINs Family and a Member of the EMI Domain-Containing Superfamily." *The Journal of Biological Chemistry* 276, no. 15 (April 13, 2001): 12003–12011. doi:10.1074/jbc.M011591200.

El Wakil, Abeer, and Enzo Lalli. "The Wnt/beta-Catenin Pathway in Adrenocortical Development and Cancer." *Molecular and Cellular Endocrinology* 332, no. 1–2 (January 30, 2011): 32–37. doi:10.1016/j.mce.2010.11.014.

Ellis, Lee M. "Epidermal Growth Factor Receptor in Tumor Angiogenesis." *Hematology/Oncology Clinics of North America* 18, no. 5 (Ottobre 2004): 1007–1021. doi:10.1016/j.hoc.2004.06.002.

Ema, Masatsugu, and Janet Rossant. "Cell Fate Decisions in Early Blood Vessel Formation." *Trends in Cardiovascular Medicine* 13, no. 6 (August 2003): 254–259.

Ferrara, N, and K Alitalo. "Clinical Applications of Angiogenic Growth Factors and Their Inhibitors." *Nature Medicine* 5, no. 12 (December 1999): 1359–1364. doi:10.1038/70928.

Ferrara, Napoleone, Hans-Peter Gerber, and Jennifer LeCouter. "The Biology of VEGF and Its Receptors." *Nature Medicine* 9, no. 6 (June 2003): 669–676. doi:10.1038/nm0603-669.

Folkman, J. "Tumor Angiogenesis: Therapeutic Implications." *The New England Journal of Medicine* 285, no. 21 (November 18, 1971): 1182–1186. doi:10.1056/NEJM197111182852108.

Folkman, Judah. "Angiogenesis." *Annual Review of Medicine* 57 (2006): 1–18. doi:10.1146/annurev.med.57.121304.131306.

Fox, S B, K C Gatter, and A L Harris. "Tumour Angiogenesis." *The Journal of Pathology* 179, no. 3 (July 1996): 232–237. doi:10.1002/(SICI)1096-9896(199607)179:3<232::AID-PATH505>3.0.CO;2-A.

Fukui, Akiko, Kouji Ohta, Hiromi Nishi, Hideo Shigeishi, Kei Tobiume, Masaaki Takechi, and Nobuyuki Kamata. "Interleukin-8 and CXCL10 Expression in Oral Keratinocytes and Fibroblasts via Toll-like Receptors." *Microbiology and Immunology* 57, no. 3 (March 2013): 198–206. doi:10.1111/1348-0421.12022.

Ge, Xueling, and Xin Wang. “Role of Wnt Canonical Pathway in Hematological Malignancies.” *Journal of Hematology & Oncology* 3 (2010): 33. doi:10.1186/1756-8722-3-33.

Geschwind, Jean-François H, and Soulen. *Interventional Oncology: Principles and Practice*. Cambridge; New York: Cambridge University Press, 2008.

Gharavi, Nima M, Jackelyn A Alva, Kevin P Mouillesseaux, Chi Lai, Michael Yeh, Winnie Yeung, Jaclyn Johnson, et al. “Role of the Jak/STAT Pathway in the Regulation of Interleukin-8 Transcription by Oxidized Phospholipids in Vitro and in Atherosclerosis in Vivo.” *The Journal of Biological Chemistry* 282, no. 43 (October 26, 2007): 31460–31468. doi:10.1074/jbc.M704267200.

Goldman, C K, J Kim, W L Wong, V King, T Brock, and G Y Gillespie. “Epidermal Growth Factor Stimulates Vascular Endothelial Growth Factor Production by Human Malignant Glioma Cells: A Model of Glioblastoma Multiforme Pathophysiology.” *Molecular Biology of the Cell* 4, no. 1 (January 1993): 121–133.

Gullick, W J. “Growth Factors, Growth Factor Receptors and Neoplasia.” *Human & Experimental Toxicology* 10, no. 6 (November 1991): 398–400.

Guruvayoorappan, Chandrasekaran, and Girija Kuttan. “Amentoflavone Inhibits Experimental Tumor Metastasis through a Regulatory Mechanism Involving MMP-2, MMP-9, Prolyl Hydroxylase, Lysyl Oxidase, VEGF, ERK-1, ERK-2, STAT-1, NM23 and Cytokines in Lung Tissues of C57BL/6 Mice.” *Immunopharmacology and Immunotoxicology* 30, no. 4 (2008): 711–727. doi:10.1080/08923970802278276.

Habas, Raymond, Igor B Dawid, and Xi He. “Coactivation of Rac and Rho by Wnt/Frizzled Signaling Is Required for Vertebrate Gastrulation.” *Genes & Development* 17, no. 2 (January 15, 2003): 295–309. doi:10.1101/gad.1022203.

Hanahan, D, and J Folkman. “Patterns and Emerging Mechanisms of the Angiogenic Switch during Tumorigenesis.” *Cell* 86, no. 3 (August 9, 1996): 353–364.

Hayward, C P. “Multimerin: A Bench-to-Bedside Chronology of a Unique Platelet and Endothelial Cell Protein--from Discovery to Function to Abnormalities in Disease.” *Clinical and Investigative Medicine. Médecine Clinique et Experimentale* 20, no. 3 (June 1997): 176–187.

Hayward, C P, T E Warkentin, P Horsewood, and J G Kelton. “Multimerin: A Series of Large Disulfide-Linked Multimeric Proteins within Platelets.” *Blood* 77, no. 12 (June 15, 1991): 2556–2560.

Hill, Victoria K, Luke B Hesson, Temuujin Dansranjavin, Ashraf Dallol, Ivan Bieche, Sophie Vacher, Stella Tommasi, et al. “Identification of 5 Novel Genes Methylated in Breast and Other Epithelial Cancers.” *Molecular Cancer* 9 (2010): 51. doi:10.1186/1476-4598-9-51.

Hinoi, Takao, Aytekin Akyol, Brian K Theisen, David O Ferguson, Joel K Greenson, Bart O Williams, Kathleen R Cho, and Eric R Fearon. “Mouse Model of Colonic Adenoma-Carcinoma Progression Based on Somatic Apc Inactivation.” *Cancer Research* 67, no. 20 (October 15, 2007): 9721–9730. doi:10.1158/0008-5472.CAN-07-2735.

Hirschi, K K, and P A D'Amore. "Pericytes in the Microvasculature." *Cardiovascular Research* 32, no. 4 (October 1996): 687–698.

Hu, Min, and Kornelia Polyak. "Molecular Characterisation of the Tumour Microenvironment in Breast Cancer." *European Journal of Cancer (Oxford, England: 1990)* 44, no. 18 (December 2008): 2760–2765. doi:10.1016/j.ejca.2008.09.038.

Jaffe, E A, R L Nachman, C G Becker, and C R Minick. "Culture of Human Endothelial Cells Derived from Umbilical Veins. Identification by Morphologic and Immunologic Criteria." *The Journal of Clinical Investigation* 52, no. 11 (November 1973): 2745–2756. doi:10.1172/JCI107470.

Janda, Claudia Y, Deepa Waghray, Aron M Levin, Christoph Thomas, and K Christopher Garcia. "Structural Basis of Wnt Recognition by Frizzled." *Science (New York, N.Y.)* 337, no. 6090 (July 6, 2012): 59–64. doi:10.1126/science.1222879.

Jeimy, Samira B, Nola Fuller, Subia Tasneem, Kenneth Segers, Alan R Stafford, Jeffrey I Weitz, Rodney M Camire, Gerry A F Nicolaes, and Catherine P M Hayward. "Multimerin 1 Binds Factor V and Activated Factor V with High Affinity and Inhibits Thrombin Generation." *Thrombosis and Haemostasis* 100, no. 6 (December 2008): 1058–1067.

Joyce, Johanna A., and Jeffrey W. Pollard. "Microenvironmental Regulation of Metastasis." *Nature Reviews Cancer* 9, no. 4 (April 2009): 239–252. doi:10.1038/nrc2618.

Jouan-Hureaux, Valérie, Cédric Boura, Jean-Louis Merlin, and Béatrice Faivre. "Modulation of Endothelial Cell Network Formation in Vitro by Molecular Signaling of Head and Neck Squamous Cell Carcinoma (HNSCC) Exposed to Cetuximab." *Microvascular Research* 83, no. 2 (March 2012): 131–137. doi:10.1016/j.mvr.2011.07.008.

Kalluri, Raghu, and Michael Zeisberg. "Fibroblasts in Cancer." *Nature Reviews. Cancer* 6, no. 5 (May 2006): 392–401. doi:10.1038/nrc1877.

Kim, Sun-Jin, Hisanori Uehara, Takashi Karashima, David L Shepherd, Jerald J Killion, and Isaiah J Fidler. "Blockade of Epidermal Growth Factor Receptor Signaling in Tumor Cells and Tumor-Associated Endothelial Cells for Therapy of Androgen-Independent Human Prostate Cancer Growing in the Bone of Nude Mice." *Clinical Cancer Research: An Official Journal of the American Association for Cancer Research* 9, no. 3 (March 2003): 1200–1210.

Kohn, Aimee D, and Randall T Moon. "Wnt and Calcium Signaling: Beta-Catenin-Independent Pathways." *Cell Calcium* 38, no. 3–4 (October 2005): 439–446. doi:10.1016/j.ceca.2005.06.022.

Krishnan, Laxminarayanan, Clayton J Underwood, Steve Maas, Benjamin J Ellis, Tejas C Kode, James B Hoying, and Jeffrey A Weiss. "Effect of Mechanical Boundary Conditions on Orientation of Angiogenic Microvessels." *Cardiovascular Research* 78, no. 2 (May 1, 2008): 324–332. doi:10.1093/cvr/cvn055.

LeBleu, Valerie S, Brian Macdonald, and Raghu Kalluri. "Structure and Function of Basement Membranes." *Experimental Biology and Medicine (Maywood, N.J.)* 232, no. 9 (October 2007): 1121–1129. doi:10.3181/0703-MR-72.

Leimeister, Cornelia, Christian Steidl, Nina Schumacher, Sabine Erhard, and Manfred Gessler. "Developmental Expression and Biochemical Characterization of Emu Family Members." *Developmental Biology* 249, no. 2 (September 15, 2002): 204–218.

Lewis, Claire E, and Jeffrey W Pollard. "Distinct Role of Macrophages in Different Tumor Microenvironments." *Cancer Research* 66, no. 2 (January 15, 2006): 605–612. doi:10.1158/0008-5472.CAN-05-4005.

Li, Vivian S W, Ser Sue Ng, Paul J Boersema, Teck Y Low, Wouter R Karthaus, Jan P Gerlach, Shabaz Mohammed, et al. "Wnt Signaling through Inhibition of B-Catenin Degradation in an Intact Axin1 Complex." *Cell* 149, no. 6 (June 8, 2012): 1245–1256. doi:10.1016/j.cell.2012.05.002.

Lobov, Ivan B, Peter C Brooks, and Richard A Lang. "Angiopoietin-2 Displays VEGF-Dependent Modulation of Capillary Structure and Endothelial Cell Survival in Vivo." *Proceedings of the National Academy of Sciences of the United States of America* 99, no. 17 (August 20, 2002): 11205–11210. doi:10.1073/pnas.172161899.

Lorenzon, E, R Colladel, E Andreuzzi, S Marastoni, F Todaro, M Schiappacassi, G Ligresti, A Colombatti, and M Mongiat. "MULTIMERIN2 Impairs Tumor Angiogenesis and Growth by Interfering with VEGF-A/VEGFR2 Pathway." *Oncogene* 31, no. 26 (June 28, 2012): 3136–3147. doi:10.1038/onc.2011.487.

Maeshima, Yohei, Akulapalli Sudhakar, Julie C Lively, Kohjiro Ueki, Surender Kharbanda, C Ronald Kahn, Nahum Sonenberg, Richard O Hynes, and Raghu Kalluri. "Tumstatin, an Endothelial Cell-Specific Inhibitor of Protein Synthesis." *Science (New York, N.Y.)* 295, no. 5552 (January 4, 2002): 140–143. doi:10.1126/science.1065298.

Mantovani, A, M Muzio, C Garlanda, S Sozzani, and P Allavena. "Macrophage Control of Inflammation: Negative Pathways of Regulation of Inflammatory Cytokines." *Novartis Foundation Symposium* 234 (2001): 120–131; discussion 131–135.

Matsuda, Yutaka, Thomas Schlange, Edward J Oakeley, Anne Boulay, and Nancy E Hynes. "WNT Signaling Enhances Breast Cancer Cell Motility and Blockade of the WNT Pathway by sFRP1 Suppresses MDA-MB-231 Xenograft Growth." *Breast Cancer Research: BCR* 11, no. 3 (2009): R32. doi:10.1186/bcr2317.

Mongiat, M, G Mungiguerra, S Bot, M T Mucignat, E Giacomello, R Doliana, and A Colombatti. "Self-Assembly and Supramolecular Organization of EMILIN." *The Journal of Biological Chemistry* 275, no. 33 (August 18, 2000): 25471–25480. doi:10.1074/jbc.M001426200.

Mongiat, Maurizio, Giovanni Ligresti, Stefano Marastoni, Erica Lorenzon, Roberto Doliana, and Alfonso Colombatti. "Regulation of the Extrinsic Apoptotic Pathway by the Extracellular Matrix Glycoprotein EMILIN2." *Molecular and Cellular Biology* 27, no. 20 (October 2007): 7176–7187. doi:10.1128/MCB.00696-07.

Mongiat, Maurizio, Stefano Marastoni, Giovanni Ligresti, Erica Lorenzon, Monica Schiappacassi, Roberto Perris, Sergio Frustaci, and Alfonso Colombatti. "The Extracellular Matrix Glycoprotein Elastin Microfibril Interface Located Protein 2: A Dual Role in the Tumor Microenvironment." *Neoplasia (New York, N.Y.)* 12, no. 4 (April 2010): 294–304.

Morin, P J, A B Sparks, V Korinek, N Barker, H Clevers, B Vogelstein, and K W Kinzler. "Activation of Beta-Catenin-Tcf Signaling in Colon Cancer by Mutations in Beta-Catenin or APC." *Science (New York, N.Y.)* 275, no. 5307 (March 21, 1997): 1787–1790.

Morris, John P, 4th, Sam C Wang, and Matthias Hebrok. "KRAS, Hedgehog, Wnt and the Twisted Developmental Biology of Pancreatic Ductal Adenocarcinoma." *Nature Reviews. Cancer* 10, no. 10 (October 2010): 683–695. doi:10.1038/nrc2899.

Nakatsu, Martin N, Jaeger Davis, and Christopher C W Hughes. "Optimized Fibrin Gel Bead Assay for the Study of Angiogenesis." *Journal of Visualized Experiments: JoVE* no. 3 (2007): 186. doi:10.3791/186.

Noonan, Douglas M, Andrea De Lerma Barbaro, Nicola Vannini, Lorenzo Mortara, and Adriana Albini. "Inflammation, Inflammatory Cells and Angiogenesis: Decisions and Indecisions." *Cancer Metastasis Reviews* 27, no. 1 (March 2008): 31–40. doi:10.1007/s10555-007-9108-5.

Nusse, R, A van Ooyen, D Cox, Y K Fung, and H Varmus. "Mode of Proviral Activation of a Putative Mammary Oncogene (int-1) on Mouse Chromosome 15." *Nature* 307, no. 5947 (January 12, 1984): 131–136.

O-Charoenrat, Pornchai, Peter Rhys-Evans, and Suzanne Eccles. "A Synthetic Matrix Metalloproteinase Inhibitor Prevents Squamous Carcinoma Cell Proliferation by Interfering with Epidermal Growth Factor Receptor Autocrine Loops." *International Journal of Cancer. Journal International Du Cancer* 100, no. 5 (August 10, 2002): 527–533. doi:10.1002/ijc.10531.

Papetti, Michael, and Ira M Herman. "Mechanisms of Normal and Tumor-Derived Angiogenesis." *American Journal of Physiology. Cell Physiology* 282, no. 5 (May 2002): C947–970. doi:10.1152/ajpcell.00389.2001.

Papkoff, J, A M Brown, and H E Varmus. "The Int-1 Proto-Oncogene Products Are Glycoproteins That Appear to Enter the Secretory Pathway." *Molecular and Cellular Biology* 7, no. 11 (November 1987): 3978–3984.

Papkoff, J, B Rubinfeld, B Schryver, and P Polakis. "Wnt-1 Regulates Free Pools of Catenins and Stabilizes APC-Catenin Complexes." *Molecular and Cellular Biology* 16, no. 5 (May 1996): 2128–2134.

Pepper, M S. "Role of the Matrix Metalloproteinase and Plasminogen Activator-Plasmin Systems in Angiogenesis." *Arteriosclerosis, Thrombosis, and Vascular Biology* 21, no. 7 (July 2001): 1104–1117.

Pietras, Kristian, and Arne Ostman. "Hallmarks of Cancer: Interactions with the Tumor Stroma." *Experimental Cell Research* 316, no. 8 (May 1, 2010): 1324–1331. doi:10.1016/j.yexcr.2010.02.045.

Polakis, Paul. “The Many Ways of Wnt in Cancer.” *Current Opinion in Genetics & Development* 17, no. 1 (February 2007): 45–51. doi:10.1016/j.gde.2006.12.007.

Prewett, M, M Rothman, H Waksal, M Feldman, N H Bander, and D J Hicklin. “Mouse-Human Chimeric Anti-Epidermal Growth Factor Receptor Antibody C225 Inhibits the Growth of Human Renal Cell Carcinoma Xenografts in Nude Mice.” *Clinical Cancer Research: An Official Journal of the American Association for Cancer Research* 4, no. 12 (December 1998): 2957–2966.

Radisky, D, C Hagios, and M J Bissell. “Tumors Are Unique Organs Defined by Abnormal Signaling and Context.” *Seminars in Cancer Biology* 11, no. 2 (April 2001): 87–95. doi:10.1006/scbi.2000.0360.

Raman, Malavika, and Melanie H Cobb. “TGF-Beta Regulation by Emilin1: New Links in the Etiology of Hypertension.” *Cell* 124, no. 5 (March 10, 2006): 893–895. doi:10.1016/j.cell.2006.02.031.

Räsänen, Kati, and Antti Vaheri. “Activation of Fibroblasts in Cancer Stroma.” *Experimental Cell Research* 316, no. 17 (October 15, 2010): 2713–2722. doi:10.1016/j.yexcr.2010.04.032.

Raza, Ahmad, Michael J Franklin, and Arkadiusz Z Dudek. “Pericytes and Vessel Maturation during Tumor Angiogenesis and Metastasis.” *American Journal of Hematology* 85, no. 8 (August 2010): 593–598. doi:10.1002/ajh.21745.

Rhodes, John M, and Michael Simons. “The Extracellular Matrix and Blood Vessel Formation: Not Just a Scaffold.” *Journal of Cellular and Molecular Medicine* 11, no. 2 (April 2007): 176–205. doi:10.1111/j.1582-4934.2007.00031.x.

Rucker, H K, H J Wynder, and W E Thomas. “Cellular Mechanisms of CNS Pericytes.” *Brain Research Bulletin* 51, no. 5 (March 15, 2000): 363–369.

Saal, Lao H, Peter Johansson, Karolina Holm, Sofia K Gruvberger-Saal, Qing-Bai She, Matthew Maurer, Susan Koujak, et al. “Poor Prognosis in Carcinoma Is Associated with a Gene Expression Signature of Aberrant PTEN Tumor Suppressor Pathway Activity.” *Proceedings of the National Academy of Sciences of the United States of America* 104, no. 18 (May 1, 2007): 7564–7569. doi:10.1073/pnas.0702507104.

Salomon, D S, R Brandt, F Ciardiello, and N Normanno. “Epidermal Growth Factor-Related Peptides and Their Receptors in Human Malignancies.” *Critical Reviews in Oncology/hematology* 19, no. 3 (July 1995): 183–232.

Sanz-Moncasi, M P, P Garin-Chesa, E Stockert, E A Jaffe, L J Old, and W J Rettig. “Identification of a High Molecular Weight Endothelial Cell Surface Glycoprotein, endoGlyx-1, in Normal and Tumor Blood Vessels.” *Laboratory Investigation; a Journal of Technical Methods and Pathology* 71, no. 3 (September 1994): 366–373.

Sato, H, T Kinoshita, T Takino, K Nakayama, and M Seiki. “Activation of a Recombinant Membrane Type 1-Matrix Metalloproteinase (MT1-MMP) by Furin and Its Interaction with Tissue Inhibitor of Metalloproteinases (TIMP)-2.” *FEBS Letters* 393, no. 1 (September 9, 1996): 101–104.

Saunders, W Brian, Brenda L Bohnsack, Jennifer B Faske, Nicholas J Anthis, Kayla J Bayless, Karen K Hirschi, and George E Davis. "Coregulation of Vascular Tube Stabilization by Endothelial Cell TIMP-2 and Pericyte TIMP-3." *The Journal of Cell Biology* 175, no. 1 (October 9, 2006): 179–191. doi:10.1083/jcb.200603176.

Schiavinato, Alvise, Ann-Kathrin A Becker, Miriam Zanetti, Diana Corallo, Martina Milanetto, Dario Bizzotto, Giorgio Bressan, et al. "EMILIN-3, Peculiar Member of Elastin Microfibril Interface-Located Protein (EMILIN) Family, Has Distinct Expression Pattern, Forms Oligomeric Assemblies, and Serves as Transforming Growth Factor B (TGF-B) Antagonist." *The Journal of Biological Chemistry* 287, no. 14 (March 30, 2012): 11498–11515. doi:10.1074/jbc.M111.303578.

Schraufstatter, Ingrid U., Khanh Trieu, Ming Zhao, David M. Rose, Robert A. Terkeltaub, and Meike Burger. "IL-8-Mediated Cell Migration in Endothelial Cells Depends on Cathepsin B Activity and Transactivation of the Epidermal Growth Factor Receptor." *The Journal of Immunology* 171, no. 12 (December 15, 2003): 6714–6722.

Segditsas, S, and I Tomlinson. "Colorectal Cancer and Genetic Alterations in the Wnt Pathway." *Oncogene* 25, no. 57 (December 4, 2006): 7531–7537. doi:10.1038/sj.onc.1210059.

Shweiki, D, A Itin, D Soffer, and E Keshet. "Vascular Endothelial Growth Factor Induced by Hypoxia May Mediate Hypoxia-Initiated Angiogenesis." *Nature* 359, no. 6398 (October 29, 1992): 843–845. doi:10.1038/359843a0.

Spessotto, Paola, Marta Cervi, Maria Teresa Mucignat, Gabriella Mungiguerra, Ida Sartoretto, Roberto Doliana, and Alfonso Colombatti. "Beta 1 Integrin-Dependent Cell Adhesion to EMILIN-1 Is Mediated by the gC1q Domain." *The Journal of Biological Chemistry* 278, no. 8 (February 21, 2003): 6160–6167. doi:10.1074/jbc.M208322200.

Starska. "Impact of EGFR Immunoexpression on STAT3 Activation and Association with Proinflammatory/regulatory Cytokine Pattern in Laryngeal Squamous Cell Carcinoma." *Oncology Reports* (July 6, 2009). doi:10.3892/or_00000255.

Steeg, Patricia S. "Tumor Metastasis: Mechanistic Insights and Clinical Challenges." *Nature Medicine* 12, no. 8 (August 2006): 895–904. doi:10.1038/nm1469.

Tsukamoto, A S, R Grosschedl, R C Guzman, T Parslow, and H E Varmus. "Expression of the Int-1 Gene in Transgenic Mice Is Associated with Mammary Gland Hyperplasia and Adenocarcinomas in Male and Female Mice." *Cell* 55, no. 4 (November 18, 1988): 619–625.

Veljkovic, V, N Veljkovic, J A Esté, A Hüther, and U Dietrich. "Application of the EIIP/ISM Bioinformatics Concept in Development of New Drugs." *Current Medicinal Chemistry* 14, no. 4 (2007): 441–453.

Wang, Yixin, Jan G M Klijn, Yi Zhang, Anieta M Sieuwerts, Maxime P Look, Fei Yang, Dmitri Talantov, et al. "Gene-Expression Profiles to Predict Distant Metastasis of Lymph-Node-Negative Primary Breast Cancer." *Lancet* 365, no. 9460 (February 19, 2005): 671–679. doi:10.1016/S0140-6736(05)17947-1.

Xia, Ling, Lijuan Wang, Alicia S Chung, Stanimir S Ivanov, Mike Y Ling, Ana M Dragoi, Adam Platt, Tona M Gilmer, Xin-Yuan Fu, and Y Eugene Chin. "Identification of Both Positive and Negative Domains within the Epidermal Growth Factor Receptor COOH-Terminal Region for Signal Transducer and Activator of Transcription (STAT) Activation." *The Journal of Biological Chemistry* 277, no. 34 (August 23, 2002): 30716–30723. doi:10.1074/jbc.M202823200.

Yancopoulos, G D, S Davis, N W Gale, J S Rudge, S J Wiegand, and J Holash. "Vascular-Specific Growth Factors and Blood Vessel Formation." *Nature* 407, no. 6801 (September 14, 2000): 242–248. doi:10.1038/35025215.

Yarden, Y. "The EGFR Family and Its Ligands in Human Cancer. Signalling Mechanisms and Therapeutic Opportunities." *European Journal of Cancer (Oxford, England: 1990)* 37 Suppl 4 (September 2001): S3–8.

Yook, Jong In, Xiao-Yan Li, Ichiro Ota, Casey Hu, Hyun Sil Kim, Nam Hee Kim, So Young Cha, et al. "A Wnt-Axin2-GSK3beta Cascade Regulates Snail1 Activity in Breast Cancer Cells." *Nature Cell Biology* 8, no. 12 (December 2006): 1398–1406. doi:10.1038/ncb1508.

Yoshida, Tatsushi, Yaqin Zhang, Leslie A Rivera Rosado, and Baolin Zhang. "Repeated Treatment with Subtoxic Doses of TRAIL Induces Resistance to Apoptosis through Its Death Receptors in MDA-MB-231 Breast Cancer Cells." *Molecular Cancer Research: MCR* 7, no. 11 (November 2009): 1835–1844. doi:10.1158/1541-7786.MCR-09-0244.

Zardawi, Sarah J, Sandra A O'Toole, Robert L Sutherland, and Elizabeth A Musgrove. "Dysregulation of Hedgehog, Wnt and Notch Signalling Pathways in Breast Cancer." *Histology and Histopathology* 24, no. 3 (March 2009): 385–398.

8 PUBLISHED ARTICLE

Journal of Pathology
J Pathol 2014; **232:** 391–404
Published online in Wiley Online Library
(wileyonlinelibrary.com) DOI: 10.1002/path.4316

ORIGINAL PAPER

EMILIN2 down-modulates the Wnt signalling pathway and suppresses breast cancer cell growth and migration

Stefano Marastoni,[1] Eva Andreuzzi,[1] Alice Paulitti,[1] Roberta Colladel,[1] Rosanna Pellicani,[1] Federico Todaro,[1] Alvise Schiavinato,[2] Paolo Bonaldo,[2] Alfonso Colombatti[1,3] and Maurizio Mongiat[1]*

[1] *Department of Translational Research, Experimental Oncology Division 2, CRO, Aviano, Italy*
[2] *Department of Biomedical Sciences, University of Padua, Italy*
[3] *MATI Centre of Excellence, University of Udine, Italy*

**Correspondence to: M Mongiat, Department of Translational Research, CRO-IRCCS, Experimental Oncology Division 2, Via Franco Gallini, 2 Aviano, PN, Italy. E-mail: mmongiat@cro.it*

Abstract

EMILIN2 is an extracellular matrix (ECM) protein that exerts contradictory effects within the tumour microenvironment: it induces apoptosis in a number of tumour cells, but it also enhances tumour neo-angiogenesis. In this study, we describe a new mechanism by which EMILIN2 attenuates tumour cell viability. Based on sequence homology with the cysteine-rich domain (CRD) of the Frizzled receptors, we hypothesized that EMILIN2 could affect Wnt signalling activation and demonstrate direct interaction with the Wnt1 ligand. This physical binding leads to decreased LRP6 phosphorylation and to the down-modulation of β-catenin, TAZ and their target genes. As a consequence, EMILIN2 negatively affects the viability, migration and tumourigenic potential of MDA-MB-231 breast cancer cells in a number of two- and three-dimensional *in vitro* assays. EMILIN2 does not modulate Wnt signalling downstream of the Wnt–Frizzled interaction, since it does not affect the activation of the pathway following treatment with the GSK3 inhibitors LiCl and CHIR99021. The interaction with Wnt1 and the subsequent biological effects require the presence of the EMI domain, as there is no effect with a deletion mutant lacking this domain. Moreover, *in vivo* experiments show that the ectopic expression of EMILIN2, as well as treatment with the recombinant protein, significantly reduce tumour growth and dissemination of cancer cells in nude mice. Accordingly, the tumour samples are characterized by a significant down-regulation of the Wnt signalling pathway. Altogether, these findings provide further evidence of the complex regulations governed by EMILIN2 in the tumour microenvironment, and they identify a key extracellular regulator of the Wnt signalling pathway.

Keywords: extracellular matrix; tumour microenvironment; Wnt signalling; breast cancer; EMILIN2

Received 22 August 2013; Revised 9 December 2013; Accepted 17 December 2013

No conflicts of interest were declared.

Introduction

The ECM moieties of the tumour microenvironment play a pivotal role in regulating tumour progression [1,2] and are endowed with biomechanical and biological properties that determine cell behaviour [3–5]. EMILIN2, an ECM molecule belonging to the EMI domain endowed (EDEN) protein family [6], whose distinctive trait is the presence of an EMI domain at the N-terminus [7,8], plays a pleiotropic role in the tumour microenvironment. EMILIN2 represents a negative regulator of tumour development: this gene is frequently methylated in breast, lung and colorectal tumours [9]. EMILIN2 affects tumour cell viability by activating the extrinsic apoptotic pathway [10,11]. It is directly up-regulated by miR-320 and is part of a fibroblast secretome profile that correlates with clinical outcome in breast cancer patients [9,12]. Despite this evidence, the molecular regulations governed by EMILIN2 in breast cancer were not investigated prior to this study. Based on a sequence analysis study, we hypothesized that EMILIN2 could represent a key regulator of the Wnt signalling pathway in this context.

The Wnt signalling pathway activates the expression of many genes regulating cell proliferation, differentiation and motility [13,14]. The Wnt secreted ligands act by engaging the Frizzled (Fz) receptors [15] at the CRD domains [16,17], leading to an increased β-catenin stability and the modulation of gene transcription. The transcriptional co-activator TAZ is an important downstream mediator of this pathway [18]. Wnt plays a crucial role both during development and in disease [13,16,19] and several tumour types [19–24], including breast cancer [25–27], are characterized by its hyper-activation. To verify our hypothesis, we manipulated the expression of EMILIN2 and of a Wnt ligand and

carried out a number of *in vitro* and *in vivo* tests to assess the activation of the Wnt signalling pathway and the tumourigenic potential of breast cancer cells.

The results presented here shed light on the role of EMILIN2 in the breast tumour microenvironment as an ECM cue that fine-tunes the Wnt signalling pathway and attenuates tumour growth.

Materials and methods

Cell cultures

MDA-MB-231, HEK293T and E293 cells came from ATCC (Manassas, VA, USA) and were cultured in Dulbecco's modified eagle's medium (DMEM) containing 10% fetal bovine serum (FBS; Gibco, Milan, Italy). The cells were maintained at 37 °C in a humidified 5% CO_2 atmosphere.

Antibodies and other reagents

Monoclonal 828B3B3 and polyclonal anti-EMILIN2 antibodies were obtained as previously described [10,11]. Anti-β-actin and anti-FLAG antibodies, FLAG peptide, anti-FLAG M2 affinity gel, FLAG-tagged BAP, human type I collagen and low-melting agarose were from Sigma-Aldrich (Milan, Italy). Cell Death Detection Fluorescein Kit was from Roche Diagnostics (Milan, Italy). Maxwell 16 Mouse Tail DNA Purification kit and Maxwell 16 instrument, Dual Luciferase Assay Kit and Caspase-Glo 8 and 3/7 assays and pRLCMV–*Renilla* vector were from Promega (Milan, Italy). Pseudopodia kit and anti-active β-catenin antibodies were from Millipore (Milan, Italy). Anti-histone H3 (pSer28) and total β-catenin were from Abcam (Cambridge, UK). Anti-total and anti-phospho-LRP6 antibodies were from Cell Signaling Technology (Danvers, MA, USA). Anti-histidine antibody was from Abgent (San Diego, CA, USA). Ni-NTA agarose was from Qiagen (Milan, Italy). Secondary AlexaFluor-conjugated antibodies, AlexaFluor 546 phalloidin and TO-PRO-3 were from Invitrogen (Milan, Italy). Matrigel™ was from BD Biosciences (Milan, Italy). Secondary HRP-conjugated antibody was from Amersham (GE Healthcare, Milan, Italy) and Trueblot was from eBiosciences (San Diego, CA, USA). EGF was from Peprotech (Rocky Hill, NJ, USA). Wnt1 pCMV6-Neo vector was from Origene (Rockville, MD, USA). Mouse Wnt1, Fz8 pcDNA and *Xenopus* Dickkopf (DKK) pCS2 constructs, TOPflash TCF reporter and *Renilla* plasmids, Axin2 activator compound XAV939, GSK3 inhibitor CHIR99021 and anti-TAZ antibody were a gift from Professor S Piccolo (University of Padua, Italy).

RT–PCR, cell transfection, recombinant protein production and adenoviral transduction

RNA for PCR analysis was extracted from manipulated/treated MDA-MD-231 cells or tumour samples using the Trizol® reagent (Invitrogen, Milan, Italy); reverse transcription was performed using AMV–RT and exanucleotides (Promega, Milan, Italy). Semi-quantitative end-point reactions (25 cycles) were performed using GoTaq DNA polymerase (Promega) and real-time PCRs with RealMasterMix SYBR ROX (5Prime, Hamburg, Germany), using the following oligonucleotides: c-myc, 5′-TCAAGA GGCGAACACACAAC-3′ and 5′-GGCCTTTTCATT GTTTTCCA-3′; axin2, 5′-AGCCAAAGCGATCTACA AAAGG-3′ and 5′-GGTAGGCATTTTCCTCCATCAC -3′; cyclin D1, 5′-GTGCTGCGAAGTGGAAACC-3′ and 5′-ATCCAGGTGGCGACGATCT-3′; CTGF/CCN2, 5′-ATGGTGCTCCCTGCATCTTC-3′ and 5′-C TGGTACTTGCAGCTGCTCT-3′; actin, 5′-AGAAAA TCTGGCACCACAAA-3′ and 5′-AGAGGCGTACAG GGATAGCA-3′. The primer efficiency was 100%, thus the comparative C_T method ($2^{-\Delta\Delta C_T}$) was applied for the analyses.

MDA-MB-231 were transfected with the various vectors using FuGene6 reagent (Promega). Wnt1-stable clones were obtained through selection with 600 µg/ml G418. E293 cells were transfected with the relative pCEP–Pu constructs, using the FuGene6 reagent, and were then selected with 250 µg/ml G418 and 0.5 µg/ml puromycin. Confluent cells were incubated in serum-free medium for 48 h, and the media were collected and the proteins purified by means of Ni-NTA or anti-FLAG beads. The EMILIN2 Δ5 deletion mutant was amplified by PCR, using the oligonucleotides 5′-CTAGCTAGCGACGGTT CTTGACCTCCAGTCT-3′ and 5′-CGGGATCCTTAA TGGTGATGGTGATGATGGAGGTGGGAAAGGAA -3′, using the EMILIN2 full-length construct as a template. Adenoviral co-transduction with the Adeno-X Tet-On construct was performed as previously reported [11] and expression was induced using 2 µg/ml doxycycline.

Luciferase assay

HEK293T cells were transfected with FuGene6, as previously reported [28]. The day after, the cells were treated, or left untreated, with 12.5 nM type I collagen, EMILIN2 or the Δ5 deletion mutant. Cells transfected with the pCS2-DKK-1 construct served as a negative control. Using the Dual Luciferase Assay Kit, luciferase activity was normalized to *Renilla* following measurement with a luminometer (Perkin-Elmer, Waltham, MA, USA). As an alternative, MDA-MB-231 and HEK293T cells were co-transfected with empty or Wnt1 pCMV vectors, empty or EMILIN2 pcDNA vectors and TopFlash and *Renilla* constructs.

MTT assay, cell cycle analysis and detection of apoptotic cells

Breast tumour MDA-MB-231 cells transfected with the EMILIN2 and/or Wnt1 constructs, or incubated with conditioned media, following or not depletion of

EMILIN2 by means of Ni-NTA resin, or treated with 50 ng/ml EGF, were incubated for 3 h with 5 mg/ml MTT and absorbance was detected at 560 nm. Cell proliferation was also monitored, using the xCELLigence system (Roche, Milan, Italy). For FACS analysis, MDA-MB-231-transfected cells were starved for 24 h, resuspended in 70% ethanol, stained with 0.1% sodium citrate supplemented with 0.1% NP40, 125 µg/ml RNase and 50 µg/ml propidium iodide and analysed on a FACScan flow cytometer (BD, Milan, Italy). Cell cycle analysis was performed using CellQuest software (BD, Milan, Italy). The apoptotic rate was determined using the Cell Death Detection ELISA^{PLUS} TUNEL assay, and Caspase-Glo 8 and Caspase-Glo 3/7 assays were performed according to the manufacturer's instructions.

Western blot analysis

Proteins resolved in 4–20% Criterion Precast Gels (Bio-Rad, Milan, Italy) were transferred onto Hybond-ECL nitrocellulose membranes, blocked with 5% dried milk in TBS-T buffer, probed with the appropriate antibodies and developed using enhanced chemiluminescence (Amersham Biosciences, Milan, Italy). Alternatively, the Odyssey Infrared Imaging System was used (Li-COR Biosciences, Lincoln, NE, USA). The breast tumour array strips were from Protein Biotechnologies (Ramona, CA, USA); strips were wetted with methanol, blocked with 5% dried milk and incubated with the monoclonal anti-Wnt1 and polyclonal anti-EMILIN2 antibodies, followed by secondary antibody incubation and acquisition using the Odyssey Infrared Imaging System. Human tissues were provided by the CRO-Biobank.

ELISA and solid-phase binding assays

EMILIN2/mock-conditioned media were coated onto ELISA plates, blocked with 2% BSA and incubated with the 828B3B3 anti-EMILIN2 antibody followed by a HRP-conjugated secondary antibody; the substrate (0.5 mg/ml ABTS/0.1 M sodium citrate solution containing 0.01% H_2O_2) was then added and the absorbance measured at 405 nm. For the EMILIN2–Wnt1 interaction studies, 0.1 µg/well of His-tagged EMILIN2 and the Δ5 deletion mutant were coated onto ELISA plates and incubated with 30 or 100 ng FLAG-tagged Wnt1 and the binding detected with an anti-FLAG antibody.

Histidine and FLAG pull-down experiments

E293 or MDA-MB-231 cells transfected with the FLAG-tagged Wnt1 pcDNA construct were lysed in HNTG buffer (20 mM HEPES, pH 7.5, 150 mM NaCl, 0.1% Triton X-100, 10% glycerol). Cell lysates (60 µg) were incubated with 7 µg His-tagged EMILIN2 or the His-tagged Δ5 deletion mutant. The FLAG–BAP protein was used as control. Proteins were captured with the anti-FLAG-conjugated or Ni-NTA beads and analysed by western blotting.

Transwell migration assay and quantitative analysis of pseudopodia

Cell migration assays were carried out as previously described [29]. Briefly, 8 µm FluoroBlok^{TM} inserts (BD, Milan, Italy) were coated with 20 µg/ml type I collagen at 4 °C and blocked with 1% BSA. Following overnight starvation, mock and EMILIN2-transfected MDA-MB-231 cells were fluorescently tagged with 5 µg/ml DiI lipophilic dye (Invitrogen, Milan, Italy) and plated in the upper chamber. Migration was monitored by independent fluorescence detection from the top and bottom sides of the membrane, using a GENios Plus microplate fluorometer (Tecan Italia, Milan, Italy). For pseudopodia analysis, starved MDA-MB-231 cells were seeded on type I collagen- or EMILIN2-coated membranes. Complete medium was used as a chemoattractant and the analysis was performed after 90 min, using the appropriate kit.

Soft agar colony assays, spheroid outgrowth and Matrigel evasion assay

MDA-MB-231 cells, 5×10^3 cells/well, were included in 0.4% low melting-point agarose, placed on top of a 0.6% agarose layer, challenged with EMILIN2 and pictures were taken after 10 days. The colony number and area of clones formed by more than 10 cells were measured using Image Tool software.

Spheroids were obtained by seeding 5×10^5 cells on six-well plates coated with 0.5% polyHEMA and included in growth factor-reduced Matrigel^{TM}. The pictures were taken after 8 h and the outgrowth was assessed. For the Matrigel evasion assay, 3×10^5/ml mock and/or Wn1-transfected cells were included in Matrigel^{TM} drops containing 12.5 nM recombinant EMILIN2 or type I collagen, or 50 ng/ml of EGF. Pictures were taken after 6 days, following crystal violet staining.

In vivo tumour growth studies

MDA-MB-231 cells (1.5×10^6) transduced with β-galactosidase or EMILIN2 adenoviral constructs and resuspended in 3 mg/ml Matrigel^{TM} were injected into the mammary fat pad of six nude mice/group. Ten nude mice were injected with MDA-MB-231 cells transfected with Wnt1 or mock pCMV constructs and/or transduced as above. Once the tumours had reached the size of about 30 mm^3, adenoviral expression was induced with 1 mg/ml doxycycline and 2.5% sucrose added to the drinking water. Twenty nude mice were injected with 1.5×10^6 MDA-MB-231 cells over-expressing or not over-expressing Wnt1 and treated with 10 µg purified EMILIN2 or PBS (five each), every other day. Another 10 mice were orthotopically injected with 5×10^5 MDA-MB-231 cells transfected

with the EMILIN2 or empty pcDNA vectors and sacrificed after 35 days. Axillary lymph nodes were collected for Alu sequence analysis. Tumour sizes were measured with a caliper and the volume calculated with the following formula: $(\pi \times \text{length} \times \text{width}^2)/6$. All the *in vivo* studies were approved by the Institutional Ethics Committee.

Tumour sample and lymph node analyses

Tumours were embedded in OCT (Kaltek Padua, Italy) and 7 µm-thick cryostat sections were obtained for immunofluorescence analyses. DNA was isolated from axillary lymph nodes using a Maxwell 16 Mouse Tail DNA Purification Kit and a Maxwell 16 instrument. Alu sequence PCR analysis was performed, using the following oligonucleotides: *Alu*, 5′-ACGCCTGTAATCCCAGCACTT-3′ and 5′-TCGCCCAGGCTGGAGTGCA-3′; *hGAPDH*, 5′-GAGAGACCCTCACTGCTG-3′ and 5′-GATGGTACATGACAAGGTGC-3′.

Software and data analysis

Graphs and statistical analyses were performed using SigmaPlot (Systat Software, San Jose, CA, USA) or Graphpad Prism 5 (Graphpad Software, La Jolla, CA, USA). Sequence analysis was performed with Workbench tools (http://workbench.sdsc.edu; San Diego, CA, USA). Gene expression data were queried using the Oncomine database (https://www.oncomine.org). Other gene expression data and relapse-free and overall survival information were downloaded from GEO (Affymetrix microarrays only), EGA and TCGA. Kaplan–Meier curves were obtained using the Kaplan–Meier plotter (http://kmplot.com). Densitometric analyses were performed with Quantity One (Bio-Rad, Milan, Italy). Cell cycle analysis was performed with CellQuest (BD, Milan, Italy). Image measurements were taken with Image Tool Software (http://en.bio-soft.net/draw/ImageTool.html; San Antonio, TX, USA). Pictures were obtained using a digital camera or a Leica AF6000 Imaging System (Leica Microsystems, Milan, Italy).

Results

EMILIN2 affects breast cancer cell proliferation and motility

The down-regulation of EMILIN2 expression by gene methylation in breast cancer suggested that EMILIN2 could affect the progression of this type of tumour. To address this question, we induced ectopic EMILIN2 expression in breast tumour MDA-MB-231 cells that do not secrete this molecule. EMILIN2 significantly reduced MDA-MB-231 cell viability in all the selected high-expressing clones (Figure 1A, B). To overcome clonogenic variability, the clones were pooled for subsequent analysis. We obtained similar results when cells were challenged with EMILIN2 and the effect was specific, since it disappeared when EMILIN2 was depleted from the medium (see supplementary material, Figure S1A). Surprisingly, unlike the findings obtained using sarcoma cells [11], the lower viability did not correlate with increased caspase-8 and caspase 3/7 activation, or with increased apoptosis (see supplementary material, Figure S1B, C). These results indicated that MDA-MB-231 cells were resistant to the EMILIN2-driven pro-apoptotic effects and suggested that EMILIN2 could alter cell cycle progression. Indeed, MDA-MB-231 cells over-expressing EMILIN2 were characterized by a significant reduction of S-phase cells (see supplementary material, Figure S1D) and by a reduced number of phospho-histone H3-positive nuclei (see supplementary material, Figure S1E, F). In addition, these cells migrated significantly less (Figure 1C), displayed fewer pseudopodial protrusions (Figure 1D) and showed a reduced migratory phenotype, as indicated by the lower elliptical factor [30] (see supplementary material, Figure S1G, H) compared to the control cells.

EMILIN2 interacts with Wnt ligands and affects the Wnt signalling pathway

During our search for new EMILIN2 molecular partners that could account for inhibition of breast cancer cell proliferation, we noticed that, similarly to what was observed for type XVIII collagen [31], the cysteine-rich EMI domain shared 42% homology with the CRD domains. The homology involved a stretch of amino acid residues indispensable for the interaction with Wnt ligands [32] (see supplementary material, Figure S2A) and, interestingly, the rooted phylogenetic tree showed a closer relation with the secreted Frizzled-related proteins (sFRPs), which are natural inhibitors sequestering the Wnt ligands [33] (see supplementary material, Figure S2B). These observations led to the hypothesis that EMILIN2 could be an extracellular regulator of the Wnt signalling pathway. Accordingly, solid-phase binding assays indicated that EMILIN2 and Wnt1 interacted (Figure 2A): the binding was confirmed by both His- (EMILIN2) and FLAG- (Wnt1) pull-down experiments and occurred using either E293 or MDA-MB-231 cell lysates (see supplementary material, Figure S2C, B, respectively). The interaction required the presence of the EMI domain, since it disappeared when using the Δ*5E2* deletion mutant lacking this domain (Figure 2C, D). We next queried whether this interaction could affect the activation of the Wnt signalling pathway. E293 cells were transfected, or not, with Wnt1 and EMILIN2 and the TOPflash reporter revealed a significant and dose-dependent decrease of active β-catenin when EMILIN2 was ectopically expressed (Figure 2E). To corroborate this finding and to avoid possible DNA toxicity following multiple transfections, we challenged *Fz8*-transfected E293 cells with recombinant EMILIN2, while type I collagen and DKK1 [34,35] were used as negative and

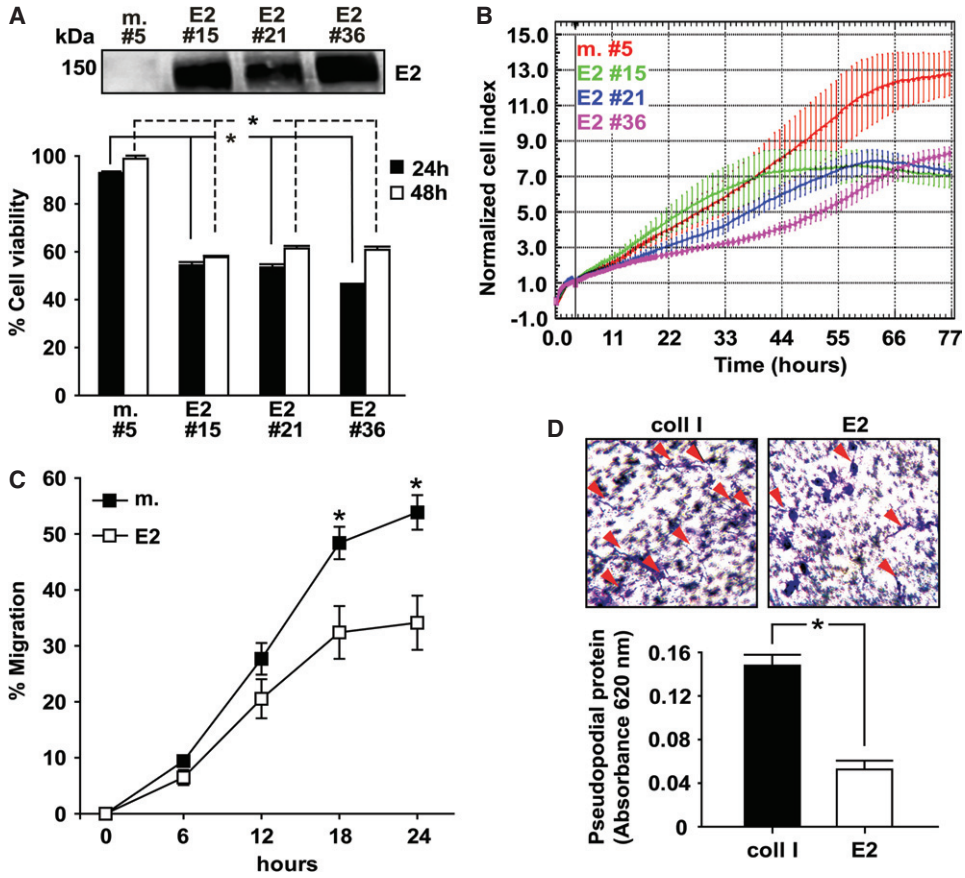

Figure 1. EMILIN2 impairs the proliferation and migration of MDA-MB-231 cells. (A) (top) Western blotting analysis of the conditioned media from MDA-MB-231 cells stably transfected with the pcDNA-EMILIN2 construct (clones E2 nos 15, 21 and 36). Mock-transfected clone 5 (m., no. 5) was used as a control; (bottom) graph reporting the percentage cell viability of the different clones at 24 and 48 h after seeding, as assessed by MTT assays. (B) Time-course analysis of cell proliferation using the same clones of (A), as assessed through the xCELLigence instrument. (C) Graph reporting the migration rate of mock- and EMILIN2-transfected MDA-MB-231 cells (m. and E2, respectively), as assessed by a Transwell migration assay. (D) (top) Representative images of the pseudopodial emissions by MDA-MB-231 cells treated with type I collagen (coll I) or EMILIN2 (E2). Pseudopodia are indicated by the arrows; (bottom) relative quantification. Values represent the mean of three replicates ± SE (*$p \leq 0.05$).

positive controls, respectively (Figure 2F). In this case, EMILIN2 also significantly impaired β-catenin activation and, in accordance with the interaction studies, the Δ*5E2* deletion mutant was ineffective (Figure 2F).

Effects of EMILIN2 on breast cancer cell proliferation and motility are Wnt-dependent

EMILIN2 also markedly reduced β-catenin activation in MDA-MB-231 cells (Figures 2G, H, 3A). To verify whether EMILIN2 attenuated the Wnt1-induced cell proliferation, we generated Wnt1 over-expressing MDA-MB-231 stable clones (Figure 3B; see also supplementary material, Figure S3A) and subsequently analysed the viability of individual clones (nos 3 and 10) and that of three combined highly expressing clones (nos 1, 3 and 10; see supplementary material, Figure S3A). EMILIN2 was able to block Wnt-driven β-catenin and LRP6 activation, as well as cell viability (Figure 3B–D) and to down-modulate the expression of the target genes cyclin-D1, c-Myc and Axin2 (see supplementary material, Figure S3B); on the other hand, EMILIN2 did not alter EGF-induced cell viability and the Δ*5E2* deletion mutant also was ineffective (Figure 3D). Accordingly, EMILIN2 did not affect the activation of the pathway downstream of Wnt/Frizzled, as indicated by the use of GSK inhibitors LiCl and CHIR99021 (Figure 3E, F). MDA-MB-231 cells treated with EMILIN2 (see supplementary material, Figure S3C) and XAV939, a promoter of Axin stabilization, displayed a substantial reduction of active β-catenin and TAZ (see supplementary material, Figure S3D, E), possibly due to inactivation of endogenous Wnt(s) caused by EMILIN2.

Next, we verified whether EMILIN2 could also affect the Wnt-driven motility of breast cancer cells. EMILIN2 significantly and specifically reduced the Wnt1-induced evasion of MDA-MB-231 cells from Matrigel™, whereas it did not affect EGF-induced evasion (Figure 4A). In a more physiological experimental setting, using polyHEMA-derived MDA-MB-231 spheroids, EMILIN2 significantly reduced cell outgrowth (Figure 4B). In contrast, the Δ*5E2* deletion mutant did not affect cell motility in this three-dimensional (3D) context (Figure 4B).

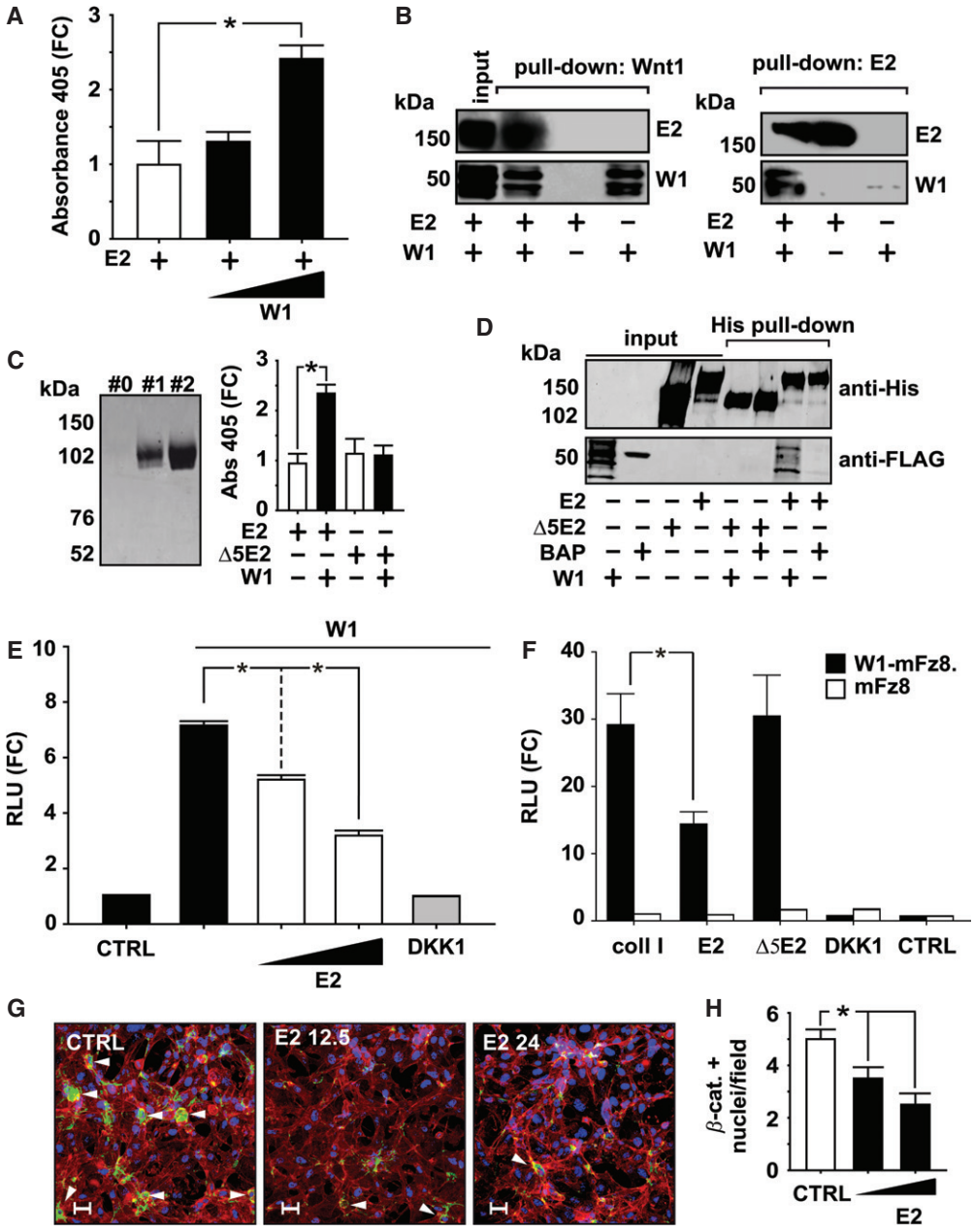

Figure 2. EMILIN2 binds to Wnt1 and inhibits Wnt1-induced signalling. (A) Graph representing the results from a solid-phase binding assay following coating of ELISA plates with EMILIN2 (E2) and incubation with 30 or 100 ng purified FLAG-tagged Wnt1. Binding was detected with a specific anti-FLAG antibody and is expressed as absorbance fold change (FC) at 405 nm. (B) Western blotting analysis of the histidine and FLAG pull-down experiment, following incubation of His-tagged EMILIN2 (E2) with cell lysates from MDA-MB-231 cells transfected with a FLAG-tagged Wnt1 construct ($W1^+$) or empty vector ($W1^-$). (C) (left) Image representing the SDS–PAGE analysis following Coomassie staining of different fractions of the His-tagged recombinant *Δ5E2* deletion mutant purification; (right) graph representing the results from a solid-phase binding assay following coating of ELISA plates with EMILIN2 (E2) or the *Δ5E2* deletion mutant and incubation with 100 ng purified FLAG-tagged Wnt1. Binding was detected with a specific anti-FLAG antibody and is expressed as absorbance fold change (FC) at 405 nm. (D) Western blotting analysis of the histidine and FLAG pull-down experiment, following incubation of the His-tagged EMILIN2 deletion mutant (*Δ5E2*) with cell lysates from MDA-MB-231 cells transfected with a FLAG-tagged Wnt1 construct (W1). His-tagged EMILIN2 and FLAG-tagged BAP were used as a positive and negative controls, respectively. (E) Graph representing the analysis of β-catenin activity following co-transfection of E293 cells with a murine pcDNA–Wnt1 construct (W1) and increasing amounts of a murine pcDNA–EMILIN2 construct (E2; 50 and 100 ng). Cells transfected with the pCS2–DKK construct (DKK1) were used as a control. (F) Graph representing the analysis of β-catenin activity in E293 cells co-transfected with the murine pcDNA–Wnt1construct (W1) and/or pcDNA-Frizzled-8 construct (Fz8) and treated with equimolar amounts (12.5 nM) of type I collagen (coll I), EMILIN2 (E2) or the *Δ5* EMILIN2 deletion mutant (*Δ5E2*). Cells transfected with the pCS2–DKK1 construct (DKK1) were used as a control. In (C, D) β-catenin activity was detected by measuring the luciferase activity following TOPflash reporter plasmid transfection (CTRL) and normalized for *Renilla*; data are expressed as the fold chance of the relative light units [RLU (FC)]. (G) Representative images of the immunofluorescence analysis of β-catenin (green), following treatment of MDA-MB-231 cells with increasing concentrations of EMILIN2 (E2; 12.5 and 24 nM); actin was stained with phalloidin (red) and nuclei with TO-PRO-3 (blue); β-catenin-positive nuclei are indicated by white arrowheads; scale bar = 35 μm. (H) Graph reporting the number of nuclear β-catenin-positive cells/field; at least 10 independent fields were examined. Values of the other graphs represent the mean of four replicates ± SE (*$p \leq 0.05$).

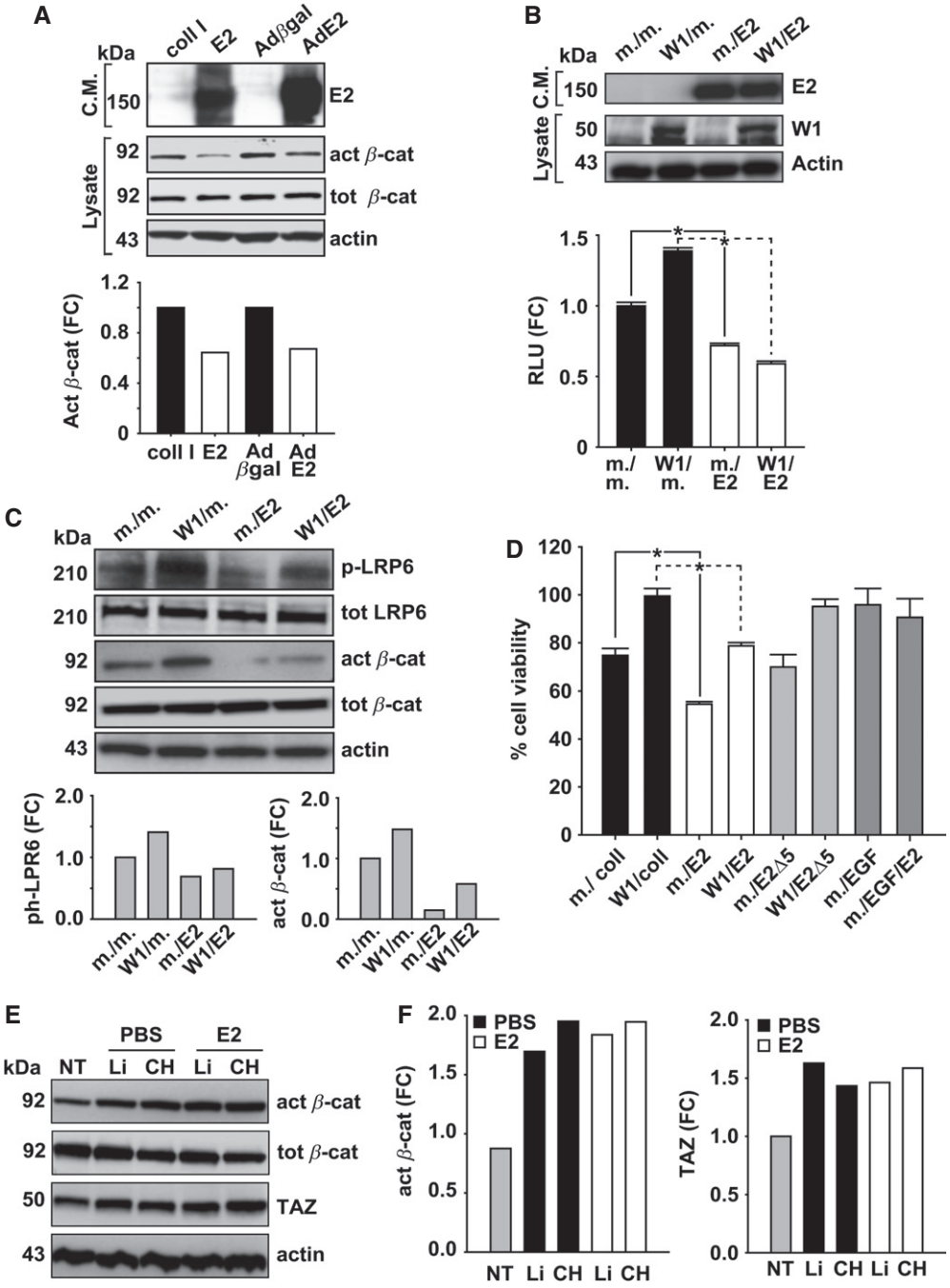

Figure 3. EMILIN2 inhibits the viability of MDA-MB-231 cells affecting Wnt signalling. (A) (top panel) Western blotting analysis of EMILIN2 in the conditioned medium (CM) and β-catenin activation (act β-cat) in MDA-MB-231 cell lysates following treatment with type I collagen (coll I) or EMILIN2 (E2) or transduction with the EMILIN2 (AdE2) or the β-galactosidase (Adβgal) adenoviral constructs. Actin was used as a normalizer of protein loading; (bottom) quantification of the fold change (FC) of the active versus total β-catenin bands. (B) (top panel) Western blotting analysis of the conditioned media (C.M.) and cell lysates to assess EMILIN2 and Wnt1 expression, respectively, following co-transfection of MDA-MB-231 cells with empty (m.) or Wnt1 (W1) pCMV vectors and/or the empty (m.) or EMILIN2 (E2) pcDNA vectors; (bottom) graph representing the analysis of β-catenin activation, detected by measuring the luciferase activity following TOPflash reporter and *Renilla* plasmid transfection; the data are expressed as the fold change of the relative light units [RLU (FC)] normalized to *Renilla*. (C) (top) Western blotting analysis of β-catenin (act β-cat) and LRP6 (p-LRP6) activation following transfection of MDA-MB-231 cells empty (m.), Wnt1 (W1) or EMILIN2 (E2) pcDNA vectors; (bottom graph) quantification of the fold change (FC) of active β-catenin and phospho-LRP6 (p-LRP6) bands. (D) Graph representing the assessment of MDA-MB-231 cell viability following co-transfection with the empty (m.) or Wnt1 (W1) pCMV vectors and treatment with equimolar amounts (12.5 nM) of type I collagen (coll I), EMILIN2 (E2) or the EMILIN2 deletion mutant (*Δ5E2*), as assessed by MTT assays; as a control, mock-transfected cells were treated with 50 ng/ml EGF plus or minus EMILIN2. (E) Western blotting analysis of TAZ and β-catenin activation performed on MDA-MB-231 cell lysates, following treatment with 12.5 nM recombinant EMILIN2 (E2) or PBS as a control, without (NT) or in the presence of the GSK3 inhibitors LiCl (Li; 40 mM) or CHIR99021 (CH; 6 μM). (F) (left and right) Graphs representing the quantification of the fold change (FC) of the active β-catenin and TAZ bands. Values represent the mean of four replicates ± SE (*$p \leq 0.01$).

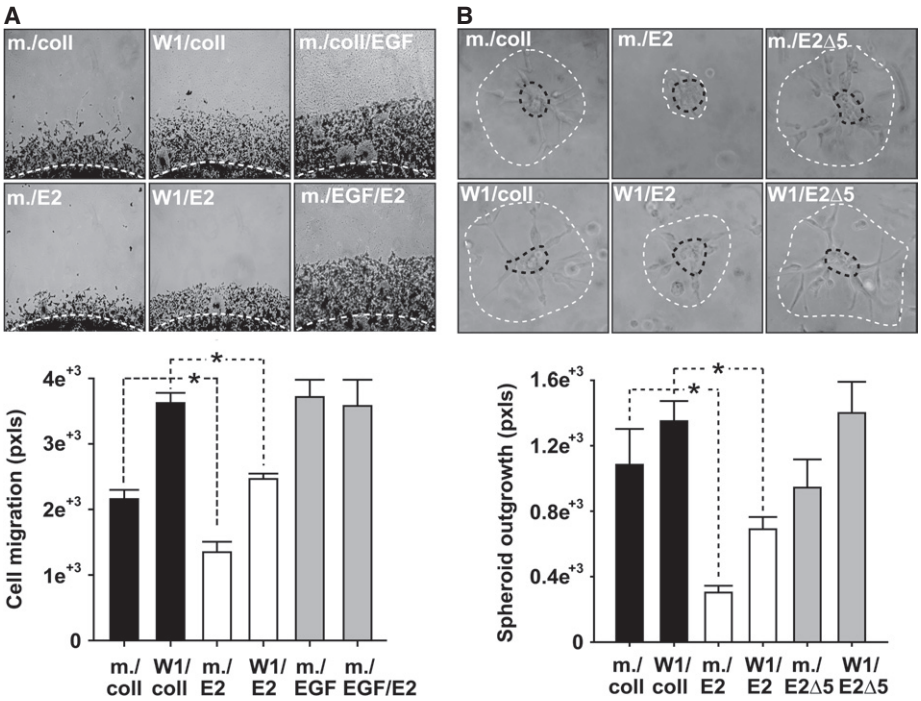

Figure 4. EMILIN2 reduces Wnt-driven breast cancer cell migration. (A) (top) Representative images of the Matrigel evasion assay, performed using MDA-MB-231 cells transfected with empty (m.) or Wnt1 pCMV (W1) constructs, following treatment with equimolar amounts (12.5 nM) of type I collagen (coll I) or EMILIN2 (E2). As a control, mock-transfected cells were treated with 50 ng/ml EGF plus or minus EMILIN2; (bottom) graph representing the quantification of the extent of cell evasion expressed in pixel (pxls). (B) (top) Representative images of the spheroid outgrowth assay performed using MDA-MB-231 cells transfected with empty (m.) or Wnt1 pCMV (W1) constructs. PolyHEMA-generated spheroids were included in Matrigel™ and treated with equimolar amounts (12.5 nM) of type I collagen (coll I), EMILIN2 (E2) or the EMILIN2 deletion mutant (*Δ5E2*); the extent of the outgrowth is indicated by white dashed circles; (bottom) graph representing the quantification of the spheroid outgrowth expressed in pixels (pxls). Values are the mean of the measurements obtained with the Image tool software and performed on 10 independent fields from three independent experiments ± SE (*$p \leq 0.006$).

EMILIN2 inhibits the tumourigenic potential of MDA-MB-231 cells, hinging on Wnt signalling

The finding that EMILIN2 negatively affected Wnt-induced breast cancer cell proliferation and motility *in vitro* led us to explore the potential anti-tumourigenic effects of EMILIN2. First, we determined that EMILIN2-transfected MDA-MB-231 cells embedded in agarose developed significantly fewer and smaller colonies compared to the control (Figure 5A). This effect also was striking with Wnt1-over-expressing cells (Figure 5B). Next, we verified the *in vivo* anti-tumourigenic potential following orthotopic injection of EMILIN2-transduced MDA-MB-231 cells. The over-expression of EMILIN2 led to the formation of significantly smaller tumours compared to the β-galactosidase-transduced controls (Figure 5C), despite the fact that caspase-3/7 and −8 activation was comparable (Figure 5D). On the other hand, the tumour samples from EMILIN2-over-expressing cells displayed a significant decrease of active and nuclear β-catenin (Figure 5E, F; see also supplementary material, Figure S4A, B) and a concurrent reduction of β-catenin and TAZ target genes (see supplementary material, Figure S4C, D).

To investigate whether EMILIN2 could also impair Wnt1-driven breast tumour cell growth *in vivo*, cells over-expressing or not over-expressing Wnt1 and transduced with the β-galactosidase or EMILIN2 adenoviral constructs were orthotopically injected in nude mice. EMILIN2 significantly decreased Wnt1-induced tumour growth (Figure 6A) and this impairment was associated with a decreased cell proliferation rate (Figure 6B). Next, to simulate a therapeutic approach, Wnt1 over-expressing tumours were challenged with EMILIN2 every other day. As shown in Figure 6C, this treatment strongly reduced tumour growth, even when boosted by Wnt1 over-expression. Finally, we verified whether the decreased cell motility induced by EMILIN2 could entail a reduced tumour cell colonization to the axillary lymph nodes; however, no difference was found between mice treated or not treated with EMILIN2 (data not shown). We then injected a lower number of cells in animals that were sacrificed after a longer observation period. EMILIN2 impaired tumour growth (Figure 6D) and, under these experimental conditions, the longer time allowed the migration of tumour cells to the axillary lymph nodes, which was significantly reduced by the over-expression of EMILIN2 (Figure 6E). Overall, EMILIN2 expression is appreciable in normal breast tissues (see supplementary material, Figure S5A) and low in some breast tumour datasets (Figure 7A, top), but a broader analysis showed a variable expression of EMILIN2

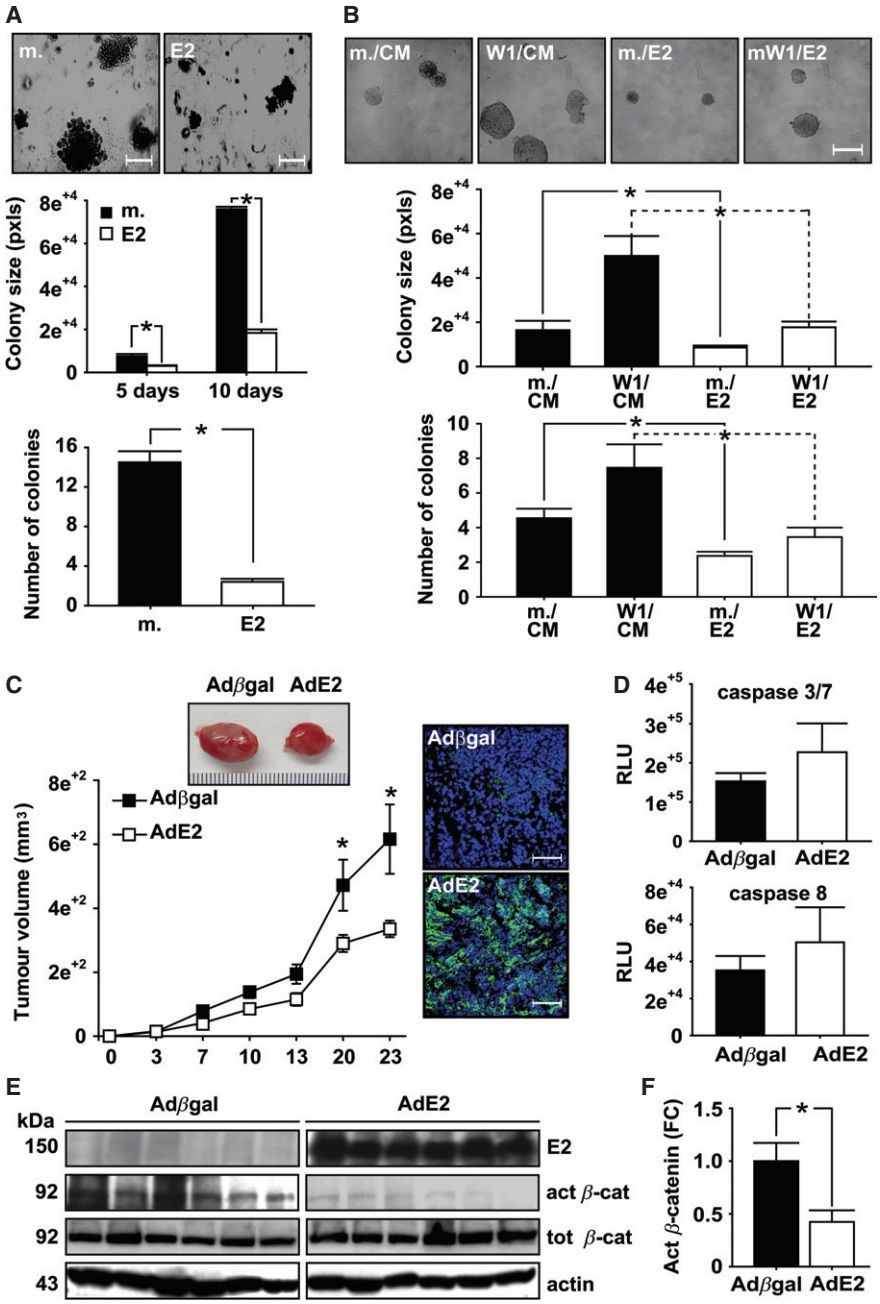

Figure 5. EMILIN2 reduces clonogenicity and tumourigenesis. (A) Representative images (top), quantification of the colony size (middle) and colony number (bottom) from soft agar colony assays, using MDA-MB-231 cells transfected with the empty (m.) EMILIN2 (E2) pcDNA vectors. (B) Representative images (top) and quantification of the colony size (middle) and colony number (bottom) from soft agar colony assays, using MDA-MB-231 cells transfected with empty (m.) or Wnt1 (W1) pCMV vectors and treated with conditioned media containing, or not containing, EMILIN2 (E2 and CM, respectively). (C) Representative images (top) and graph representing the tumour growth curves (bottom) following orthotopic injection of MDA-MB-231 cells transduced with β-galactosidase (Adβgal) or EMILIN2 (AdE2) adenoviral constructs in nude mice; (right panel) immunofluorescence analysis of the intra-tumoural deposition of EMILIN2 by the transduced tumour cells. (D) Graph representing the analysis of the active caspase-3/7 and −8 in tumours from Adβgal- and AdE2-transduced cells, as assessed with Caspase-Glo assays. (E) Western blotting analysis of EMILIN2 expression and β-catenin activation, performed on six samples of Adβgal and AdE2 tumours; actin was used as a normalizer. (F) Graph representing the quantification of the fold change (FC) of the active β-catenin bands reported in (E). Analysis in (A, B) was performed on 10 independent fields; analysis in (C) was performed using six mice/group. Values represent mean ± SE (*$p \leq 0.05$). Bars = (A, B) 10 μm; (C) 75 μm.

[36] (Figure 7A, bottom; see also supplementary material, Table S1), and this was confirmed by analysis of a human normal and breast tumour array for EMILIN2 and also Wnt1 (Figure 7B; see also supplementary material, Figure S5B). In accordance with our study, an *in silico* meta-analysis of gene expression profiles performed on a cohort of 2878 breast cancers showed an inverse correlation between EMILIN2 and Wnt target genes in relation to relapse-free survival (Figure 7C; see also supplementary material, Figure S5C). Taken together, these results demonstrate that high EMILIN2 expression negatively

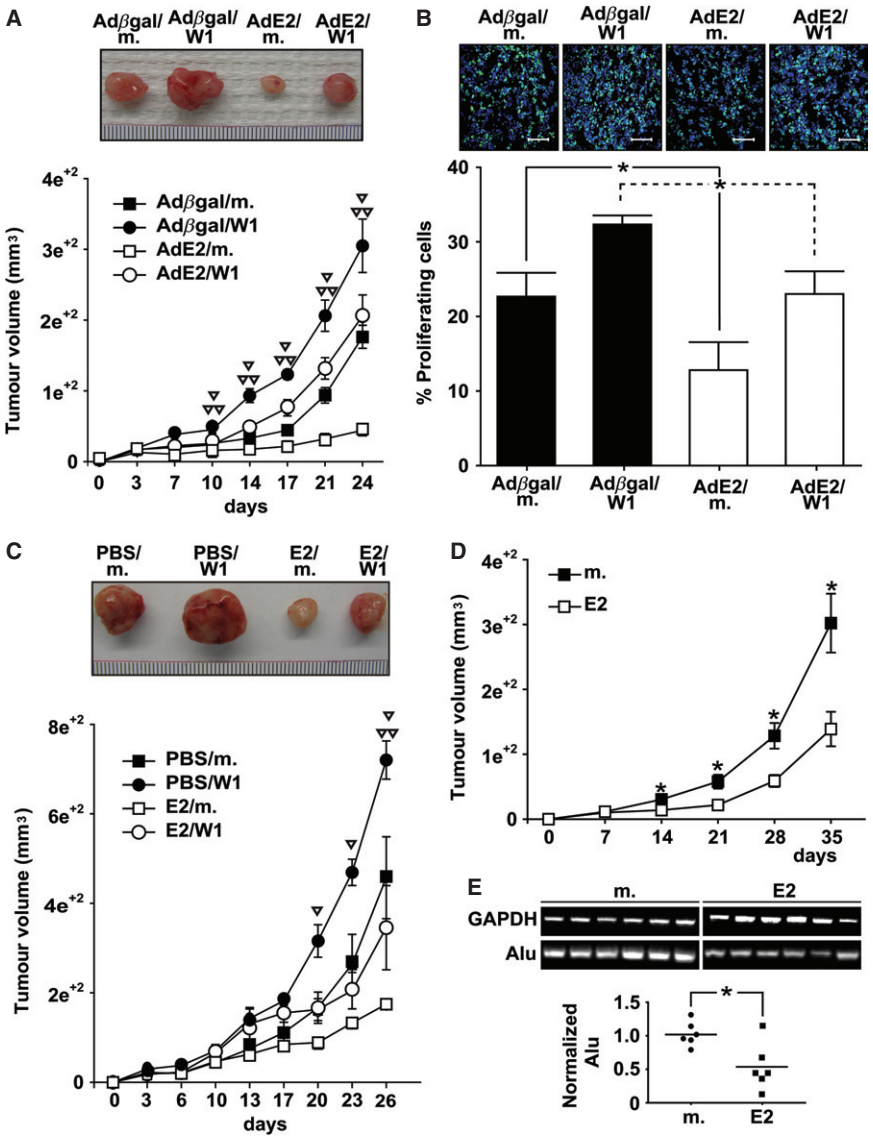

Figure 6. EMILIN2 inhibits breast tumour growth. (A) (top panel) Representative images of the tumours obtained following orthotopic injection in nude mice of MDA-MB-231 cells transfected with the empty (m.) or Wnt1 (W1) pCMV vectors and/or transduced with EMILIN2 (AdE2) or β-galactosidase (Adβgal) adenoviral constructs; (bottom) graph representing the tumour growth curves. (B) (top panel) Representative images of the Ki67 immunofluorescence analysis performed on tumour sections from experiment in (A); (bottom) graph representing the Ki67 staining quantification analysing 10 independent fields. (C) (top panel) Representative images of the tumours obtained following orthotopic injection of MDA-MB-231 cells transfected with empty (m.) or Wnt1(W1) pCMV vectors and treatment with PBS or recombinant EMILIN2 (E2); (bottom) graph representing the tumour growth curves. (D) (top) Graph representing the tumour growth curves following the injection of MDA-MB-231 cells transfected with the empty (m.) or EMILIN2 (E2) pcDNA vectors. (E) (top) Image of agarose gel analysis of PCR-amplified Alu sequences, using as a template DNA from mouse lymph nodes from the experiment in (D); *GAPDH* was used as a control; (bottom) graph representing the quantification of the Alu bands normalized to the *GAPDH* bands (*$p \leq 0.05$); ∇, statistical significance between controls and EMILIN2 treated tumours (∇ ≤ 0.02); ∇∇, statistical significance between Wnt1 and Wnt1 plus EMILIN2 treated tumours (∇∇ ≤ 0.01).

affects the proliferation and dissemination of breast cancer cells by directly attenuating the Wnt signalling pathway, and the results are schematized in Figure 7D.

Discussion

In this study, we identified EMILIN2 as a novel molecular partner of Wnt1 and demonstrated that this interaction led to a significant inhibition of the Wnt signalling pathway. EMILIN2 decreased LRP6 phosphorylation and β-catenin activation, thus halting the expression of β-catenin target genes. Accordingly, the downstream mediator TAZ [18] and its *CTGF*/*CCN2* target gene were also down-modulated by EMILIN2. In support of an extracellular role of EMILIN2, the pathway activation downstream of the Frizzled receptors was not affected, as indicated by the use of GSK3 inhibitors. In turn, Wnt signalling attenuation negatively affected cell viability as well as motility, and reduced tumour growth and lymph node metastasis.

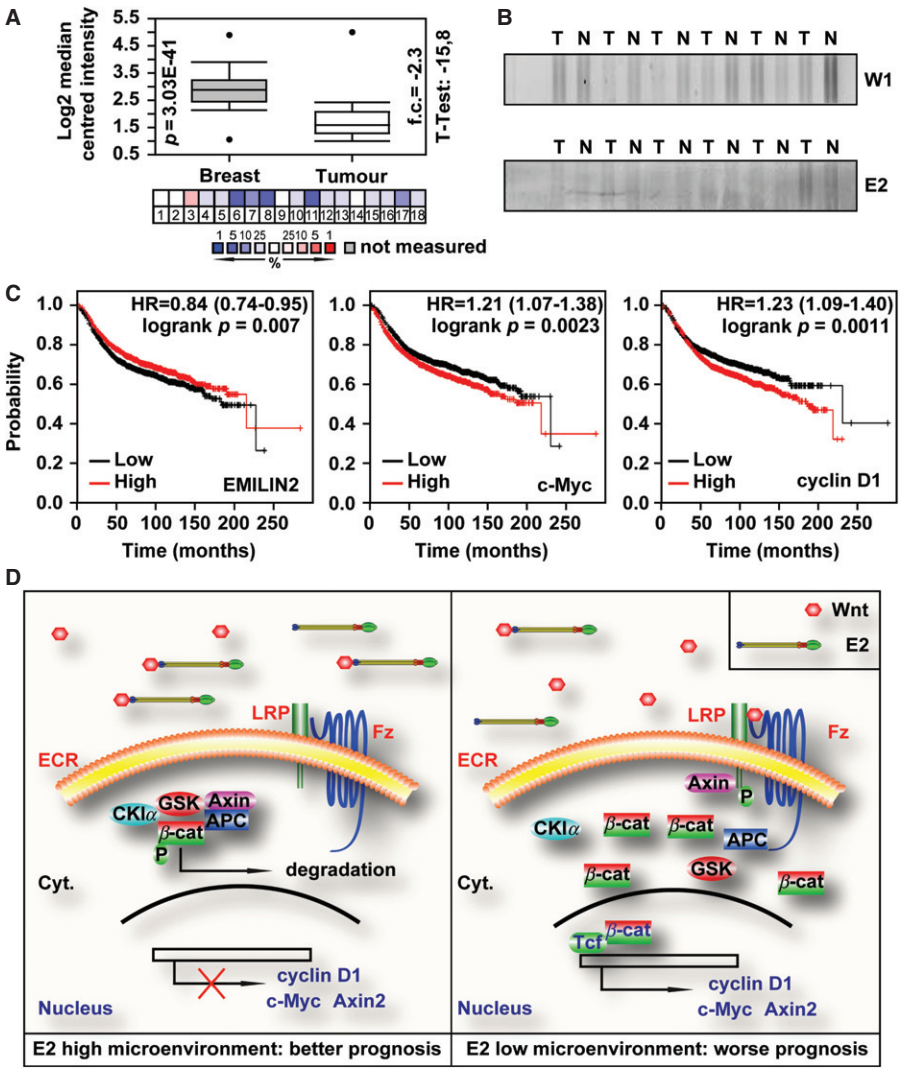

Figure 7. A low EMILIN2 expression in human breast tumours correlates with an increased expression of β-catenin target genes. (A) (top) Box plot representing the expression of EMILIN2 in the Curtis breast dataset from the Oncomine database, including 148 cases of breast tumour and 144 cases of normal tissue; the *p* value, *t*-test analysis and fold change (f.c.) are reported; (bottom) panel reporting the complete EMILIN2 expression profile in the Curtis breast dataset, including 2136 cases (see also supplementary material, Table S1). (B) Analysis of EMILIN2 (E2) and Wnt1 (W1) expression in an array of human normal (N) and tumoural (T) breast samples. An evaluation of the relative band intensity of the slot blot is shown in Figure S4F (see supplementary material). (C) Kaplan–Meier survival curves showing the probability of relapse-free survival in relation to the expression of EMILIN2, c-Myc and cyclin D1. The analysis was performed using the Kaplan–Meier plotter (http://kmplot.com) and was run on a cohort of 2878 breast cancer patients. (D) Schematic representation of the effects of low or high concentrations of EMILIN2 (E2) in the tumour microenvironment on the regulation of the Wnt signalling pathway. The extracellular region (ECR) cytoplasm (cyt.) and nuclear compartments of breast cancer cells are indicated and colour-coded; the components of the β-catenin (β-cat) destruction complex casein kinase α (CKIα), Axin, GSK3β (GSK) and APC, as well as the LPR6 (LRP) and Frizzled (Fz) receptors, are indicated. P, protein phosphorylation.

The microenvironment fine-tunes Wnt responses; many ECM molecules, including biglycan [37], glypican-3 [38] and syndecan-1 [39], as well as heparan sulphate chains [40,41], are positive regulators of Wnt signalling, whereas type XVIII collagen is a negative regulator [42]. The first clue indicating that EMILIN2 could affect Wnt signalling emerged from the observation that the EMI domain shared homology with the CRD domains, and the highest homology was found in a stretch of amino acid residues critical for Wnt binding [32]. A closer relation was found with secreted FRPs [33], suggesting that EMILIN2 might behave as an effective inhibitor.

The pleiotropic effects of EMILIN2 (ie pro-apoptotic for a number of tumour cell lines [10,11], pro-angiogenic [11,12], and the Wnt signalling regulatory function discussed in this paper) are dependent on different domains. The reason why MDA-MB-231 cells are resistant to the EMILIN2-driven pro-apoptotic effects is unknown; it is possible that EMILIN2 may alter the expression of the death receptors at the cell surface, as observed with TRAIL [43].

The EMI domain interacted with Wnt1 and promoted the Wnt signalling inhibitory effects, since the use of a deletion mutant abolished the effects, as did the removal of EMILIN2 from the medium, further

implying a direct role of EMILIN2 in Wnt signalling modulation. The EMI domain represents a potential reservoir of Wnt molecules that could compete with Wnt receptor(s), depending on the relative affinities.

The proto-oncogene Wnt1 was one of the first members of this family of ligands to be described in the mammary gland [44], but breast cancer is usually not characterized by mutations of the APC or β-catenin genes [45]. On the contrary, in this tumour misregulations of ligand–receptor interactions and altered expression of the ligands, receptors or secreted inhibitors have been described [46–49]. In line with our results, the *EMILIN2* gene is frequently methylated in breast and other tumours, and this correlates with a worse prognosis [9]. It is conceivable to speculate that decreased EMILIN2 expression deprives the tumour microenvironment of Wnt signalling-suppressive cues, granting an advantage to cancer cells. In this view, tumour microenvironments with low EMILIN2 concentrations display high c-Myc and cyclin D1 expression and are more permissive to cancer progression (see Figure 7C, D), although no similar correlation was found for the β-catenin target gene *Axin2*.

In the *in vivo* studies, we have attempted a therapeutic approach by switching on EMILIN2 expression in established tumours or by intratumoural injections of the recombinant molecule: in both cases, the striking outcome highlighted the therapeutic potential of this molecule. Furthermore, the reduction of Wnt-enhanced breast cancer cell migration to the lymph nodes prompted by EMILIN2 was of even greater impact. Breast cancer cell motility is profoundly affected by Wnt signalling [26] and may be hampered in EMILIN2-rich microenvironments, thus jeopardizing tumour cell spreading to different organs. This effect could be amplified by the EMILIN2-driven down-regulation of the TAZ target gene *CTGF/CCN2*, which enhances the osteolytic metastasis of breast cancer [50]. Thus, the methylation of EMILIN2 and the subsequent down-regulation of its expression in breast cancer may endow the cancer cell with an increased aptitude to metastasize to distant organs, through direct EMILIN2/Wnt-dependent mechanisms and/or an indirect CTGF/CCN2-dependent mechanism. Despite the remarkable results obtained with the xenograft models, the human breast cancer dataset analyses indicated a significant but less compelling link between EMILIN2 and patient survival, possibly due to the complex regulations occurring during natural tumour progression.

In conclusion, we present *in vitro* and *in vivo* data showing that EMILIN2 binds to Wnt1 and impairs Wnt signalling activation. As a consequence, EMILIN2 slows cell cycle progression and reduces cell motility, impairing breast cancer cell growth and development. These findings reveal a further mechanism by which EMILIN2 suppresses tumour growth, provide additional evidence of the pivotal role of the microenvironment during tumour development and reinforce the therapeutic potential of this molecule.

Acknowledgements

We gratefully thank Dr Monica Schiappacassi for her valuable help with the adenoviral system; Giovanni Ligresti for starting pilot studies not included in the current publication; Professor Stefano Piccolo and collaborators for the generous gift of valuable reagents; the Pathology Unit of the CRO for help with the human tissue samples; and Ms Anna Vallerugo MA for English editing. We also thank the ISS-ACC Program 2 (Grant No. ISS-ACC/R5.5, to AC), the Italian Association for Cancer Research (AIRC; Grant No. IG-2012-12718, to MM) and the Italian Ministry of Education, University, and Research (MIUR; Grant No. RBRN07BMCT, to AC) for supporting this study.

Author contributions

SM conceived and performed most of the experiments; EA performed some of the *in vitro* cell tests; AP performed pull-down experiments; RC performed some of the *in vitro* studies; RP performed tumour array database analyses; FT produced recombinant molecules; AS performed part of the TOP-flash analyses; PB and AC critically reviewed the manuscript; and MM conceived some of the experiments and wrote the manuscript.

References

1. Hanahan D, Coussens LM. Accessories to the crime: functions of cells recruited to the tumor microenvironment. *Cancer Cell* 2012; **21**: 309–322.
2. Lu P, Weaver VM, Werb Z. The extracellular matrix: a dynamic niche in cancer progression. *J Cell Biol* 2012; **196**: 395–406.
3. Paszek MJ, Zahir N, Johnson KR, *et al.* Tensional homeostasis and the malignant phenotype. *Cancer Cell* 2005; **8**: 241–254.
4. DuFort CC, Paszek MJ, Weaver VM. Balancing forces: architectural control of mechanotransduction. *Nat Rev Mol Cell Biol* 2011; **12**: 308–319.
5. Hynes RO. The extracellular matrix: not just pretty fibrils. *Science* 2009; **326**: 1216–1219.
6. Braghetta P, Ferrari A, De GP, *et al.* Overlapping, complementary and site-specific expression pattern of genes of the EMILIN/Multimerin family. *Matrix Biol* 2004; **22**: 549–556.
7. Doliana R, Bot S, Bonaldo P, *et al.* EMI, a novel cysteine-rich domain of EMILINs and other extracellular proteins, interacts with the gC1q domains and participates in multimerization. *FEBS Lett* 2000; **484**: 164–168.
8. Doliana R, Canton A, Bucciotti F, *et al.* Structure, chromosomal localization, and promoter analysis of the human elastin microfibril interfase located protein (EMILIN) gene. *J Biol Chem* 2000; **275**: 785–792.
9. Hill VK, Hesson LB, Dansranjavin T, *et al.* Identification of five novel genes methylated in breast and other epithelial cancers. *Mol Cancer* 2010; **9**: 51.
10. Mongiat M, Ligresti G, Marastoni S, *et al.* Regulation of the extrinsic apoptotic pathway by the extracellular matrix glycoprotein EMILIN2. *Mol Cell Biol* 2007; **27**: 7176–7187.
11. Mongiat M, Marastoni S, Ligresti G, *et al.* The extracellular matrix glycoprotein elastin microfibril interface located protein 2:

a dual role in the tumor microenvironment. *Neoplasia* 2010; **12**: 294–304.
12. Bronisz A, Godlewski J, Wallace JA, *et al.* Reprogramming of the tumour microenvironment by stromal PTEN-regulated miR-320. *Nat Cell Biol* 2012; **14**: 159–167.
13. Archbold HC, Yang YX, Chen L, *et al.* How do they do Wnt they do?: regulation of transcription by the Wnt/β-catenin pathway. *Acta Physiol (Oxf)* 2012; **204**: 74–109.
14. Li VS, Ng SS, Boersema PJ, *et al.* Wnt Signaling through inhibition of β-catenin degradation in an intact Axin1 complex. *Cell* 2012; **149**: 1245–1256.
15. Bhanot P, Brink M, Samos CH, *et al.* A new member of the frizzled family from *Drosophila* functions as a Wingless receptor. *Nature* 1996; **382**: 225–230.
16. Clevers H, Nusse R. Wnt/β-catenin signaling and disease. *Cell* 2012; **149**: 1192–1205.
17. Janda CY, Waghray D, Levin AM, *et al.* Structural basis of Wnt recognition by Frizzled. *Science* 2012; **337**: 59–64.
18. Azzolin L, Zanconato F, Bresolin S, *et al.* Role of TAZ as mediator of Wnt signaling. *Cell* 2012; **151**: 1443–1456.
19. Polakis P. The many ways of Wnt in cancer. *Curr Opin Genet Dev* 2007; **17**: 45–51.
20. El WA, Lalli E. The Wnt/β-catenin pathway in adrenocortical development and cancer. *Mol Cell Endocrinol* 2011; **332**: 32–37.
21. Morris JP, Wang SC, Hebrok M. KRAS, Hedgehog, Wnt and the twisted developmental biology of pancreatic ductal adenocarcinoma. *Nat Rev Cancer* 2010; **10**: 683–695.
22. Armengol C, Cairo S, Fabre M, *et al.* Wnt signaling and hepatocarcinogenesis: the hepatoblastoma model. *Int J Biochem Cell Biol* 2011; **43**: 265–270.
23. Ge X, Wang X. Role of Wnt canonical pathway in hematological malignancies. *J Hematol Oncol* 2010; **3**: 33.
24. Hinoi T, Akyol A, Theisen BK, *et al.* Mouse model of colonic adenoma–carcinoma progression based on somatic Apc inactivation. *Cancer Res* 2007; **67**: 9721–9730.
25. Zardawi SJ, O'Toole SA, Sutherland RL, *et al.* Dysregulation of Hedgehog, Wnt and Notch signalling pathways in breast cancer. *Histol Histopathol* 2009; **24**: 385–398.
26. Matsuda Y, Schlange T, Oakeley EJ, *et al.* WNT signaling enhances breast cancer cell motility and blockade of the WNT pathway by sFRP1 suppresses MDA-MB-231 xenograft growth. *Breast Cancer Res* 2009; **11**: R32.
27. Yook JI, Li XY, Ota I, *et al.* A Wnt–Axin2–GSK3β cascade regulates Snail1 activity in breast cancer cells. *Nat Cell Biol* 2006; **8**: 1398–1406.
28. Wu W, Glinka A, Delius H, *et al.* Mutual antagonism between dickkopf1 and dickkopf2 regulates Wnt/β-catenin signalling. *Curr Biol* 2000; **10**: 1611–1614.
29. Spessotto P, Lacrima K, Nicolosi PA, *et al.* Fluorescence-based assays for *in vitro* analysis of cell adhesion and migration. *Methods Mol Biol* 2009; **522**: 221–250.
30. Grande-Garcia A, Echarri A, de RJ, *et al.* Caveolin-1 regulates cell polarization and directional migration through Src kinase and Rho GTPases. *J Cell Biol* 2007; **177**: 683–694.
31. Xu YK, Nusse R. The Frizzled CRD domain is conserved in diverse proteins including several receptor tyrosine kinases. *Curr Biol* 1998; **8**: R405–406.
32. Dann CE, Hsieh JC, Rattner A, *et al.* Insights into Wnt binding and signalling from the structures of two Frizzled cysteine-rich domains. *Nature* 2001; **412**: 86–90.
33. Bovolenta P, Esteve P, Ruiz JM, *et al.* Beyond Wnt inhibition: new functions of secreted Frizzled-related proteins in development and disease. *J Cell Sci* 2008; **121**: 737–746.
34. Glinka A, Wu W, Delius H, *et al.* Dickkopf-1 is a member of a new family of secreted proteins and functions in head induction. *Nature* 1998; **391**: 357–362.
35. MacDonald BT, Tamai K, He X. Wnt/β-catenin signaling: components, mechanisms, and diseases. *Dev Cell* 2009; **17**: 9–26.
36. Curtis C, Shah SP, Chin SF, *et al.* The genomic and transcriptomic architecture of 2000 breast tumours reveals novel subgroups. *Nature* 2012; **486**: 346–352.
37. Berendsen AD, Fisher LW, Kilts TM, *et al.* Modulation of canonical Wnt signaling by the extracellular matrix component biglycan. *Proc Natl Acad Sci USA* 2011; **108**: 17022–17027.
38. Capurro MI, Xiang YY, Lobe C, *et al.* Glypican-3 promotes the growth of hepatocellular carcinoma by stimulating canonical Wnt signaling. *Cancer Res* 2005; **65**: 6245–6254.
39. Alexander CM, Reichsman F, Hinkes MT, *et al.* Syndecan-1 is required for Wnt-1-induced mammary tumorigenesis in mice. *Nat Genet* 2000; **25**: 329–332.
40. Ai X, Do AT, Lozynska O, *et al.* QSulf1 remodels the 6-*O* sulfation states of cell surface heparan sulfate proteoglycans to promote Wnt signaling. *J Cell Biol* 2003; **162**: 341–351.
41. Lin X. Functions of heparan sulfate proteoglycans in cell signaling during development. *Development* 2004; **131**: 6009–6021.
42. Quelard D, Lavergne E, Hendaoui I, *et al.* A cryptic frizzled module in cell surface collagen 18 inhibits Wnt/β-catenin signaling. *PLoS One* 2008; **3**: e1878.
43. Yoshida T, Zhang Y, Rivera Rosado LA, *et al.* Repeated treatment with subtoxic doses of TRAIL induces resistance to apoptosis through its death receptors in MDA-MB-231 breast cancer cells. *Mol Cancer Res* 2009; **7**: 1835–1844.
44. Nusse R, Varmus HE. Many tumors induced by the mouse mammary tumor virus contain a provirus integrated in the same region of the host genome. *Cell* 1982; **31**: 99–109.
45. Lin SY, Xia W, Wang JC, *et al.* β-Catenin, a novel prognostic marker for breast cancer: its roles in cyclin D1 expression and cancer progression. *Proc Natl Acad Sci USA* 2000; **97**: 4262–4266.
46. Bafico A, Liu G, Goldin L, *et al.* An autocrine mechanism for constitutive Wnt pathway activation in human cancer cells. *Cancer Cell* 2004; **6**: 497–506.
47. Schlange T, Matsuda Y, Lienhard S, *et al.* Autocrine WNT signaling contributes to breast cancer cell proliferation via the canonical WNT pathway and EGFR transactivation. *Breast Cancer Res* 2007; **9**: R63.
48. Milovanovic T, Planutis K, Nguyen A, *et al.* Expression of Wnt genes and frizzled 1 and 2 receptors in normal breast epithelium and infiltrating breast carcinoma. *Int J Oncol* 2004; **25**: 1337–1342.
49. Wong SC, Lo SF, Lee KC, *et al.* Expression of frizzled-related protein and Wnt-signalling molecules in invasive human breast tumours. *J Pathol* 2002; **196**: 145–153.
50. Shimo T, Kubota S, Yoshioka N, *et al.* Pathogenic role of connective tissue growth factor (CTGF/CCN2) in osteolytic metastasis of breast cancer. *J Bone Miner Res* 2006; **21**: 1045–1059.

SUPPLEMENTARY MATERIAL

The following supplementary material may be found in the online version of this article:

Figure S1. (A) Graph reporting the MTT activity following treatment of MDA-MB-231 cells with EMILIN2 or its depletion from the medium. (B, C) Graphs reporting the caspase 8, caspase 3/7 and apoptotic rate of MDA-MB-231 cells following treatment with EMILIN2, respectively. (D)

Graphs representing the cell cycle of MDA-MB-231 following EMILIN2 over-expression. (E, F) Immunofluorescence analysis and quantification of the phospho-histone H3-positive nuclei in control and EMILIN2-transfected cells. (G, H) Analysis of the elliptical factor of MDA-MB-231 cells plated on EMILIN2

Figure S2. (A, B) Sequence alignment between EMILIN2, frizzled receptors and FRP3 and rooted phylogenetic tree from the alignment. (C) Pull-down of EMILIN2 and Wnt1 from transfected 293 cells

Figure S3. (A) Wnt1 expression following transfection of MDA-MB-231 cells and MTT activity of the different clones. (B) Real-time PCR analysis of β-catenin target genes in mock and EMILIN2-transfected MDA-MB-231 cells. (C) EMILIN2 expression in transfected 293 cells. (D, E) β-Catenin and TAZ expression following treatment with EMILIN2 and XAV939

Figure S4. (A) Immunofluorescence of β-catenin in control and EMILIN2 over-expressing tumours. (B) Evaluation of the number of β-catenin positive nuclei in control and EMILIN2 over-expressing tumours. (C) PCR analysis of the β-catenin target genes in control and EMILIN2 over-expressing tumours. (D) PCR analysis of the TAZ target gene *CTGF*/*CCN2* in control and EMILIN2 over-expressing tumours

Table S1. Complete EMILIN2 expression profile reported in the Curtis breast dataset

Supplementary references

ACKNOWLEDGMENTS

This work was performed in the Division of Experimental Oncology 2 at National Cancer Institute (CRO) of Aviano, directed by Prof. Alfonso Colombatti.

I would like to acknowledge the "Tumor microenvironment and Angiogenesis" group, in particular my PhD advisors, Dr. Maurizio Mongiat and Prof. Alfonso Colombatti, for supporting me during these years.